UNIVERSITY OF Hull

Novel Photochromic Liquid Crystals

A Thesis submitted for degrees of Doctor of Philosophy by

James Hussey MChem(Hons)

September 2016

PhD Thesis

The combination of photochromic units and liquid crystal mesogens has over the years been investigated intensively. However the focus of this work has been on very few photochromic groups. The overall aim of this work is to combine photochromic groups, that have not been used in combination with liquid crystal phase behaviour inducing groups, with the aim to generate new liquid crystalline photochromes. The imidazole based lophine group was functionalised symmetrically to induce liquid crystalline properties. The modification of the lophine core involved the introduction of a spacer using hydrocarbon and siloxane groups, a mesogenic group and the variation of the spacing between the mesogenic groups and the imidazole. The first room temperature liquid crystalline triphenyl imidazoles were thus generated and the photochromic and liquid crystal properties were explored using UV-Vis spectroscopy, optical polarising microscopy, differential scanning calorimetry and X-ray diffraction methods. Additionally the synthesis and the functionalisation of a diazocine unit, which is a derivative of the commonaly known *trans*-azobenzene compound was explored.

The results of the work carried out was the synthesis of a set of novel photochromic liquid crystalline materials, with the alteration of the structure and the method of linking the liquid crystalline mesogen and the photochromic unit. This reduced the transition temperatures to the isotropic phase by 2°C and causing a shift in the absorption spectra if the irradiated species from 450nm to 550nm. It was also observed that the irradiation and subsequent radicalisation of the hexaarybiimidazole group did not alter the liquid crystalline properies but did induce a bulk colour change in the material in the smectic A phase.

Acknowledgements

I would like to thank Prof G. H. Mehl for the opportunity to carry out this work and the support throughout the project. I would also like to thank Dr C. Welch for the support in the synthetic discussions and the help throughout. I would also like to thank Dr Z. Ahmed for the help with XRD and advice, Mr D. Allan for the help with programs and the superior knowledge of LaTeX. Finally I would like to thank my wife Sandie, my parents and Jamie Moore for their support (emotional and financial) without whom I would have struggled to complete this project.

Contents

List of Figures

List of Schemes

List of Tables

List of Symbols & Abbreviations

ϵ Extinction coefficient

ϵ Extinction coefficient

Φ Photoisomerisation quantum Yields

(LC) Liquid crystal

(ppm) Parts per million

(SAX) Small angle X-ray diffraction

(WAX) Wide angle X-ray diffraction

K Thermal relaxation barrier

DSC Differential scanning calorimetry

FRET flurescance resonance energy transfer

HABI Hexaarylbiimidazol

HPLC High performance liquid chromatography

LED Light emiting diode

NMR Nuclear magnetic resonance

OPM Optical polarising microscopy

SmA Smectic A

SmB Smectic B

SmC Smectic C

SmF Smectic F

SmI Smectic I

Tg Glass transition

TLC Thin layer chromatography

TPM triphenylmethyl

UV Ultra violet

Chapter 1 Introduction to liquid crystals

1.1 General overview

The overall aim of the project was to investigate the effects of photochromism on the liquid crystal properties of a novel photochromic core group. The combination of liquid crystal (LC) mesogens with molecules that exhibit both photochromic properties and piezochromic properties has yet to be investigated. The core molecule which shows both of these characteristics is the 2,4,5-triphenylimidazole molecule, the liquid crystal arm is a functionalised cyanobiphenyl group attached via a combined hydrocarbon-siloxane linker system.

1.2 A brief overview of Liquid Crystals, their structure and phase properties.

Liquid crystals are a class of molecules which, upon heating, show a state of matter that is neither isotropic liquid nor crystalline. Properties of molecules that exhibit liquid crystal behaviour can be classed as crystalline like, with some of the positional and orientational order of crystalline molecules.[1] In addition to this (limited order positionally and orientationally) they also behave like liquid for example, they flow like a liquid. There are many different forms of liquid crystal molecules which have different properties and behave in different ways as shown in Figure 1.1.

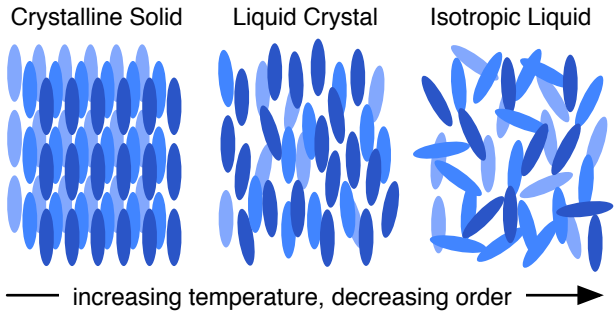

Figure 1.1. Schematic transition sequence for thermotropic liquid crystals.

Liquid crystals can be split into two categories: lyotropic and thermotropic compounds. Thermotropic liquid crystals undergo the transition from a crystalline state to a LC state when heated. Lyotropic liquid crystals, on the other hand, are formed by mixing the lyotropic LC mesogen with an isotropic solvent.[2] Thermotropic LC's can be further subdivided by the phase structure. For most materials there is a clear link between their anisotropic structure and the formation of a liquid crystalline phase. Most rod-shaped liquid crystals form nematic and/or smectic phases. The general definition of a nematic liquid crystal phase is that the molecules have orientational order but no positional order. This means that the long axis of the molecule is in the average direction of the orientation of the molecules for rod like mesogens, an example, is shown in Figure 1.2. There has been much work focusing on the incorporation of low mass liquid crystal mesogens into polymers and elastomers, which has the effect of altering the properties of the polymer. Rod shaped liquid crystals have been used in many elastomers[3] because of the ability of the mesogen to respond to many stimuli, such as strain, temperature, light, and electric fields.

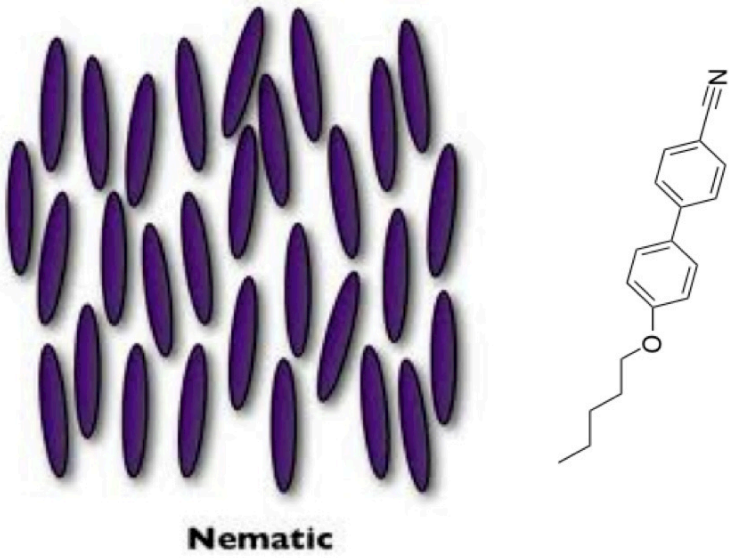

Figure 1.2. Basic representation of a Nematic liquid crystal phase based on 5CB

The direction of the LC mesogens is the term given to the averaging of the orientation of the molecules in space in the LC phase. The properties and the shape of the mesogens can give rise to different orientations such as molecules that have inherent chiral properties, where the molecules will twist with respect to one another forming a layer twisting director, these are known as the chiral nematic or cholesteric phase.

Smectic LC phases are different from nematic phases as they have orientational order and one or two-dimensional positional order. They can be subdivided into categories depending on the degrees of order that the molecules have, the most common of the smectic phases are the A, B, C, F, and I phase (SmA,SmB, SmC, SmF, SmI). The SmA phase is layered with the molecules having an average orientation of 90° with respect to the layer normal. In the SmC phase the molecules are tilted with respect to the layer normal, see Figure 1.3.[1] Both the SmA and the SmC phases have limited positional ordering within the layers. The other common smectic phases have two-dimensional positional ordering.

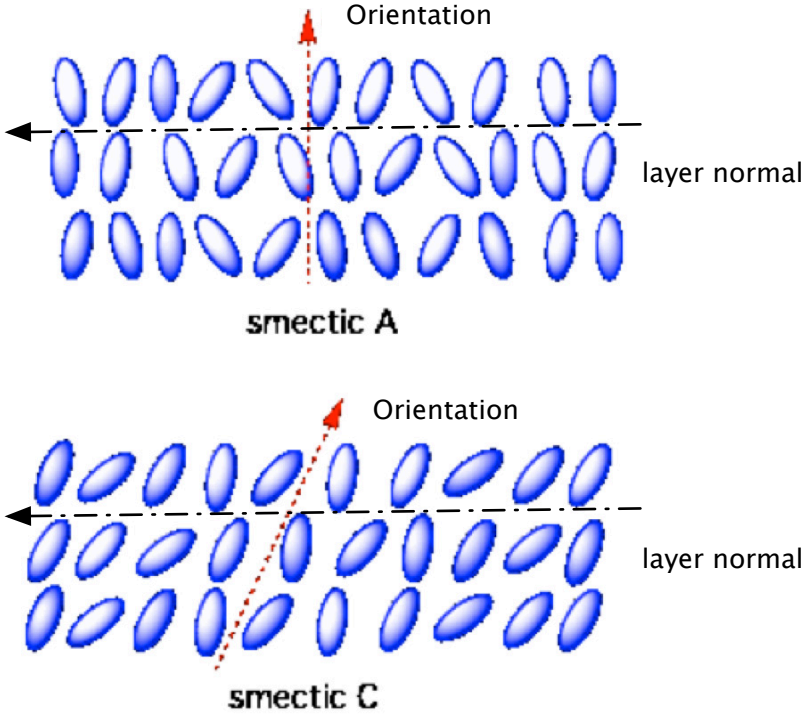

Figure 1.3. Depiction of an SmA phase and a SmC phase.

An example of this is the hexagonal structure of the molecules positioned orthogonal to the layer planes which is seen in the SmB phase or with a tilted hexagonal structure as in the SmF or SmI phases.

1.3 Characterisation methods

There are many methods used to characterise both the molecules and the LC phases. The main methods used for the general purity and molecular structure determination are ^{1}H-NMR spectroscopy, mass spectrometry, and high performance liquid chromatography (HPLC), they all report different properties of a molecule or a sample. The methods for the determination of the LC phase are DSC DSC(differential scanning calorimetry) and OPM (optical polarizing microscopy) together with a hot stage. OPM is a method for the initial determination of liquid crystal transitions. OPM works by heating up the sample and using optical polarizers at 90° to one

another. The transition from the crystal to the LC phase to the isotropic phase is then observed by the user as a disaperance of birefringence see Figure 1.4.

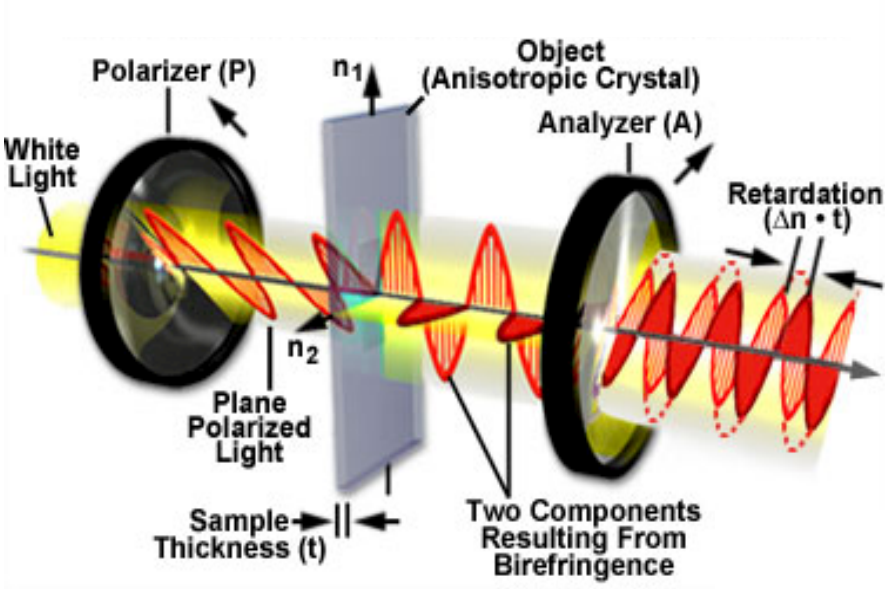

Figure 1.4. Representation of OPM setup

The sample is illuminated by linear polarized light. Once the polarized light has passed through the sample, if the sample is a liquid crystal, the light is split into the ordinary and extraordinary rays, which then pass through the second polarizer and to the eyepiece. The splitting of the light into the ordinary and extraordinary rays is due to the material having different refractive indices in different directions. This causes the light passing through the material to have different speeds. This property of the material gives rise to birefringence. The birefringence of the material can be calculated using the formula $\Delta n = n_e - n_o$.[1] Δn is the birefringence of the material, n_e is the term for the refractive index of the extraordinary ray, finally n_o is the term for the refractive index of the ordinary ray.

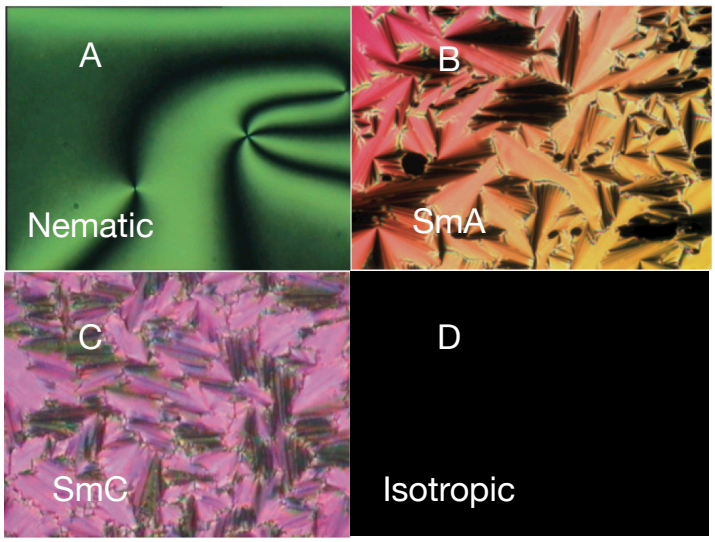

Figure 1.5. Examples of LC textures and the isotropic phase on non aligned microscope slides. A = nematic schlieren texture, B = smectic A focal conic fans, C = smectic C broken focal conic fans, D = isotropic non berefingent.

This formation of the ordinary and extraordinary rays gives rise to the well known LC birefringent textures, like the streak or thread like texture of the nematic known as the Schlieren texture, see Figure 1.5 **A**. Depending on the LC phase a different texture is observed. In the smectic phases there are often focal conic fans with areas of non birefringence which is typical for the SmA phase, see Figure 1.5 **B**. The smectic C phase has an similar texture to the smectic A phase, with focal conic fans though giving non-orthogonal crosses and additionally the non birefringent areas now show birefringence see Figure 1.5. The final image in Figure 1.5 is the isotropc phase where there is no birefringence and the light does not pass through the sample. Once the phase transition and the temperature are recorded, the next step is to confirm it by using DSC see Figure 1.6.

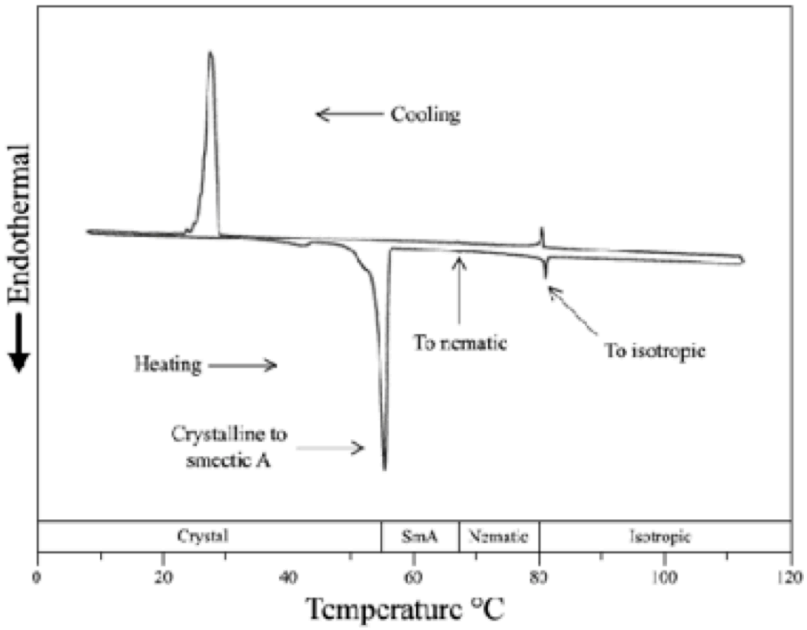

Figure 1.6. Basic representation of a DSC plot of a liquid crystal compound.

Differential scanning calorimetry (DSC) uses a method based on the thermal energy required to induce phase change. The instrument is calibrated against a standard; both internally and externally. The common external standard is indium, which has known values, indium (6.37mg, 20µL aluminium pan) enthalpy 28.51J g^{-1} and onset of the melting temperature of 156.5985°C. The common internal standard is gold. When a sample with liquid crystal properties is analysed, the increase in energy needed to overcome the phase transitions on heating is shown on the plot as a peak, on cooling it is shown as a negative peak, see Figure 1.6. The LC sample is heated at a uniform rate against an internal standard, under an inert atmosphere to stop oxidation of the sample under heating, see Figure 1.7. The LC sample and the gold reference sample are heated at a constant uniform rate, at the point of transition from the crystal to LC, and then the LC to isotropic, more energy is required to keep the heating of the LC sample and the gold internal sample is needed. This increase in energy is measured and outputted as a graph of temperature against energy, see Figure 1.6.

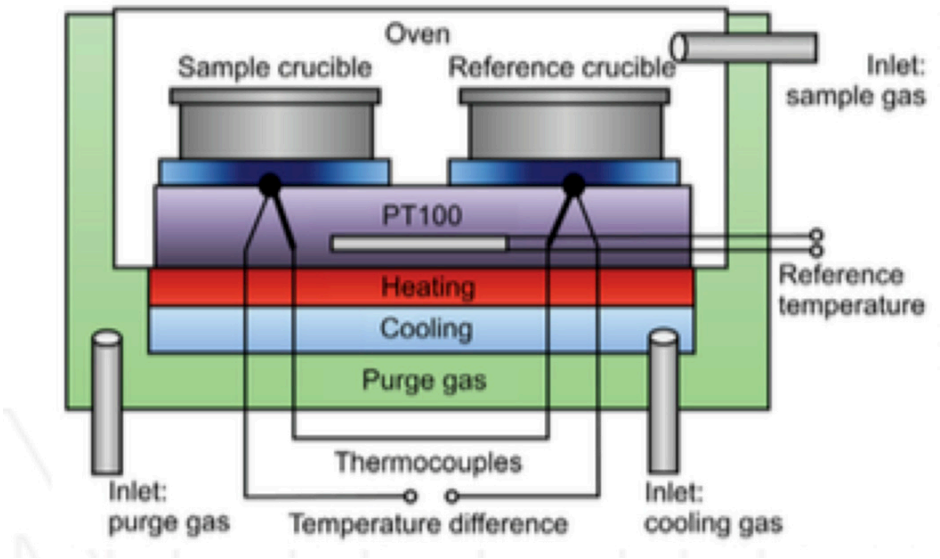

Figure 1.7. The internal workings of a differential scanning calorimeter.

This value is then compared with known literature values of smectic and nematic phase transitions to determine an unknown phase and confirm transitions observed by OPM. The LC phase can be further verified using XRD (X-ray diffraction), the sample is heated through the crystalline phase to the LC phase and the sample is exposed to a beam of X-rays. The sample scatters the X-rays and this pattern is recorded see Figure 1.8. This 2D pattern can then be translated into a 1D plot and analysed using Bragg's diffraction law: $n\lambda = 2dsin\theta$. The 1D plot is used to calculate the pseudo lattice associated with the reflection patterns.

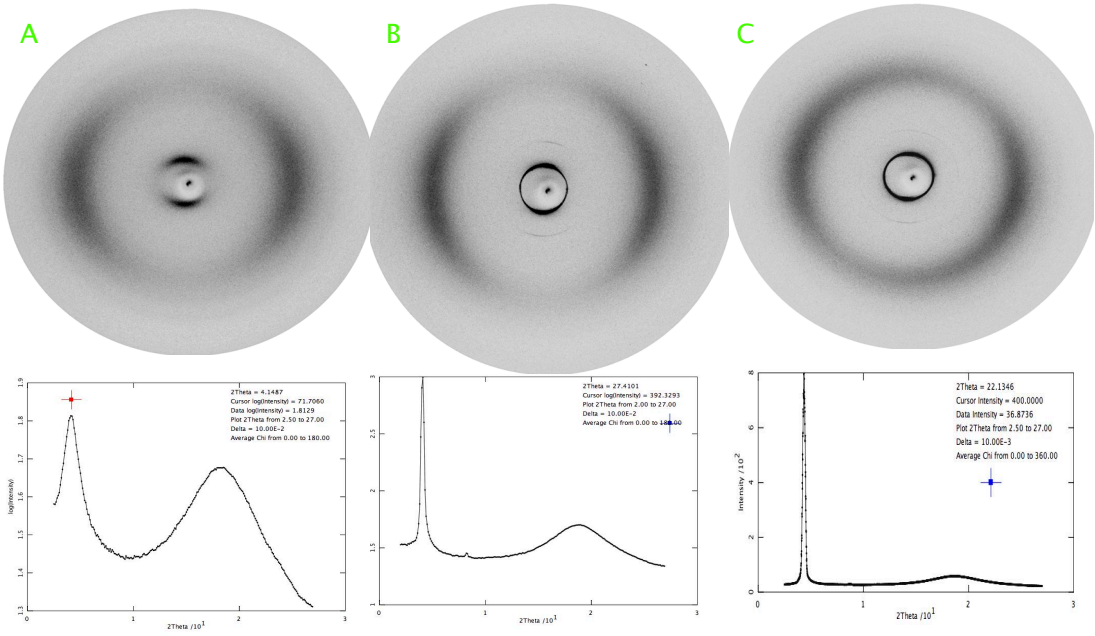

Figure 1.8. Examples of A = Nematic phase at 190°C, B = Smectic A phase at 166°C, C = Smectic C phase at 160°C.

The differences in the LC phases can be seen in the 1D and 2D diffractagrams obtained from XRD experiments. Figure 1.8 shows the 1D and 2D plots of a nematic phase, smectic A and smectic C respectively. The 2D plot of the nematic phase shows two reflections, one in the wide angle area (WAX) and one in the small angle (SAX). The reflections in the SAX region denote the overall average repeat units of the molecular lenghts of the molecule, due to the low positional and orientational order the reflections are diffuse. This is mirrored in the broadness of the 1D 2θ plots below the 2D scattering pattern see Figure 1.8. The second reflection is in the WAX area. This reflection is attributed to the lateral intermolecular distance of the mesogens in the LC phase. The second plot **B** is for the SmA phase. The SAX reflections of the SmA phase compared to the nematic phase are narrower and sharper. This is due to the increase in the order and the layers that are formed in the SmA phase, see Figure 1.3. The second section in the SmA reflections is the WAX reflection. This reflection, when compared to the nematic phase, is narrower and this is caused by the increase in the orientational order and positional order of the system. The increase in the positional and orientational order from the nematic phase to the SmA phase

can be seen in the narrowing and sharpening of the 1D 2θ plot.

The final reflection is of the SmC phase. This has a very similar reflection pattern to the SmA phase, with narrow reflection in the WAX and SAX areas because of the higher orientational and positional order in the LC phase. The tilt in the reflections is due to the tilt in the SmC mesophase, the degrees of tilt in the phase can be calculated from the tilt in the reflection. The narrowing of the WAX reflection can be attributed to the increase in the positional order of the system. This can also be seen in the 1D 2θ plot. The differences in the reflections between the phases can be used to back up the results from the OPM images of the LC texture and confirm the phase, or help to determine the LC phase structure when the OPM image is inconclusive.

References

(1) P. J. Collings and M. Hird, *Introduction to liquid crystals: chemistry and physics*, 1997.

(2) I. Dierking, *Textures of Liquid Crystals*, Wiley-VCH Verlag GmbH & Co. KGaA, Weinheim, Germany, 2003.

(3) P. Palffy-Muhoray, *Phys Today*, **60**, 54–60.

Chapter 2 Photochromism

2.1 Introduction to photochromism

Photochromism is a 'reversible transformation of a molecular entity between two forms, A and B, resulting in different absorption spectra, induced in one or both directions by absorption of electromagnetic radiation. The spectral change produced is typically, but not necessarily, of visible colour and is accompanied by differences in other physical properties.'[4] The first report of this effect was in 1867 by J. Fritzsche and studied more indepth by I. Frisch in 1988.[5] He observed the change in colour of a tetracene solution in the presence of air and light and then the reversible change with the exclusion of light. A similar effect was observed later on a painted gatepost which was black in the daylight and white at night (the paint was zinc based) by E. Ter Meer in 1876.[6] The main interest in these early years of the research on photochromism was the speed of the relaxation reaction from the irradiated coloured form back to the non-coloured ground state, as well as the degradation of the molecules. This early work led on to further investigation based around some of the key photochromic groups. These have been the basis of much photochromic research, due to their high resistance to photo-degradation and the tuneability of the effective wavelength of light and the speed of relaxation.

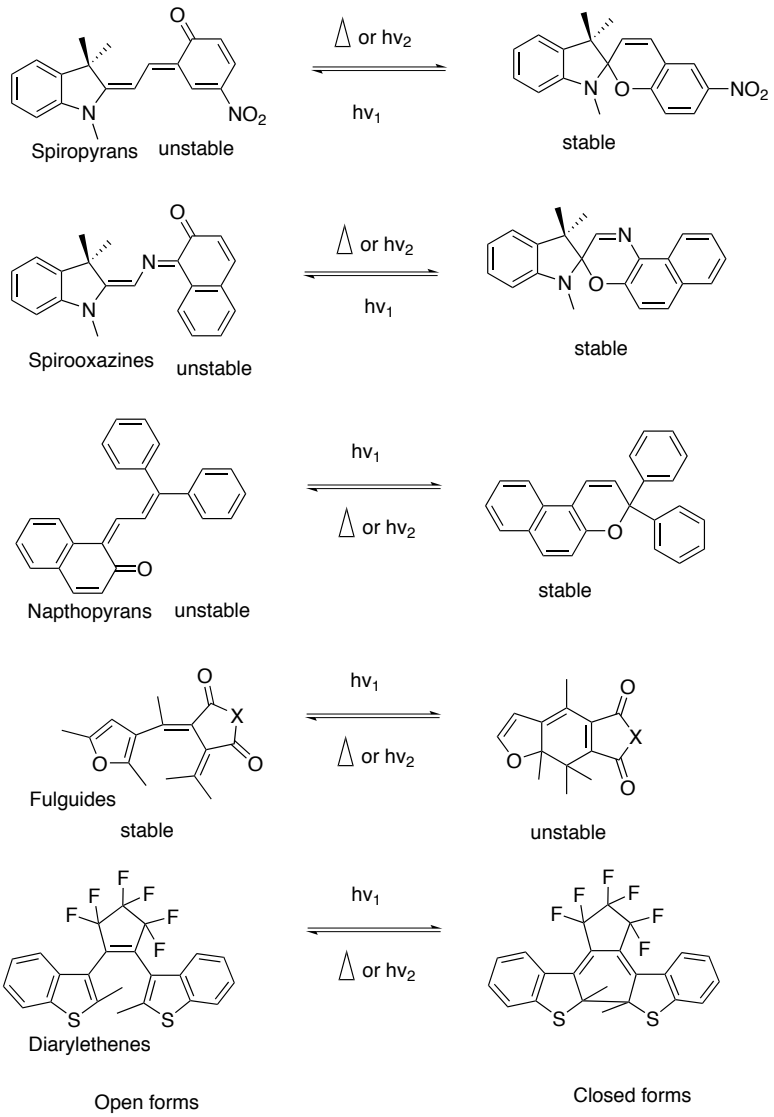

Figure 2.1. Example of the main groups of photochromic materials in open and closed form.

2.2 Main photochromic molecules and derivatives

The main groups of molecules that exhibit photochromic properties that will be discussed are spiropyrans, spirooxazines, chromenes (which are also known as naphthopyrans and benzopyrans), fulgides and diarylethenes, see Figure 2.2. The rate of relaxation, or thermal stability, is the rate at which the excited unstable photochromic compound switches back to the more stable confomer of the molecule.

The number of cycles of irradiation and then relaxation the specific molecule can withstand before any changes in the structure occur (leading to non-photochromic products) is known as the photostability. The stability of different groups can be altered by small changes in the structure of the molecule. For example going from benzopyrans to naphthopyrans will often cause a bathochromic shift (shift in the maximum of the absorption or transmittance to a longer wavelength). This can also be achieved by the introduction of aromatic rings in the 3 and 3' positions of the molecule of the hydrogens in ortho position with bulky groups. This has the effect of slowing the fade rate of the open form of the molecule and also causes a bathochromic shift.

Much work has been done with photochromic molecules; one of the most well known is with photoreactive lenses for spectacles, in optical devices, and data storage systems.[7,8] Here a photochromic group such as a derivative of the illustrated diarylethene[9] in Figure 2.1 is employed. This application uses the diarylethene derivative fully dispersed in a polymer matrix; this means it can be formed into different shapes and thin films easily. It also means that different derivatives of the diarlyethene can be dispersed in the matrix in a controlled fashion, thus creating a multi-colour changing material.[9] In more recent work with photoreactive contact lenses,[10] the polymer matrix that makes up the base of the contact lens is fabricated with channels in which a photoreactive dye is placed. This creates contact lenses that change colour when exposed to UV-light. Multi-coloured photochromic materials are made possible by the difference in the absorption of the individual photochromic groups such as naphthopyrans[11] and diarylethenes[12] groups of the photochromic molecules. Another factor that also aids the versatility of these compounds is the effect of changing the substituents on the 'backbone' of the molecule which in turn shifts the absorption of the mesogen.[13] An example of this is the combination of diarylethene with a naphthopyran, resulting in a biphotochromic system.[14]

The main photochromic molecules are split into two groups. One is where the closed form is the most stable form, see Figure 2.1. This is the case for the spiropyrans, spirooxazines, and the naphthopyrans. Here a weak bond proximal to a sp^3 hybridized carbon is broken under irradiation and a planar more conjugated and coloured yet thermodynamically unstable structure is generated. The diarylethenes and the fulgides on the other hand undergo [4+2] light mediated electrocyclisation

reaction.

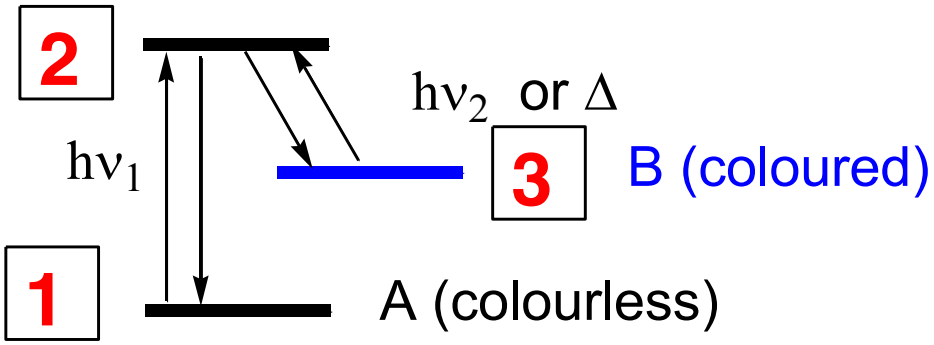

Figure 2.2. Simplified representation of the excitation of the photochromic material.

Photochromic molecules go through an excited state when exposed to light. When excited electrons move from the ground state **1** to the excited state **2**, they can either then relax to a lower state **3** which is coloured or return straight back to the ground state **1**.

2.3 Cleavage of HABI into two radicals.

The photochromic group that is of interest is based on 2,4,5-triphenylimidazole which was first reported in the 1950's. The 2,4,5-triphenylimidazole group (lophine) is unlike the other photochromic groups shown in, Figure 2.1. When irradiated the molecule splits from the dimer into two radicals, see Figure 2.3.

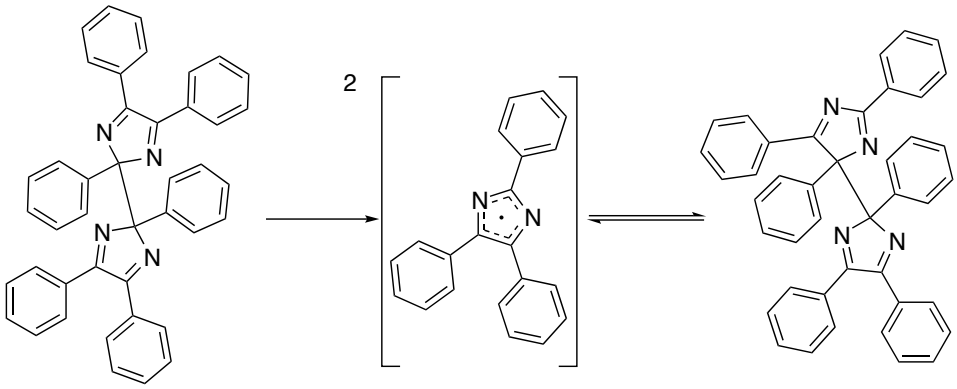

Figure 2.3. Radicalisation of imidazole dimer under irradiation and the formation of the more stable isomer.

Homolytic cleavage is the formation of two smaller molecules from the parent molecule, through the splitting of a pair of electrons between the two new species; this will always form a radical molecule. Free radical formation can lead to atomic or molecular species with unpaired electrons or an open shell configuration. The formation of radical species often means that they are highly reactive, which means they play a crucial role both in many chemical reactions and in industrial processes such as radical polymerisation, combustion, and biochemistry. They also have a role in atmospheric chemistry in the formation of ozone. In 1900, M. Gomberg, often referred to as the father of free radical chemistry, synthesised the first organic free radical in the form of triphenylmethyl (TPM), whilst trying to form the highly crowded hexaphenylethane. The triphenylmethane radical turned out to be hard to isolate due to the highly reactive free radical, instead it was isolated as the peroxide product. This discovery opened up the field of organic free radical chemistry.

Around 50 years after the start of free radical chemistry, an increase in interest in hexaarylbiimidazole (HABIs) and its properties as a free radical was shown through publications,[15,16] and patents at DuPont industries. The reason for this surge of interest in HABIs was the observation of a huge increase in the stability of the free radical compared to earlier TPM free radicals due to the oxygen sensitivity of TMP. Therefore the very short free radical half-life was of little interest in industry. However the increase in the stability of the radical to oxidation had may industrial uses for DuPont, for example: the potential uses of HABI as a photooxidant and as a photoinitiator for polymerisation reactions. The increase in the stability of the free

radical is due to the delocalisation of the free electron around the hetrocycle core of the HABIs.

This behaviour sparked a large amount of research into the altering of the properties of the HABIs and the speed at which they form a free radical when irradiated, and in turn the speed at which they return to the dimer. This also led to the tuning of the wavelength of light that causes the dissociation of the dimer. The altering of the speed of dissociation and of reassociation was shown to be related to the substituent; the position of the substituent on the aromatic rings, which can be seen in Figure 2.5. The subsitution also effected the position of the bond forming the dimer and with that the stability of the dimer. This was shown by work done in the 1970's by L.A.Cescon *et al.*[17] Their work showed that there were two main isomerisation products, see Scheme 2.1.

Species **54** isomer **1,2′** shown in Scheme 2.1 is the most stable of the two confomers and species **55** at higher temperatures converts back to species **53** and then in turn to the more stable form **54**. Species **55** shown in Scheme 2.1 can be isolated by splitting the dimer of species **54** at low temperatures and then allowing the association of the free radicals to form at this lowered temperature, this does not result in quantative formation of species **55**, but the yield is very close to this. The differences in points of attachment of the dimer was first proposed by D.M.White and H.Zimmerman in 1963[16] who suggested that there could be six possible dimer structures. These possible structures can be seen in Figure 2.4

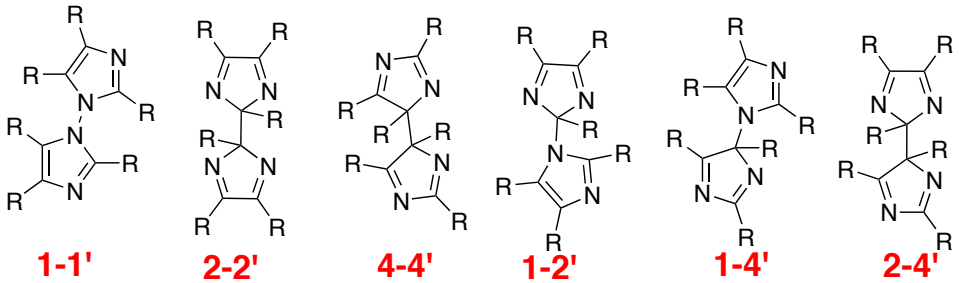

Figure 2.4. The six possible structures of hexaarybiimidazole.

The imidazole dimer is formed through oxidation of the monomer using ferrocyanate. Once the monomer has been oxidised the radical is formed, this is indicated by the appearance of an intense violet colour. This initial dimer is the piezochromic dimer

which has low stability, this means that when it is dissolved in benzene the formation of the intense violet colour indicates that the piezochromic dimer has dissociated and radicals have been formed. The reformation of the dimer from the radical in solution is discussed above. The reformed dimer was initially thought to be two isomers, **1,2′** and **4,4′** see Figure 2.4. This was explored by H.Tanino *et al*[18] who proposed (based on NMR data) that there was a third and fourth form of the imidazole dimer, see Scheme 2.2.

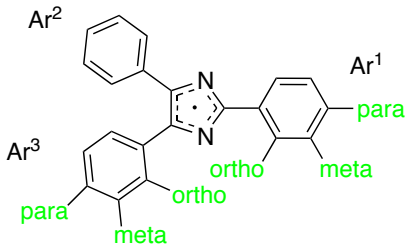

Figure 2.5. substitution on a HABI radical.

This work involving substitution in the *ortho*, *meta* and *para* positions on the aromatic rings demonstrated the effect of the substitution on the association and dissociation of the dimers and radicals. This effect was explored using chlorine to substitute in the *ortho* position on **Ar1**, see Figure 2.5. The chlorine in the *ortho* position has the largest effect on the dimer formation, when compared to the substitution of the *para* position on $\mathbf{Ar}^1$. The difference in effect of substitution between the *para* and the *ortho* positions was noticed for positions on $\mathbf{Ar}^2$ and $\mathbf{Ar}^3$, the effect of the the subsitution had a greater effect on the dimer formation in positions $\mathbf{Ar}^2$ and $\mathbf{Ar}^3$ than in $\mathbf{Ar}^1$. This trend was also observed for bromine and methoxy substitution, the rate was not noticeably altered by *meta* and *para* substitution.

This led to two hypotheses which were mainly investigated in the 1970's and 1980's. **Hypothosis A** stated that the substitution of the $\mathbf{Ar}^1$ resulted in an initially different isomer product. **Hypothesis B** stated that the destabilising effect of the ortho substituents was due to the inability of the radical to form a planar molecule. The planar form has been shown to stabilise the radical and as previously mentioned, results in an increase in delocalisation of the free radical and a lower transition state of **54**. These two hypotheses result in different products as the stable molecule and the processes are represented schematically in three charts, see Figure 2.6.

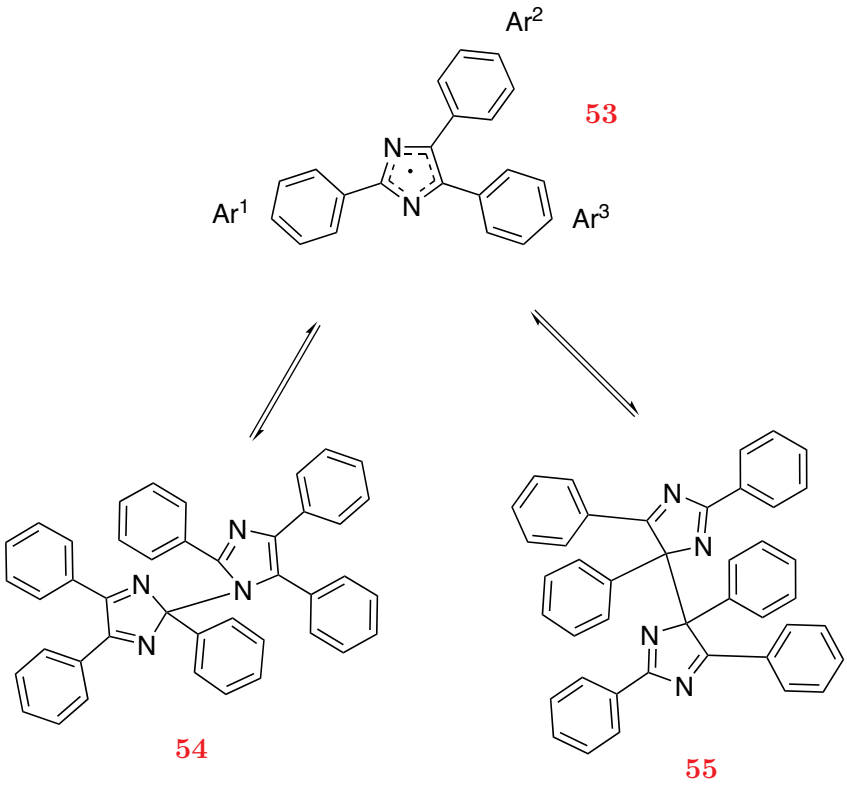

Scheme 2.1. Proposed HABI isomers L.A.Cescon *et al.*[19]

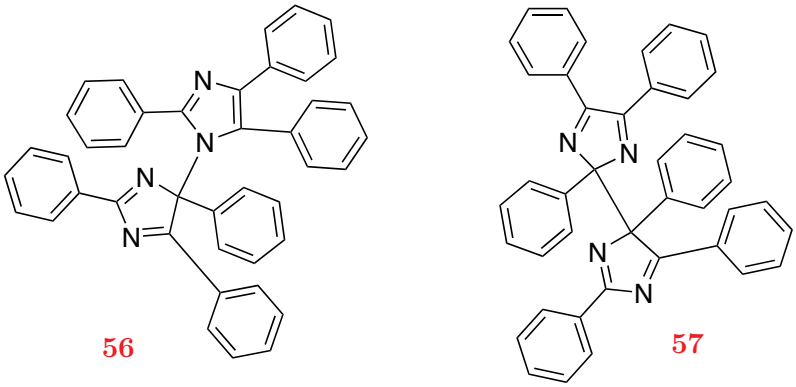

Scheme 2.2. Additional confomers proposed by H.Tanino *et al.*[18]

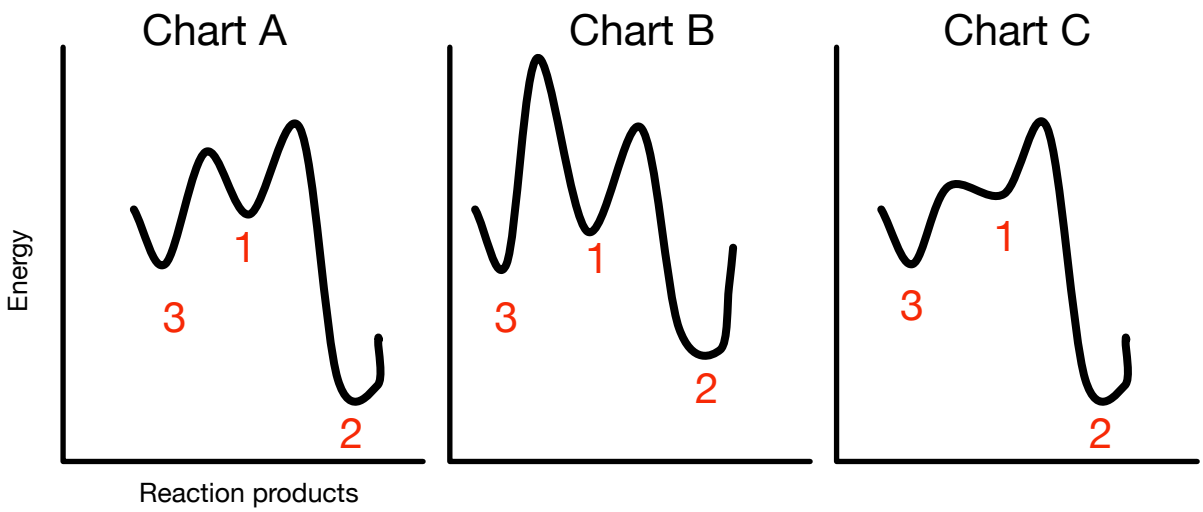

Figure 2.6. Depiction of energy diagrams for imidazole dimer association method with energy on the y axis, reaction coordinate x axis.

Figure 2.6 is a simplified depiction of the energy required to form the two different isomers **53** and **54** illustrated by Scheme 2.1.

The energy profile of the unsubstituted HABIs, see Figure 2.6, can be represented by **chart A**, this is true for both the hypotheses.[20] The example of ortho-chloro HABIs represented in **chart B** however, was not found to be supported by experimental results from the literature as this would show a precedent for the stabilisation of the coupling at the most hindered position when ortho-HABIs were involved. The hypothesis indicated that the reduction of the energy required to form **2** from **1** in preference of **3**. This can be seen by the reduction of the barrier from **1** to **2**, shown in Figure 2.6, **chart B**. This was shown to be not correct. This was based on and supported by the kinetic studies of the low temperature association of the same isomers form low temperature radicals.

Hypothesis **(B)** still fits the original **chart A** for the unsubstituted HABIs. Unlike hypothesis **(A)** which is in line with the reaction process outlined in **chart B** to represent the substituted HABI's, hypothesis **B** is in line with the results for the ortho-chloro subsituted HABIs in **chart C**. **Chart C** comforms with radical destabilisation due to the inability of the radical **53**, the ortho substituted rings to sit coplanar. Hypothesis **B** unlike **A** indicates the reduction of the energy barrier going from **53** to **55** thus making this the favoured association product. This conclusion

was supported by X-ray crystallography as the restriction of rotation due to the presence of the ortho group which does not allow **53** and the heterocyclic core to sit coplanar. The conclusion drawn from these studies is that the introduction of ortho substitution on **Ar1** alters the dimer state in favour of **55** as it has the lowest energy barrier as represented in chart **A**.

With further modeling it was also shown that unsubstituted HABIs **53** do sit coplanar to the heterocylic core and that **54** and **55** cannot simultaneously be coplanar with the core. Furthermore, there is no appreciable gain of resonance stabilisation of the dimer or radical species from **54** and **55**. The kinetics of the equilibria show that the ortho substitution at these points is not greatly effected.[17]

There has been much discussion on the correct form of the dimer that recombines upon relaxation of the molecule, notably by H. Tanino[18] and over the years many others.[10,15,21] More recently this has been investigated by J.Abe *et al.*[22] This more recent work supports the earlier theories and observations. Building upon previous work undertaken on the alteration of the dissociation and recombination speed there has been revitalised interest in HABIs and the possibileties to alter the dissociation and recombination speed through substitution[23] or using magnetic fields.[24] The earlier work was improved upon by the incorporation of naphthalene backbones.[23] it was found that the speed of the thermal relaxation of the radical back to the dimer is dramatically reduced. This improvement of the association speed has led to further alterations in structure through increased conjugation and the introduction of greater steric crowding.[25] This can lead to what is known as negative photochromism, which is the reversible loss of colour upon irradiation and then the formation of colour with the exclusion of light or thermally. An example of this negative photochromisum induced by the increase in conjugation and steric crowding can be seen in Figure 2.7

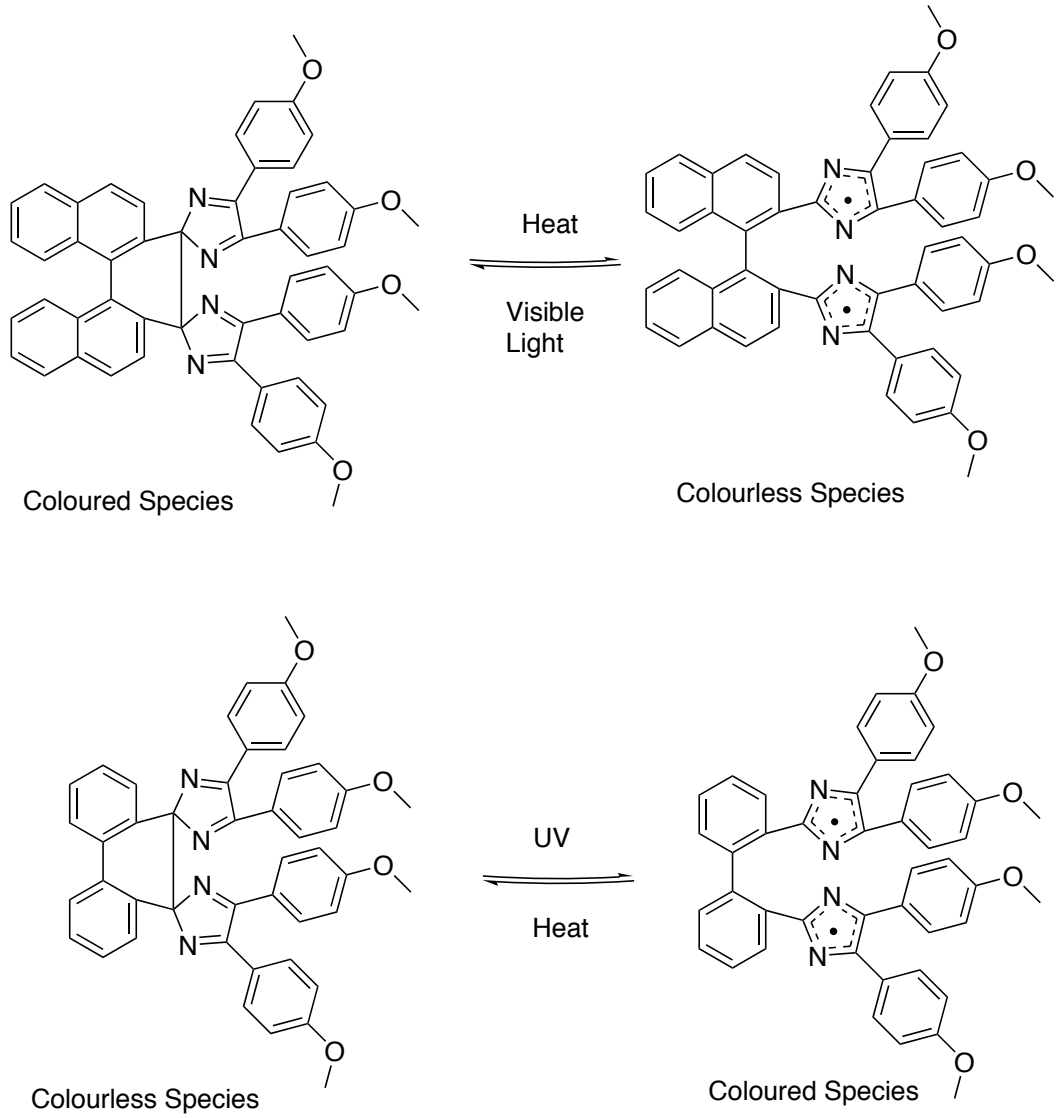

Figure 2.7. An example of negative photochromisum unduced through steric hinderance and increased conjugation compaired to the similar HABI derivative.[25]

The restriction of the mobility of the free radicals has been shown to lead to an increase in association speed. This was shown by the introduction of a naphthalene bridge[23] shown in Figure 2.8, this shows two possible methods of restricting the movement of the HABI radicals. It has however also been observed that through altering this method of restriction, the isomer of the dimer that is formed after dissociation can change from the previously mentioned naphthalene bridged materials. This is a 1,2'-isomer,[23] but with the addition of a second ring on the bridging unit to form 1-phenylnaphathlene shown in Figure 2.8, the number of other isomers that HABIs

can form are increased.[26] The increase in the possible number of confomers formed created a multistate photochromic bridged HABI derivative. Further effects on the association speed were investigated, primarily the effect of increased pressure, as it is known that increasing the pressure in a reaction causes the reaction to progress faster.

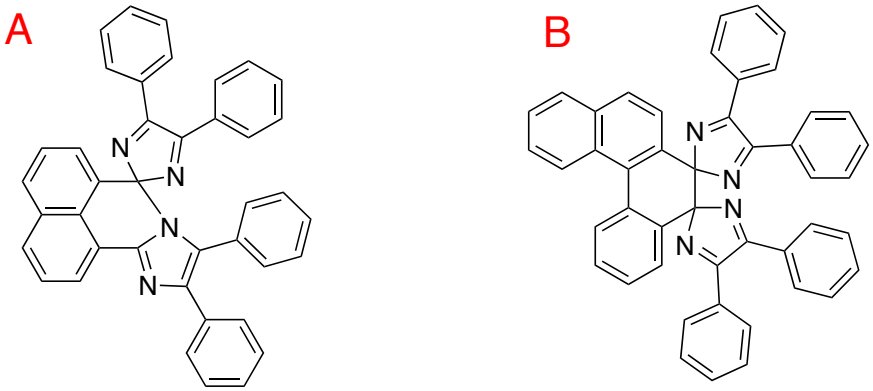

Figure 2.8. A= Naphathlene bridged HABI,[27] B= 1-phenylnaphathlene bridged HABI.[26]

This principle was applied to the association of free radicals.[28] The results show a dramatic increase in speed with the increase in pressure form 0.1MPa to 400MPa. Finally, there has been interest in improving the fatigue resistance of the HABIs, as like all free radicals they can react with anything reactive in their vicinity. This is the reason they are good radical initiators for polymerisation reactions. This was achieved by changing one of the imidazole radicals with $4H$-cyclohexadienone ring. The two radical species are linked using an aromatic ring. This compound and its derivatives show higher fatigue resistance and improved performance when inserted into a polymer matrix, when compaired to the original HABI material. The speed and the colour of the irradiated form can be altered as well through the functionalisation of the $4H$-cyclohexadienone ring.[29]

2.4 *Cis-Trans* Isomerisation

The main photochromic molecule that undergoes cis-trans isomerization is the azobenzene group. Azobenzene was first reported by E. Mitscherlich[30,31] in 1834, it has been used in many dyes due to its ability to alter the absorption through altering

the functionalisation. The original synthesis of the azobenzene was carried out by the formation of a diazonium salt from aniline.

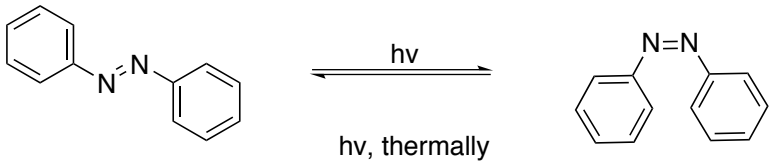

Figure 2.9. *cis-trans* Isomerisation of azobenzene.

There has been a large body of work concerning the synthesis of the azo link, see Figure 2.9.[32,33] The most simple form of the azobenzene that can be formed is due to the coupling of aniline and phenol to form aniline yellow. The reaction proceeds via a diazomiun salt formation and the homocoupling of aniline derivatives through oxidative dimerization.[34,35] The reaction of aniline and nitrobenzene also leads to the same product via the formation of a nitroso intermediate. Many different reagents and reaction conditions have been explored for the formation of the azo link.

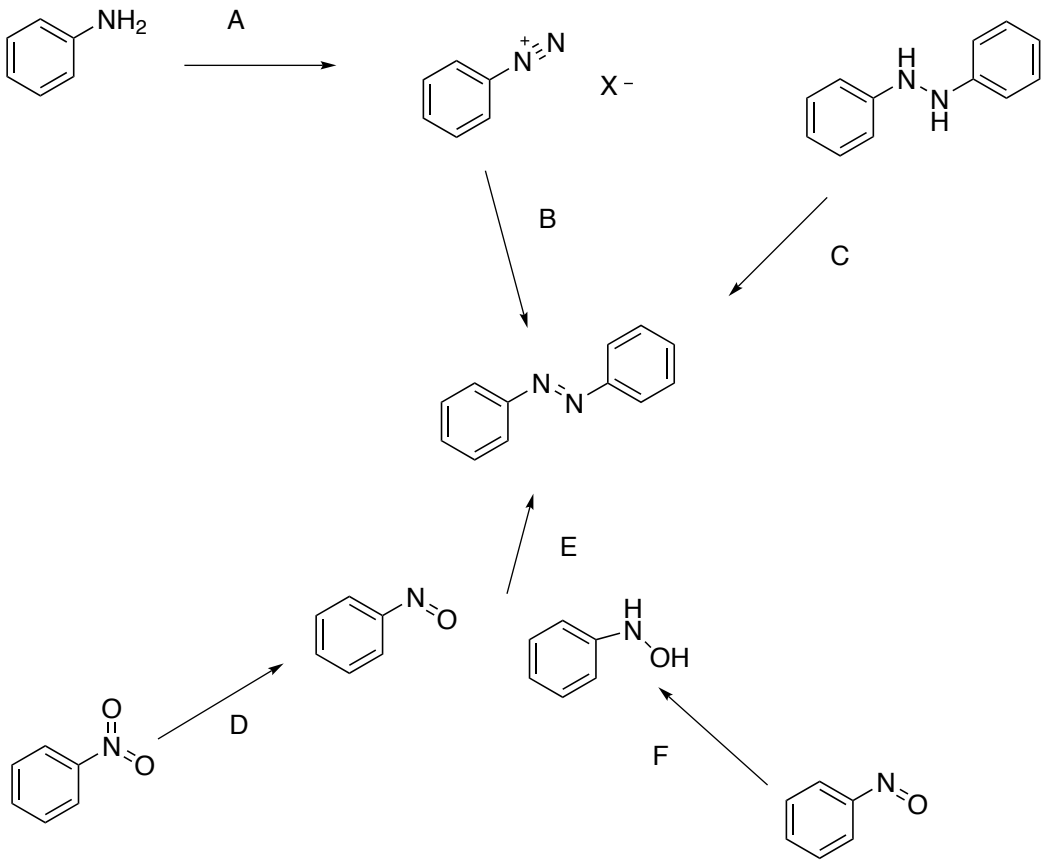

Figure 2.10. Classical methods for the synthesis of azobenzenes.

Considering the extensive knowledge gained over the 150 years this group has been known, investigations into azo compounds is still a surprisingly active research area. The use of metal catalysts such as bismuth[36] or titanium (0)[37] has been investigated. The problem with using these materials is their cost and their toxicity. For the azo coupling there has been interest in using more common and less toxic reagents such as tin chloride[38] and copper (I) oxide.[39] Using copper (I) oxide has been reported to show increased yields on highly substituted materials, due to the mild reaction conditions favorable to molecules with poor stability in harsh environments, when compared to the more traditional methods.[40] A large amount of research has focused on the optimization of the properties of azobenzenes. Beyond dyes there is a wide

range of applications reported for substituted azobenzenes in polymers, including materials where the *cis-tans* isomerization of the azo group causes a growth and shrinkage of a film and the uptake of molecules.[41] There are also applications in biological systems, an example is the control of the gliding mobility of microtubuals by the introduction of an azobenzene molecule in the supporting layer.[42] The reason for the high interest in azobenzene and its derivatives is the stability of the compound under multiple and long term irradiation relaxation cycles, there is very limited fatigue and no side products are produced. The limitation of azobenzene derivatives is that the stable conformer is the *trans* form and the *cis* form is relatively unstable which can limit the uses and applications. The stability of the cis confomer can be improved through substitution of the aromatic ring with sterically bulky groups, the addition of electron withdrawing groups can also effect the stability of the *cis* isomer.

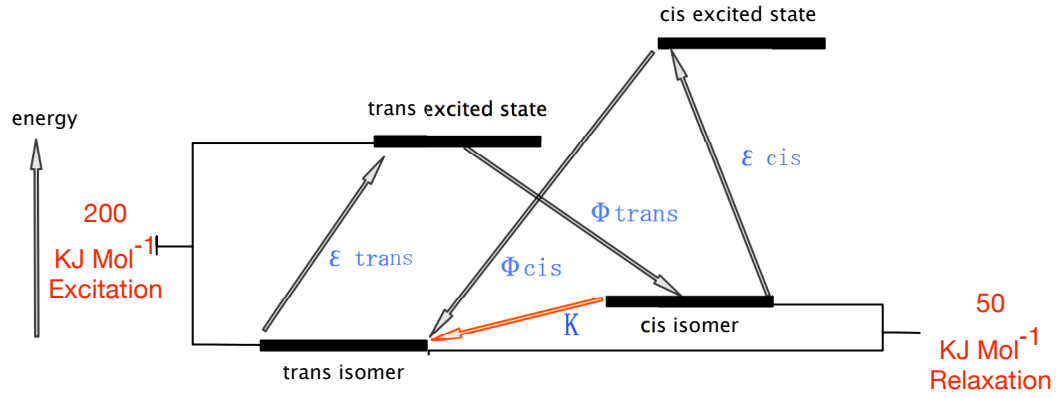

Figure 2.11. Simplified excitation and relaxation model for azobenzene with ϵ denoting the extinction coefficient and Φ the photoisomerisation quantum Yields.[43]

As illustrated by Figure 2.11. Irradiation of the ground state *trans* isomer of azobenzene results in isomerisation through the excited state where the double bond is broken. The molecules rotate to the **cis**-confomer, the double bond reforms giving the *cis* isomer. This excitation of the *trans* will not always form the cis confomer but it can relax back to the ground state. The amount of isomerisation is dependent on Φ the photoisomerisation quantum yields. The thermal relaxation barrier K, for this reaction, see Figure 2.11, is very low, which means this process is fast and the *cis* form is less stable. Altering this value K, the energy required for the thermal

relaxation, through functionalisation and *fixing* the geometry, where the molecule is forced into the *cis* confomer is possible through the introduction of a linking unit. The length of this linking unit denotes the effect on stability,[44] this can be further expanded by linking two azobenzene moeties using linkers of different lengths.[45] The downside to the stabilisation of the *cis* form through functionalisation or *fixing* can be the reduction of the photoisomerisation quantum yields of the *trans* to *cis* transformation.

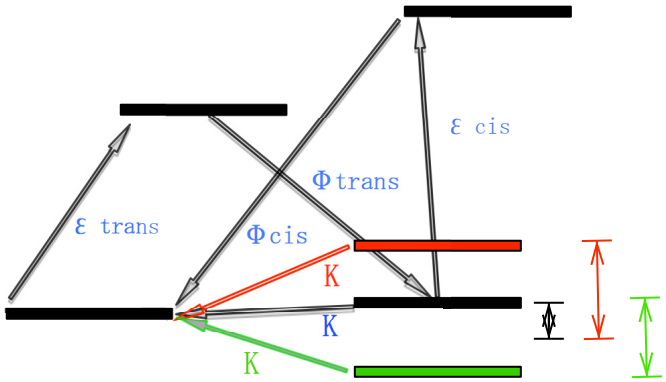

Figure 2.12. Simplified excitation and relaxation model for azobenzene with ϵ denoting the extinction coefficient and Φ the photoisomerisation quantum yields.[43] The red indicting the basic azobenzene, black to represent the functionalised azobenezene, the green representing a *fixed* azobenzene.

With the functionalisation of the azobenzene, see Figure 2.12, the **K** barrier is reduced which stabilises the *cis* form. The introduction of a *fixed* (see Figure 2.13) component to the azobenzene will further reduce the K barrier below that of the *trans* form. The lower the K barrier, the higher the stability of the *cis* isomer. There is a linear correlation to the length of the *fixing* unit.[44,45] With further reduction in the length of the bridging hydrocarbon chain, see Figure 2.13, the predominant form becomes the *cis* isomer.

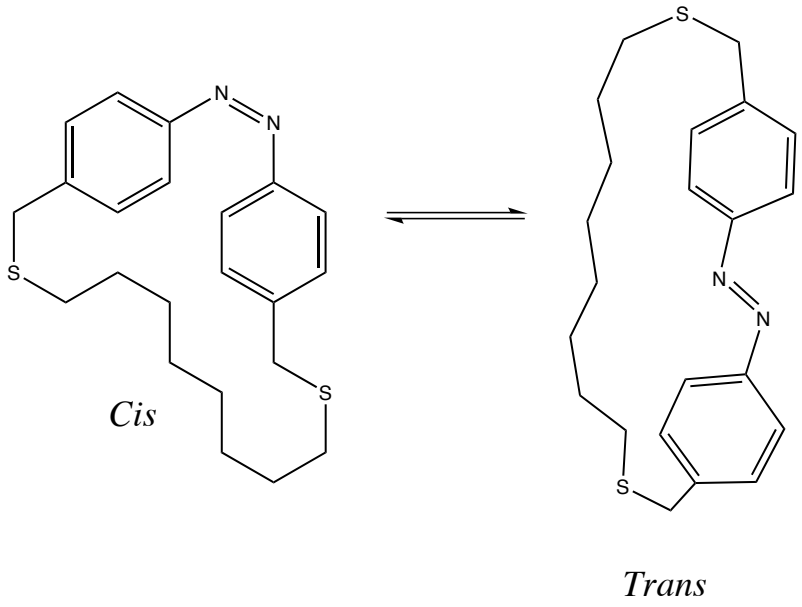

Figure 2.13. *Fixed* azobenzene using C7 hydrocarbon chain.

In the 1960s W. W. Paudler and A. G. Zeiler[46] published work on a bridged azobenzene often referred to as diazocine, where the most stable confomer is in the *cis* form. This result showed the potential to open up new applications, see Figure 2.15. The reported materials were difficult to synthesise. Since then there has been little work involving the azocine molecule; the properties were characterised in more detail in 2009 by Herges *et al*[47] **58** shown in Figure 2.14. Investigation of the azocine molecule has progressed from the 1960s due to the work done by Herges *et al* focused on a more viable method for the formation of the azo link. This group reported a method using the oxidative-reductive capabilities of D-glucose in the presence of a base to form the azo link. They reported diazocine derivatives which are functionalised symmetrically[48] **60** and non-symmetrically[49] **59**, see Figure 2.14.

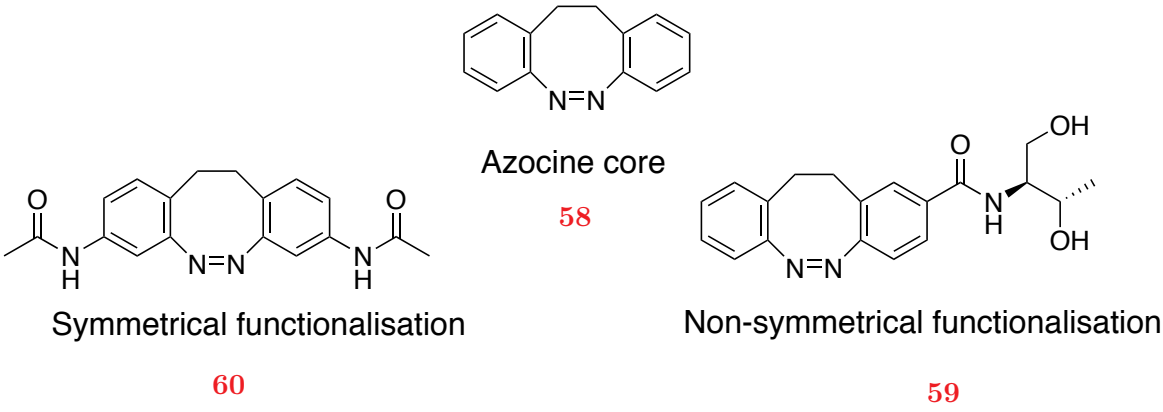

Figure 2.14. 58 Original material, 60 Symmetrical substitution,[48] 59 non-symmetrical substitution.[49]

The combination of the azobenzene moiety with liquid crystal mesogens has been investigated. One such area is the induction of a phase change by using the azobenzene as a dopent added to the LC mesogens,[50] or as a single photochromic LC mesogen.[51] The combination of the bridged azobenzene with LC moieties has yet to be explored. Here, the aim is that the cis form will be in the isotropic phase and, upon irradiation and the isomerization, to the trans form there will be a change to a liquid crystal phase.

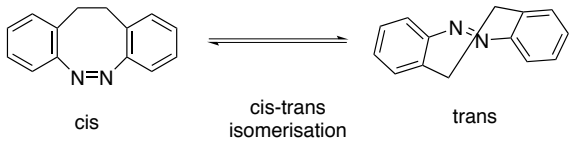

Figure 2.15. *Cis-trans* isomerisation of Diazocine molecule

The combination of photochromic molecules with LC mesogens is relatively unexplored. There has been some work in the combination of napthopyrans[52] with cyanobiphenyl LC mesogens. Related work has been carried out on the diarylethenes[53] and the combination with LC mesogenic group based on the cyanobiphenyl moiety. There has also been work using the photochromic molecule to induce LC phases.[54]

2.5 UV-Vis measurements of photochromic materials

UV-Vis (ultraviolet-visible) spectroscopy works on the principle that each molecule has a different absorption or transmittance based on the structure. The sample is irradiated with a wide range light source, typically a mercury vapour lamp or a xenon flash lamp. The light is monochromated using a prism and once the light is split into the components it passes through an exit slit, this filters off the other wavelengths and lets only specific ones through to irradiate the sample. The absorbance or the transmittance is recorded by a detector.

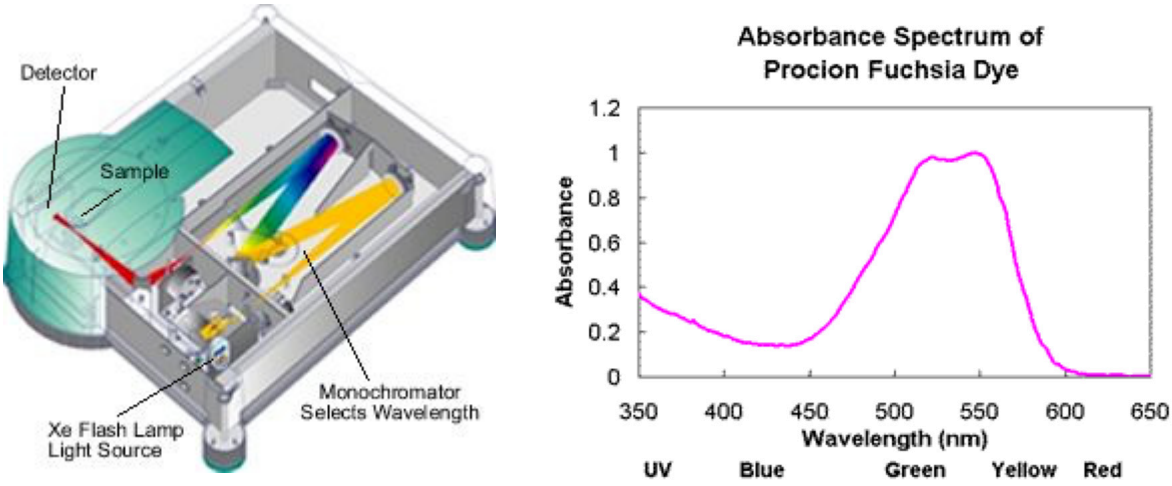

Figure 2.16. Left depiction of the internal arrangement of the Varian Carry 50. Right: the absorbance spectrum of procion fuchsia dye in solution.

The sample is irradiated by each of the wavelengths ranging from ultraviolet (110nm) to near infrared (900nm). This can be used to produce a spectrum. The higher the conjugation the greater the red shift of the spectrum. For molecular absorbance spectroscopy a sample is irradiated over the full range of the spectrum, the light that is absorbed by the sample is indicated by the peaks in the spectrum, see Figure 2.16, and the transmitted light by the troughs. The peaks (absorbance) occur where the molecule absorbs the light. This is linked to the excitation of the correct amount of energy required to excite electrons from the ground state to the higher energy levels,

see Figure 2.17. The transmittance (T) is defined as the ratio of P_o/P the power of the incident light and the power of the incident light after passing through the sample. The absorbance **A** is equal to $-log(P_o/\mathrm{P})$. Therefore the absorbance **A** is directly linked to the amount of energy required for the excitation of electrons. This absorbance can be altered by the chemical structure of the irradiated compounds structure as this changes the energy required for the excitation, see Figure 2.18.

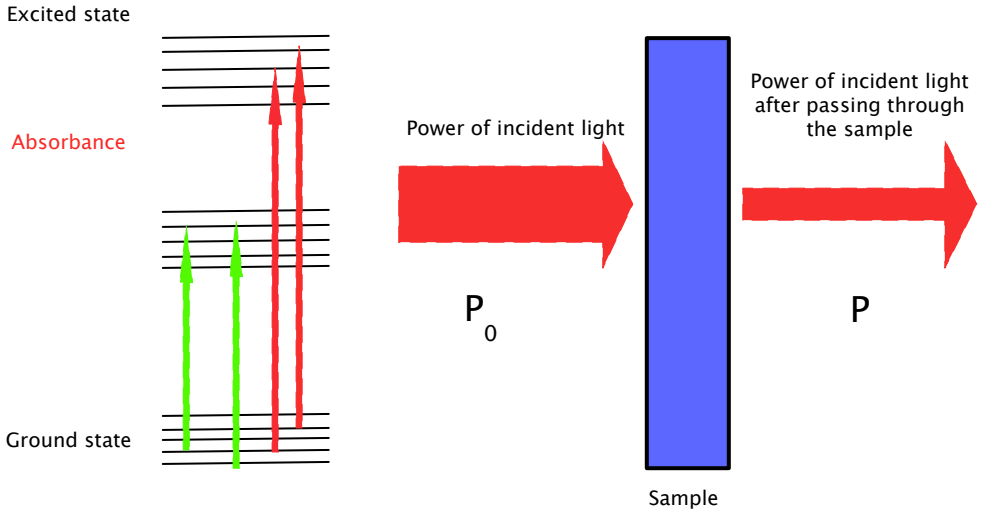

Figure 2.17. Left Simplified diagram of the excitation of electrons from the ground state to excited and the absorbance. Right correlation of P_O and P.

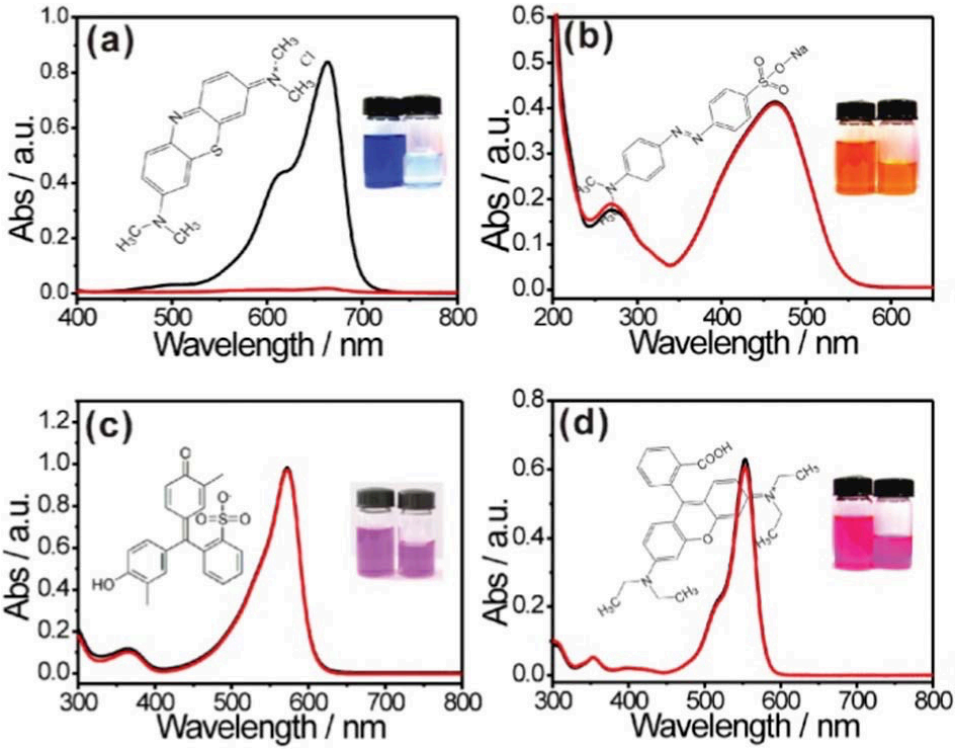

Figure 2.18. Examples of the alterations of the structure of a molecule leading to a shift in the absorbance.[55]

2.5.1 UV-Vis instrumentation modification

The standard form of irradiation of photochromic samples is via a broad range mercury vapour bulb or tungsten lamp. This broad light source is then monochromated via a grating or prism and split into the component wavelengths. The monochromated light then passes through a fibre optic cable to the sample. The main experimental issue related to this method is the low power of irradiation at a given wavlength. Though the initial power output of a typical light bulb is around 40W. After passing through the monochromator and the selection of the individual wavelength, there is a reduction of a factor of 100 of the power in the middle of the range (400nm-550nm) of the spectrum and even more in the low UV region (<400nm) and close to the near IR (>550nm).

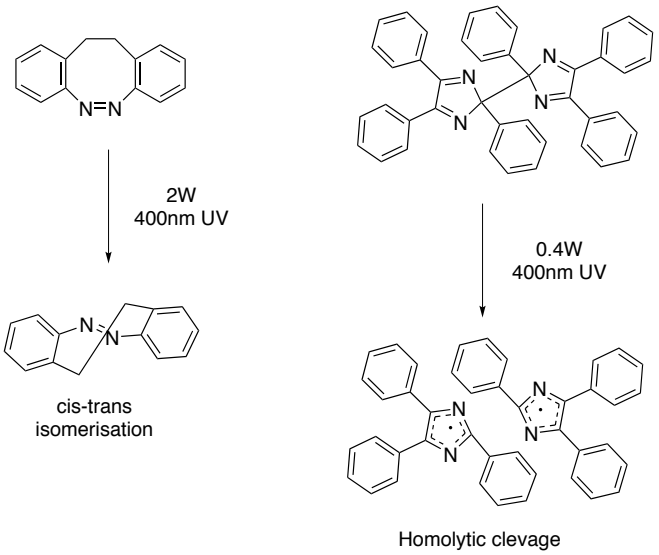

Figure 2.19. The representation of the estimated difference in power needed for the *cis-trans* isomerisation of the diazocine compared to the power needed for homolytic cleavage of HABI. Wavelength 400nm, diazocine value known for LED 1A, 14V, HABI value estimation based on 40W source lamp.

This type of irradiation is powerful enough for the imidazole dimers to cause the radicalisation upon irradiation. When diazocines where investigated it became apparent that the use of monochromated light from a 40W XeHg lamp was not sufficient, see Figure 2.19. The isomerisation of a referance material required a stronger source of irradiation. This became apparent with use of the diazocine reference material, after comparing to the orginal work by Herges *et al*[47] The solution to this problem was the use of LEDs. The power output of the LEDs can be tuned from 600mW to 12W. The UV-Vis spectrophotometer was modified to accommodate the LED and the heat sink. The power of the LEDs was controlled using a power pack (Tenma 30V, 3A) where the current and voltage can be controlled and altered to ajust for the different LED light sources. There is no loss from the monochromation of the light source as the LED's operate at a specific wavelength eg. 365nm, 400nm, 430nm, 450nm, and 500nm with a spectral spread of 10nm. After the collection of the absorbance of the sample in the ground state before irradiation, using the data the correct LED can be chosen and the sample can be irradiated.

2.6 Objectives of the project

The main objective of the project was to design, synthesise, and investigate new photochromic liquid crystals. The first target was the functionalisation of the HABI core. This was to be achived by decoupling the HABI core from the LC mesogen using a range of spacers of varying structures. The photochromic and liquid crystal properties were to be investigated by UV-Vis spectroscopy, DSC, OPM and XRD studies. Correlations between the designed structure and the photochromic and liquid crystal properties where to be made. Additionally the design, synthesis, and functionalisation of a diazocine core with LC mesogens was to be investigated for the LC properties.

References

(4) S. E. Braslavsky, *Pure Appl Chem*, 2007, **79**, 293–465.

(5) F. Fages, J.-P. Desvergne, I. Frisch and H. Bouas-Laurent, *J. Chem. Soc., Chem. Commun.*, 1988, 1413–1415.

(6) E. ter Meer, *Justus Liebigs Ann Chem.*, 1876, **181**, 1–22.

(7) W. Geng, S. Cui and S. Pu, Adv. Mat. Rev. Trans Tech Publications, 2012, pp. 109–112.

(8) Y. Hirshberg, *J. Am. Chem. Soc.*, 1956, **78**, 2304–2312.

(9) H. Nishi, T. Namari and S. Kobatake, *J. Mater. Chem.*, 2011, **21**, 17249–17258.

(10) K. Maeda, in *Processes in Photoreactive Polymers*, Springer US, Boston, MA, 1995, pp. 90–110.

(11) S. Delbaere, G. Vermeersch, M. Frigoli and G. H. Mehl, *Org Lett*, 2010, **12**, 4090–4093.

(12) A. Perrier, F. Maurel and D. Jacquemin, *Acc. Chem. Res.*, 2012, **45**, 1173–1182.

(13) G. Liu, S. Pu and R. Wang, *Org Lett*, 2013, **15**, 980–983.

(14) S. Delbaere, G. Vermeersch, M. Frigoli and G. H. Mehl, *Org. Lett.*, 2006, **8**, 4931–4934.

(15) B. S. Tanaseichuk, *Chem Heterocycl Compd*, 1972, **8**, 1173–1180.

(16) H. Baumgärtel and H. Zimmermann, *Z. Naturforsch. B Chem. Sci.*, 1963, **18**, 406–412.

(17) G. R. Coraor, L. A. Cescon, R. Dessauer, E. F. Silversmith and E. J. Urban, *J. Org. Chem.*, 1971, **36**, 2262–2267.

(18) H. Tanino, T. Kondo, K. Okada and T. Goto, *Bull. Chem. Soc. Jap*, 1972, **45**, 1474–1480.

(19) L. A. Cescon and R. Dessauer, US Pat. 358 503 8A, 1971.

(20) D. M. White and J. Sonnenberg, *J. Am. Chem. Soc.*, 1966, **88**, 3825–3829.

(21) Y. Zhou, W. E. Baker, P. M. Kazmaier and E. Buncel, *Can. J. Chem*, 2011, **76**, 884–895.

(22) S. Delbaere, M. Orio, J. Berthet, M. Sliwa, S. Hatano and J. Abe, *Chem. Commun.*, 2013, **49**, 5841–5843.

(23) Y. Harada, S. Hatano, A. Kimoto and J. Abe, *J. Phys. Chem. Lett.*, 2010, **1**, 1112–1115.

(24) H. Sato, K. Kasatani and S. Murakami, *Chem. Phys. Lett*, 1988, **151**, 97–101.

(25) S. Hatano, T. Horino, A. Tokita, T. Oshima and J. Abe, *J. Am. Chem. Soc.*, 2013, **135**, 3164–3172.

(26) T. Yamaguchi, S. Hatano and J. Abe, *J Phys Chem A*, 2014, **118**, 134–143.

(27) K. Fujita, S. Hatano, D. Kato and J. Abe, *Org Lett*, 2008, **10**, 3105–3108.

(28) K. Mutoh and J. Abe, *Phys. Chem. Ch. Ph.*, 2014, **16**, 17537–17540.

(29) H. Yamashita, T. Ikezawa, Y. Kobayashi and J. Abe, *J Am Chem Soc*, 2015, **137**, 4952–4955.

(30) E. Mitscherlich, *Ann. Pharm.*, 1834, **12**, 311–314.

(31) E. Merino and M. Ribagorda, *Beilstein J. Org. Chem*, July 2012, **8**, 1071–1090.

(32) H. M. D. Bandara and S. C. Burdette, *Chem. Soc. Rev.*, 2012, **41**, 1809–1825.

(33) A. Goulet-Hanssens and C. J. Barrett, *J. Photochem. Photobiol. C*, 2014, **294**, 62–67.

(34) Á. Georgiádes, S. B. Ötvös and F. Fülöp, *ACS Sustainable Chem. Eng.*, 2015, **3**, 3388–3397.

(35) S. Okumura, C.-H. Lin, Y. Takeda and S. Minakata, *J. Org. Chem.*, 2013, **78**, 12090–12105.

(36) S. Wada, M. Urano and H. Suzuki, *J. Org. Chem.*, 2002, **67**, 8254–8257.

(37) M. Malinowski, *J. Prakt. Chem.*, 1988, **330**, 811–813.

(38) L. Racané, H. Čičak, Z. Mihalić, G. Karminski-Zamola and V. Tralić-Kulenović, *Tetrahedron*, 2011, **67**, 2760–2767.

(39) J. Wang, J. He, C. Zhi, B. Luo, X. Li, Y. Pan, X. Cao and H. Gu, *RSC Adv.*, Apr. 2014.

(40) X. A Zhang, H. Zhao, Y. Gao, J. Tong, L. Shan, Y. Chen, S. Zhang, A. Qin, J. Z. Sun and B. Z. Tang, *Polymer*, 2011, **52**, 5290–5301.

(41) Y. Hayata, S. Nagano, Y. Takeoka and T. Seki, *ACS Macro Letters*, 2012, **1**, 1357–1361.

(42) M. K. A. Rahim, T. Fukaminato, T. Kamei and N. Tamaoki, *Langmuir*, 2011, **27**, 10347–10350.

(43) K. G. Yager and C. J. Barrett, *J. Photochem. Photobiol. C*, 2006, **182**, 250–261.

(44) U. Funke and H.-F. Grützmacher, *Tetrahedron*, 1987, **43**, 3787–3795.

(45) Y. Norikane, K. Kitamoto and N. Tamaoki, *J. Org. Chem.*, 2003, **68**, 8291–8304.

(46) W. W. Paudler and A. G. Zeiler, *J. Org. Chem.*, 1969, **34**, 3237–3239.

(47) R. Siewertsen, H. Neumann, B. Buchheim-Stehn, R. Herges, C. Näther, F. Renth and F. Temps, *J. Am. Chem. Soc.*, 2009, **131**, 15594–15595.

(48) H. Sell, C. Näther and R. Herges, *Beilstein J. Org. Chem.*, 2013, **9**, 1–7.

(49) D. K. Joshi, M. J. Mitchell, D. Bruce, A. J. Lough and H. Yan, *Tetrahedron*, 2012, **68**, 8670–8676.

(50) C. H. Legge and G. R. Mitchell, *J Phys. D Appl. Phys.*, 1992, **25**, 492–499.

(51) A. Sobolewska, S. Bartkiewicz, J. Mysliwiec and K. D. Singer, *J. Mater. Chem. C*, 2014.

(52) M. Frigoli and G. H. Mehl, *Chem. Commun. (Camb.)*, 2004, 2040–2041.

(53) M. Frigoli and G. H. Mehl, *Chem. Commun. (Camb.)*, 2004, 818–819.

(54) T. Kosa, L. Sukhomlinova, L. Su, B. Taheri, T. J. White and T. J. Bunning, *Nature*, 2012, **485**, 347–349.

(55) S. Xie, B. Zheng, Q. Kuang, X. Wang, Z. Xie and L. Zheng, *Cryst. Eng. Comm*, 2012, **14**, 7715–6.

Chapter 3 Imidazole

3.1 Imidazole - previous work and background

The use of single molecule LC photochromic mesogens is a rather under-investigated area with the majority of the work limited to diarylethenes[53,56] and naphthopyrans,[52,54] and the combination of these to form biphotochromic systems.[11,14,57,58] Derivatives of the compounds have been explored to induce rigidity and conjugation to the system upon irradiation. Most of the work on LC photochromes relates to the manipulation of liquid crystal side chain polymers, where some of the side chains bear photochromic groups. These materials would be LC-photochrome co-polymers. Surprisingly the 2,4,5-triphenylimidazole has not been considered in this single molecule structure. The single molecule structure refers to the combination of the photochromic mesogen with the LC mesogen, rather than the use of LC mesogen or photochromic dopants to mixtures. The synthesis and properties of imidazoles and its derivatives is well known and widely investigated but only for the photochromic properties. The majority of the recent work has been carried out by J. Abe *et al.*[22,23,27,59] This group have functionalised the referance imidazole core shown here in Figure 3.1 with different derivatives to increase the relaxation from the radical state to the dimer.[17]

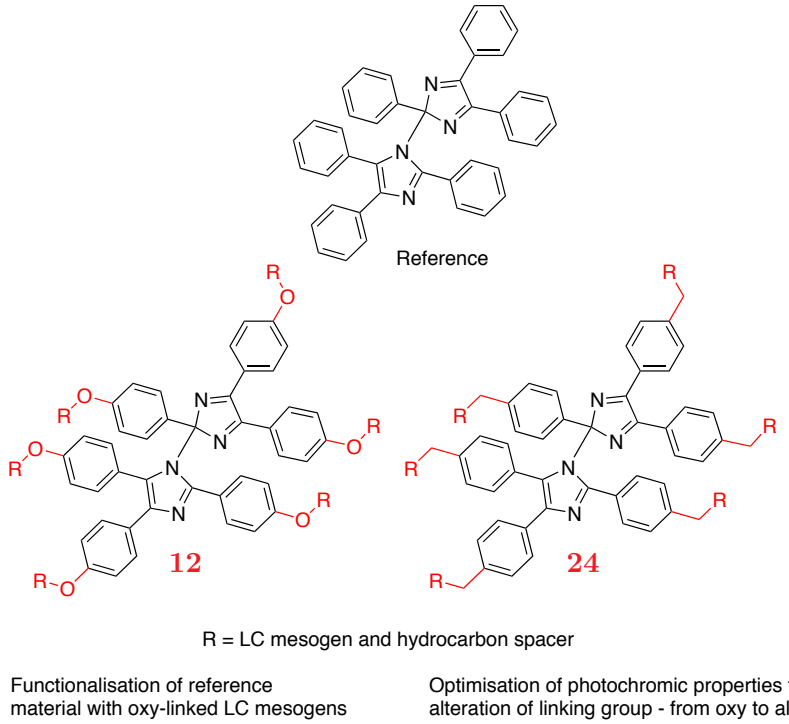

Figure 3.1. Steps for the optimisation of properties, starting from the HABI reference material through the design changes of **12** to **24**.

J. Abe *et al* have done this using different functional groups,[27] as well as the introduction of a rigid back bone to restrict the movement of the imidazole radical.[23]

3.2 Synthetic design of a photochromic LC mesogen based around the HABI group.

The aim of this work was to design and synthesise a photochromic LC mesogen, based around the HABI group shown in Figure 3.1. The design needs to take a number of issues into consideration including the glass transition Tg of the material and the LC mesogen. The LC mesogen of choice is a cyanobiphenyl group. This mesogen was chosen due to the ability of the mesogen to induce LC phase behaviour. The ability to induce LC phase behaviour comes from the rod like structure of the mesogen (this can be seen in 5CB) and also gives a good comparison to other LC mesogens and as this is a standard mesogen, to compare the detected solid state properties with other

materials. The second consideration in the design is the glass transition of the final compound. The desired glass transition is to be as close to room temperature as possible, to reduce the possibility of the HABI radical reacting at high temperatures in the LC phase. The low glass transition also eliminates the design issue that has to be dealt with, the thermochromic properties that most photochromic materials exhibit at high temperatures. The first option to introduce LC behaviour would be the direct attachment of the aromatic LC mesogen to the photochromic core. This however would result in a highly crystalline material and no LC phase behaviour as the resulting photochromic LC mesogens have restricted movement and hence a reduced ability to form an LC phase. This has been shown and explained in the literature.[1] The introduction of an LC phase is achieved throught the reduction of the glass transition and the introduction of liquid crystal phases can be achieved by the decoupling of the LC mesogen from the central core via a hydrocarbon spacer which is known to reduce the melting point of LC materials.[53] The separation of the central core from the LC mesogen also aids the formation of an LC phase as the LC mesogen has a greater degrees of freedom to form an LC phase. This decoupling of the LC mesogen from the photochromic core via a hydrocarbon spacer was initially explored by J. Hussey *et al*,[60] see Figure 3.2.

The decoupling of the LC mesogen from the central core by the introduction of an undecene hydrocarbon spacer attached via an alkoxy link reduced the overall rigidity of the material sufficiently and no vitrification (Tg) could be detected. The material was found to have a melting point of 150°C and showed no LC phase behaviour. The lowering of the melting point, the introduction of a glass transition and the induction of the LC phase was thus to be achieved by using a siloxane linker and the lenghthening of the hydrocarbon spacer. The introduction of the siloxane linker allows greater freedom of rotation of the **Si-O** bond compared to the **C-C** bond this is known to reduce the Tg of polymers. This principle can be translated into the linking of hydrocarbon spacers as, with the increased rotation at the siloxane link, the melting point is lowered. This effect has been seen in photochromic systems with lateral mesogens.[56]

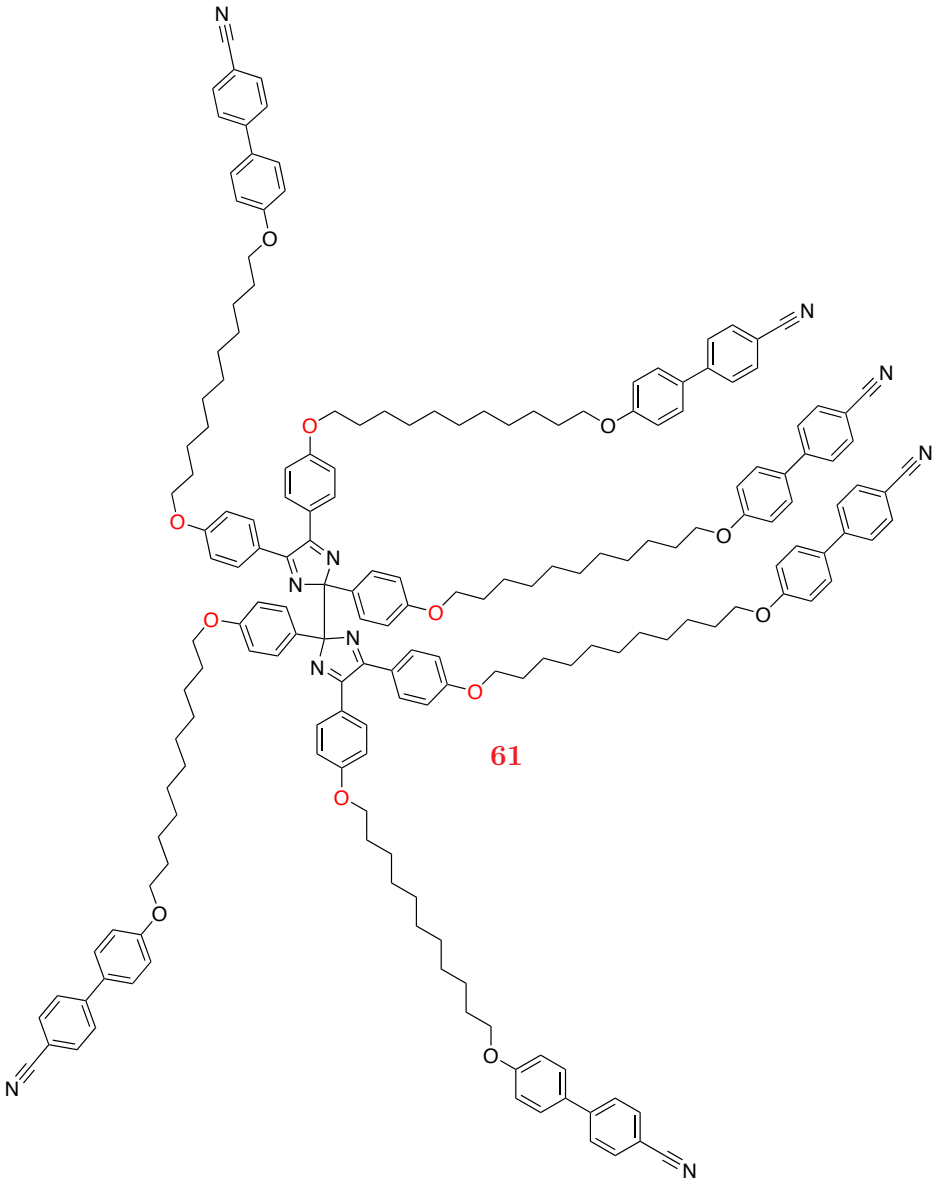

Figure 3.2. The full structure of **61** from previous work by J.Hussey.

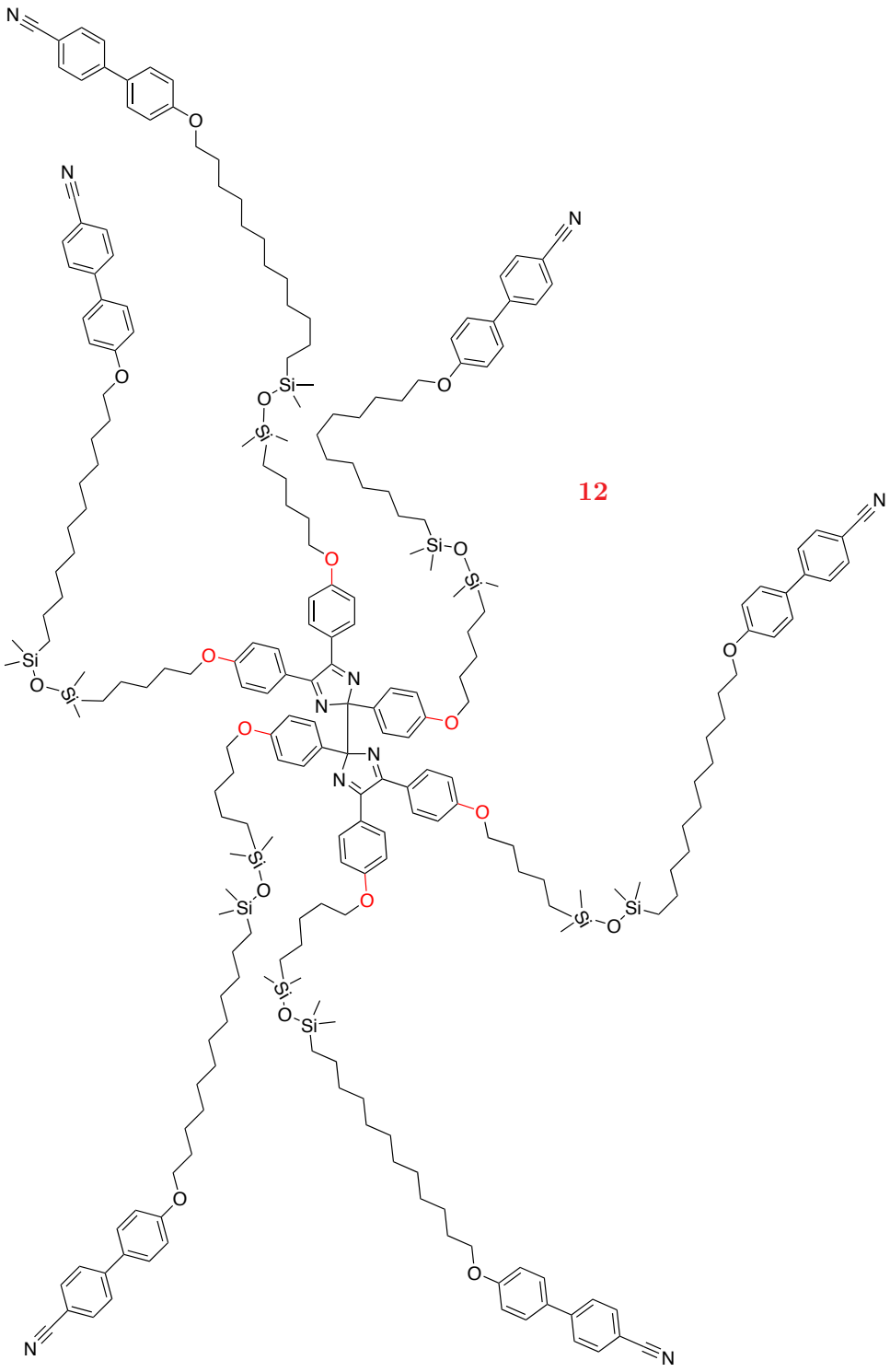

Figure 3.3. The full structure of target material **12**.

Figure 3.3 shows the full structure of **12** with the LC mesogen and the photochromic core decoupled from each other via a hydrocarbon spacer with siloxane linker. The addition of the siloxane and the increase in the length of the hydrocarbon chain was designed to reduce the melting point to be close to room temperature and to stabilise the LC phase behaviour. The increase of the length of the hydrocarbon spacer allows further decoupling of the LC mesogen from the HABI core. This allows the hydrocarbon spacer to behave as a flexible chain to the LC mesogen, which is known to stabilise LC phase behaviour and to induce especially Smectic phases[61] due to the microphase seperation.

The final consideration of the design in the material is the photochromic properties. The introduction of electron donating and withdrawing groups on photochromic molecules alters their properties[17] and, in the case of HABI, the dissociation and recombination speed. The alkoxy linker to the hydrocarbon spacer to the HABI core has an induction effect on the photochromic properties, reducing the association rate of **12**. With this in mind the structure was further altered and the removal of the alkoxy link directly attached to the HABI core was replaced with a hydrocarbon link resulting in **24** the full structure is shown in Figure 3.4. The removal of any strong electron withdrawing or donating groups attached directly to the HABI core will eliminate the potential association speed alterations.

The decoupling of the LC mesogen from the photochromic core also eliminates the possibility of competing absorption in the UV region of the LC mesogen and the photochrome, therefore reducing the possibility of the anisotropic FRET (Fluorescence Resonance Energy Transfer). This allows for better control of the electronic properties, in so far as the absorption from irradiation and the excitation of the electrons is transfered. The extent of energy transfer is determined by the distance between the donor (LC mesogen) and the acceptor (photochrome). This has the potential to effect the photochromic properties, and through that the LC phase.

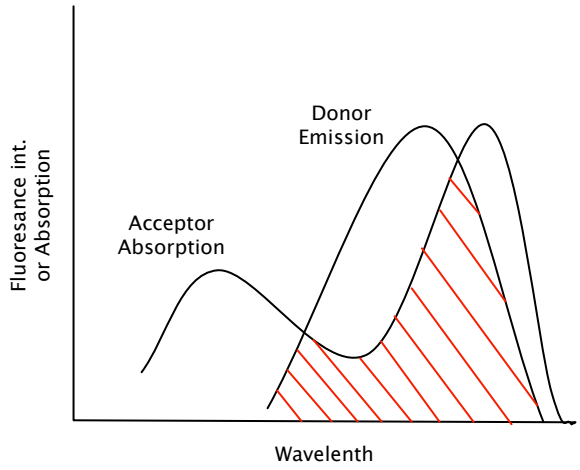

Figure 3.5. General depiction of spectral overlap for fluorescence resonance energy transfer.

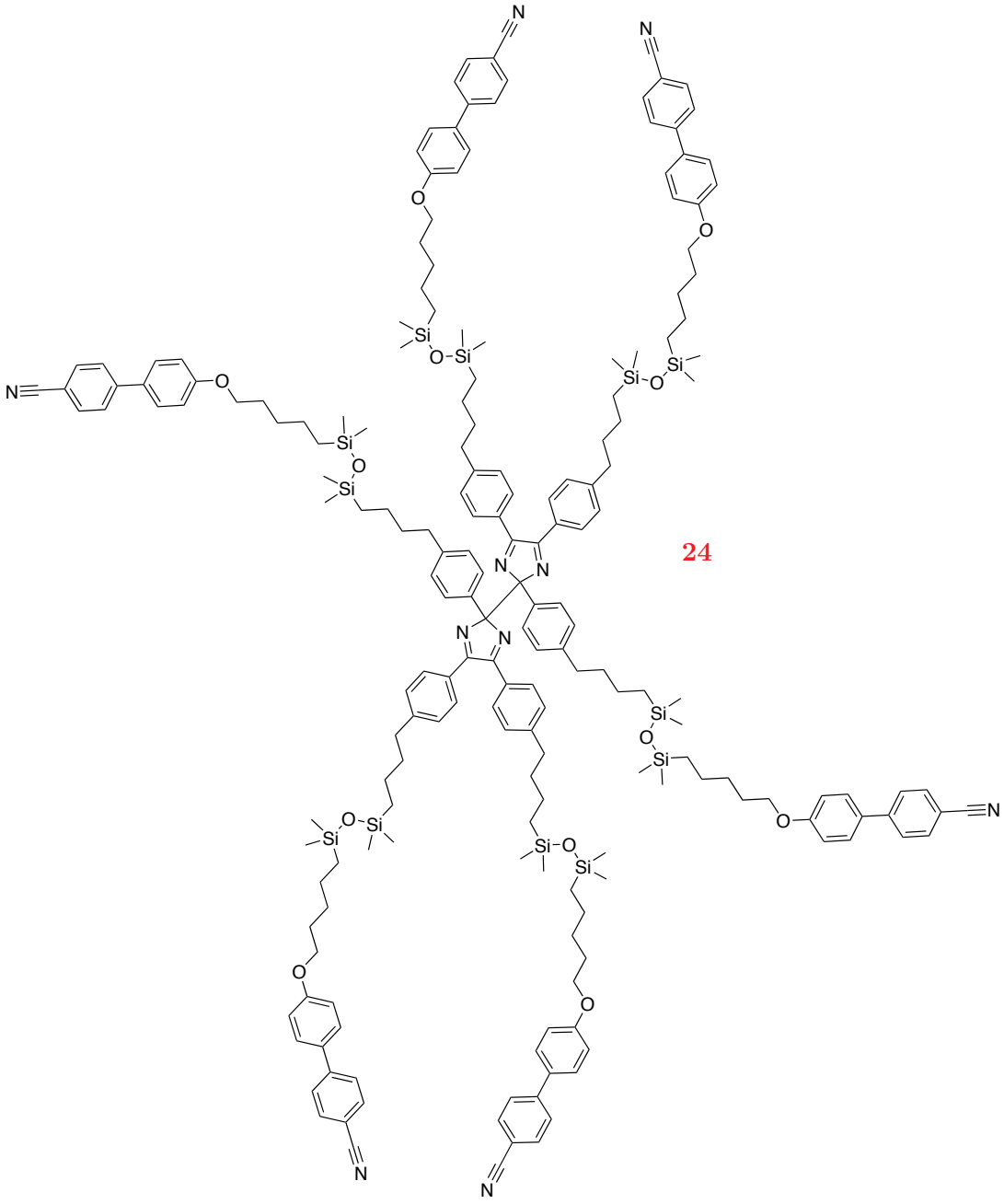

Figure 3.4. The full structure of target material **24**.

3.3 Synthesis discussion

The synthesis of the final materials was achieved via a modular approach, where the functionalised HABI monomer mesogen was first synthesised. Separately to that the liquid crystal mesogen was functionalised with a hydrocarbon spacer. The formation of the seperate modules required another step, in linking the separate modules to form the final material. The core HABI group module was then further broken down to the formation and functionalisation of the separate sections that make up the HABI monomer. The first step in the synthesis of the HABI module was the formation of the diketone **2** using a Friedel-Crafts acylation using oxalyl chloride as shown in Figure 3.6 **step 1**. 1,2-Bis(4-methoxyphenyl)ethane-1,2-dione was deprotected to give the 4-hydroxyphenyl derivative **3** **step 2**. The next step, the attachment of the 1-pentene chain, was attempted following a Mitsunobu procedure[62] see Figure 3.6 route **A**, using 4-pentene-1-ol, and DIAD and triphenylphosphine to activate the alcohol. This did not work in satisfactory yields so an alternative route was tried. The alternative route **B**, using a classical etherification of the alcohol with 1-bromo-4-pentene, see Figure 3.6, to yield **4**.

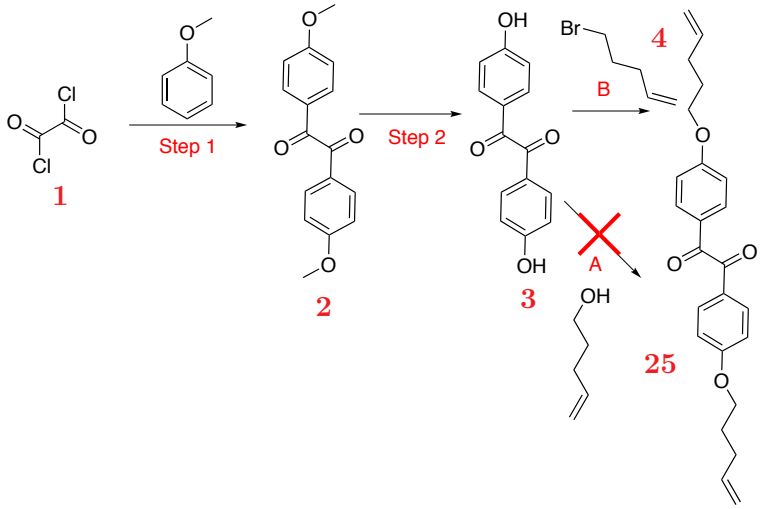

Figure 3.6. The functionalisation and formation of the first HABI group monomer module.

The second step in the formation of the HABI module was the funtionalisation of the 4-hydroxybenzaldehyde with 1-bromo-4-pentene, via a classical etherification. The formation of the 2,4,5-triphenylimidazole dimer has been attempted by many

approaches. The critical steps are the cyclisation of the aldehyde **6** and di-ketone **4**, the standard method is outlined by Harwood *et al.*[63] This method uses acetic acid as the solvent. This method can cause problems, when acid sensitive functional groups are present limiting the scope of functionalisation. An alteration to this method is the use of zinc oxide[64] in a solvent free reaction, the introduction of catalysts such as indium chloride[65] has been reported, this was shown to have inconclusive results and sometimes costly reagents. An alternative method was tried. This alternative method for the synthesis of the imidazole by the combination of three aldehyde molecules in the presence of HMDS (hexamethyldisilazane),[66,67] see Figure 3.7, was carried out following the reported literature procedure. This reaction was found to be unsuccessful.

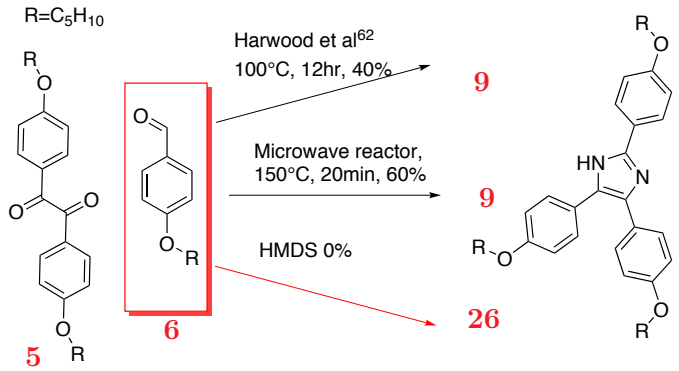

Figure 3.7. Synthetic routes tried for the formation of the HABI group monomer.

With the recent increase in the interest and use of microwave methods a relevant report by Khmelnitsky *et al*[68] discusses an increase in yield with faster reaction times, with the same reactants and reagents used in the original method by Harwood *et al.*[63] The synthesis of the imidazole monomer **9** was modified compared to the literature method, using a higher yielding method with the aid of a microwave reactor.[68,69] The reagents and reactants where dissolved mixed in a 10ml microwave reaction vessel and sealed using a teflon rubber cap, the reaction was heated to 150°C under 827kPa for 20 minutes. The introduction of the high pressure increased the yield from 40% to 60% see Figure 3.7. The use of a microwave reactor increased the yield of the monomer formation and also decreased the reaction time. This reduction in the reaction time would allow a larger number of test reactions to form variations on the HABI group monomer to be carried out. This would be a viable way of forming

many structural variations of the HABI group monomer in a short time. The increase in the speed of the formation of the HABI group monomer would allow the formation of a large structural variations to be tested to optimise the photochromic properties of the HABI group.

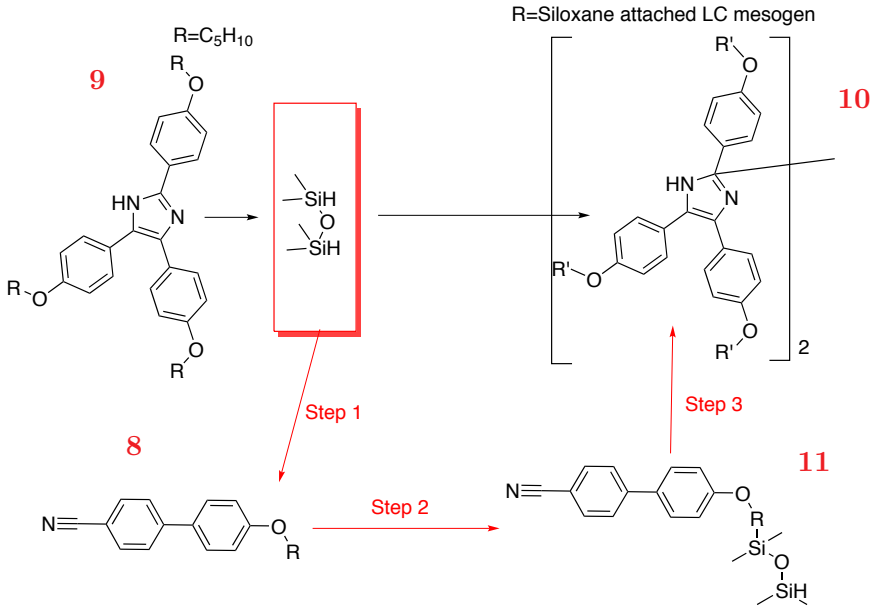

Figure 3.8. Formation of the HABI-LC final compound, R denoting the hydrocarbon spacer length and R′ the LC mesogen.

With the formation of the HABI monomer optimised through the utilisation of microwave reactions. The next step was the radicalisation and subsequent formation of the HABI group dimer. The formation of the dimer **9** was lower yielding than required at 70% using the traditional method outlined by Harwood *et al.*[63] The low yielding reaction to form **9**, would introduce more impurities and therefor further purification future steps, to yield a pure material. An alternate method used by J. Abe *et al*,[27] reported higher yields and therefore a reduction in the impurities present. This was a change from the original method, outlined by Harwood *et al*, which involved the addition of the potassium hexacyano ferrate to the cooled HABI monomer solution. The alternative method reported by J. Abe *et al*, involves adding all the reagents and stirring at room temperature for 16hr with the exclusion of light. The downside to this method was that if the light was not completely excluded from the vessel during the reaction the yield dramatically reduced, due to the formation of a side product that is identified by the presence of an intense blue colour. The method

reported by J. Abe *et al* was tried and with optimisation and full exclusion of light. There was an increased yield from 70% to 90%, of the HABI dimer. The second step in the modular building of the target was the attachment of the liquid crystal mesogen via the hydrocarbon spacer. It was decided that the best method of attachment was via a siloxane linking group. The first route tried, shown in black in Figure 3.8, was the attachment of the siloxane linker to the HABI core. This resulted in a very poor yield and difficult work-up and purification. The main problem was the separation of partially reacted groups and the cross-linking of reacted groups. The second route taken was the hydrosilation of the alkene on the LC mesogen shown in **step 1** in Figure 3.8. The addition of the siloxane linker at the LC module of the final material increased the ability to tailor in this approach. Reactive siloxanes could be prepared and purified (**step 2**) which in the following **step 3** could be reacted with the HABI core. This method could be modified with different LC mesogens to alter the final material to introduce different LC mesogens. The products of this approach were easier to purify and the reaction higher yielding.

Following the formation of the HABI monomer as well as the formation of the dimer optimised and the route for the attachment of the LC mesogen. The second module can be assembled. The formation of the liquid crystal mesogen shown in Figure 3.9 **step B**. Cyanobyphenyl is functionalised with and undecene spacer via a classical williamson esterfification **step B**. The final step to form the liquid crystal mesogen is the attachemnt of the siloxane linker. As mentioned previously this increased the ability to taylor the lC properties. The attachment of the siloxane was done via a typical hydrosilation using 1,1,3,3-tetramethydisiloxane and Karsteds catalyst. The crude product was purified using columb chromatography. The resulting material was stored in the fridge to reduce the possibily of homo-coupling of the siloxane linkers.

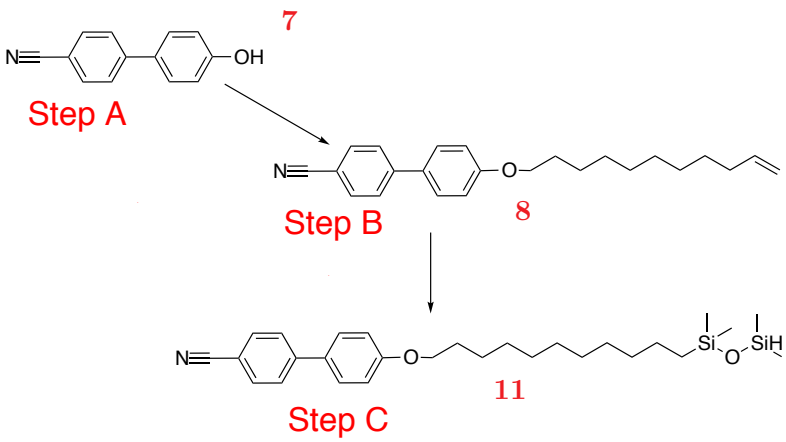

Figure 3.9. Formation and functionalisation of the LC masogen

The last part in the formation of the liquid crystal mesogen functionalised HABI moiety is the combination of the two modules that have been synthesised. This was achieved by hydrosilation of the siloxane functionalised LC mesogen to the core module. The reaction was carried out in the same way as attaching the siloxane linker to the LC mesogen using 1,1,3,3-tetramethyldisiloxane and Karstedt's catalyst in xylene. The final material **12** can be seen in Figure 3.10

The final material **12** shown in Figure 3.10 was analyised using OPM to idenify initially the transition temperatures and the presence of liquid crystal properties. The photochromic properties were also analysed using UV-Vis spectroscopy. The conclusion drawn was that the removal of the ethoxy linker between the hydrocarbon spacer and the HABI core in **12**, improved the association speed of the HABI radical as it would remove the increase in radical stabilisation that is caused by the presence of the oxy group.

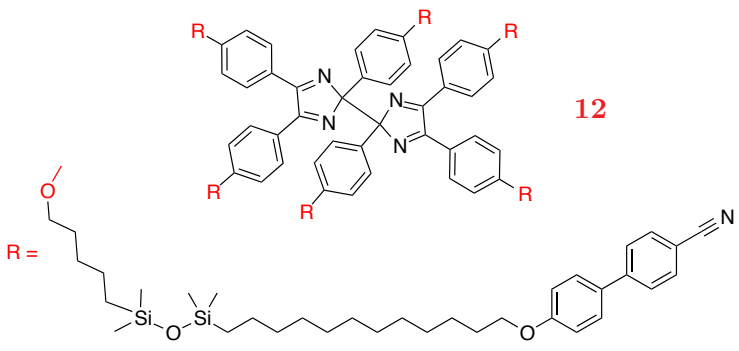

Figure 3.10. Final photochromic LC material.

A similar effect can be observed in napthopyrans when electron-donating groups are introduced into the system.[70,71]

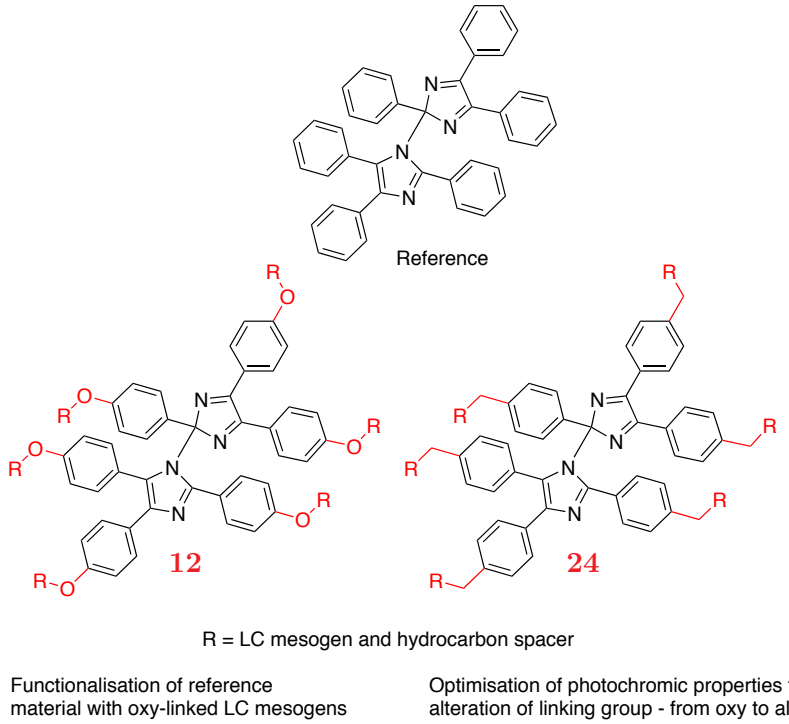

Figure 3.11. Functionalisation of the HABI reference material and optimisation of the properties.

A possible solution to the problem is shown in Figure 3.11 with compound **24** . This involves the removal of the oxy group linking the LC unit and photochromic core, and the direct attachment of the hydrocarbon spacer to the phenyl ring. The synthesis was one again broken down into modules the first being the HABI monomer and the second the liquid crystal mesogen. The HABI monomer was futher divided into the key componets to the formation of the heterocyclic core. With the alteration of the method of attaching the hydrocarbon spacer arose a new set of issues to overcome. With the removal of the oxygen linking the hydrocarbon spacer to the central HABI core this altered the synthesis of the di-ketone. The addition of the spacer via etherification was no longer a viable option, due to the lack of the oxygen. With this the next logical step was the formation of the diketone via Friedel-Crafts acylation using oxalyl chloride and bromobenzene, the major product formed would be the ortho substituted due to the directing effect of bromine. The issue with this

is the second step the attachment of the spacer, with the diketones present many of the traditional methods of carbon carbon bond formation are not possible, such as the use of a Grignard reagent, this would attack the ketons and form unwanted side reactions. For the diketone two literature reported routes were avalible. The first utilises a Friedel-Crafts acylation, using but-3-en-1-ylbenzene and oxalyl chloride, this is shown in Figure 3.12. This method proved to be low yielding, identity of the product was only verified using ^{1}H-NMR. The second method was to couple two 4-(3-buten-1-yl)benzaldehyde molecules **19** using potassium cyanide[72] shown in Figure 3.12 **step 1**. This was found not to produce satisfactory results. Additionally the use of potassium cyanide made the work-up and purification more complicated due to the toxic nature of the potassium cyanide. Therefore it was decided to synthesize the diketone **18** through an alternative route.

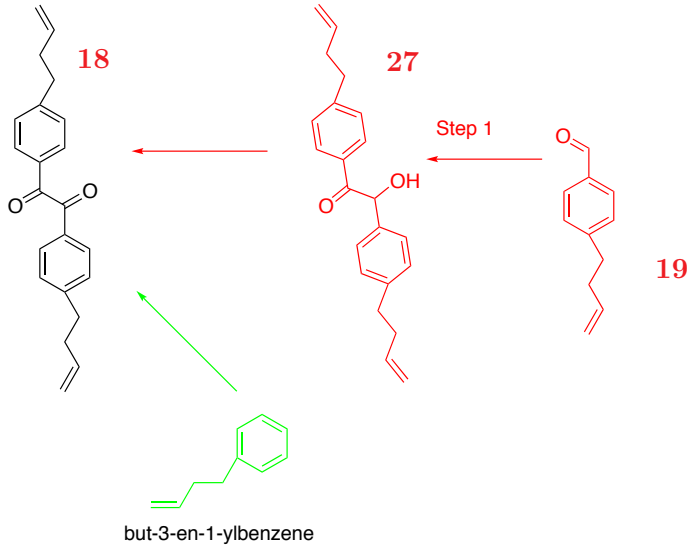

Figure 3.12. Attempted methods for the fomation of the diketone.

The alternative route is shown in Figure 3.13 and Figure 3.14. It can be broken down into sections. The attachment of the alkene and the the formation of the intermediate tolane **17** and then the formation of the diketone. The first step in building the tolane **17**, was the attachment of the alkene chain using a Grignard reagent and bromobenzyl bromide to give **14**, seen in Figure 3.13 **step 1**. The formation of the tolane can then be started, firstly by the attachment of trimethylsilyl acetylene to **14** to form **15** via a Sonagashira reaction in **step 2**. The following step required the deprotection of the alkyne which involved the removal of the trimethylsilane from **15**

to produce **16** shown in Figure 3.13 **step 3**. The trimethylsilane was removed under basic conditions to yield **16** in a near quantative yield; **step 3**. The product **16** of **step 3** was extracted into dichloromethane and dried over magnesium sulphate, the resulting oil was used with no further purification. The final step in the formation of the tolane was the coupling of **14** synthesised in **step 1** shown in Figure 3.13 with the previously synthesised material in **step 3** compound **16**. The tolane derivative **17** shown in Figure 3.13 **step 4**. The tolane produced in **step 4** was analysed for liquid crystal properties and it was found that it exhibted a SmA phase from 103°C to 107°C. This is in line with results from other tolanes[73]

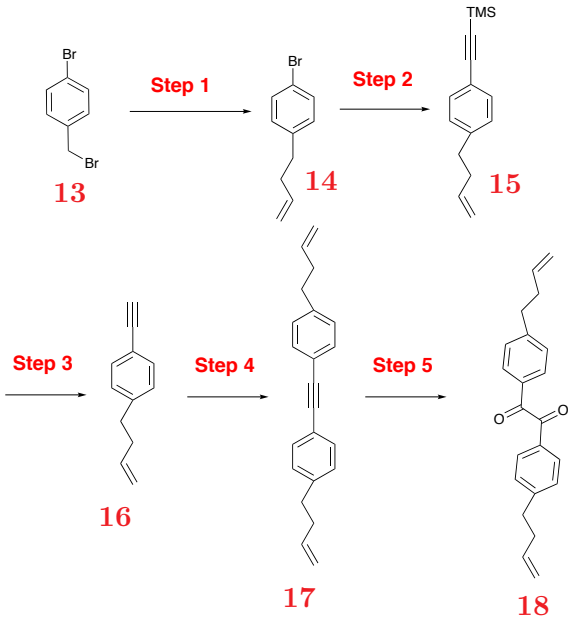

Figure 3.13. Synthetic steps for the formation of the tolane, the first section.

This tolane **17** shown in Figure 3.13, was then oxidised to form the diketone **18** shown in Figure 3.15. There are few reported literature methods for the oxidation of alkyne bonds to ketones. The use of [(NHC)Au^{I}]- a catalytic amount of (NHC = N-heterocyclic carbene) in acid free conditions, is a very promising method, with the need for a very low catalytic loading and with reported good yields.[74] Another method is the hydroborination of alkynes using pyridine borane. The advantage of this method is in the low temperature conditions as it is carried out at room temperature. The problem with the above mentioned methods, the *N*-heterocyclic carbene and the pyridine borane is that they only report conversion of the alkyne to

a single ketone. The desired method needs to convert the alkyne to diketone. With this in mind the chosen method outlined by Ang Gao *et al*[75,76] used DMSO as the solvent and Cu(II)Br/$Pd(OAc)_2$ as the catalyst, to convert the tolane derivative **17** to the diketone shown in Figure 3.14 **step 6**. The yield of the final diketone **18** was through optimisation 45%. With the formation of the diketone in **step 6** optimised, the next challenge is in the formation of the 4-(3-buten-1-yl)benzaldehyde the route taken is oulined in **step 7 and 8**.

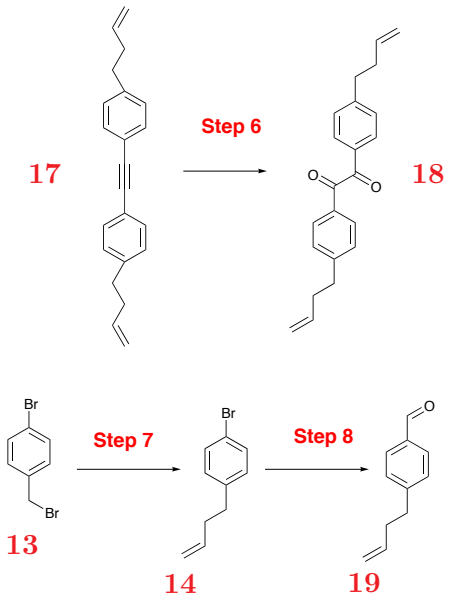

Figure 3.14. Synthetic steps for the formation of the HABI monomer.

The first step in the formation of this module of the HABI monomer is the attachment of the butene spacer chain via a Grignard reaction. The allyl magnesium bromide is commercially available. The allyl magnesium bromide was added dropwise to a solution of 4-bromobenzyl bromide in tetrahydrofuran at room temperature. This is a higly selective reaction due to the difference in reactivity of the bromo groups on the benzene ring. The next step, the formation of the aldehyde to complete this module of the HABI monomer. The product from **step 8 14** shown in Figure 3.14, was first

lithiated using n-butyllithium at -78°C under an inert atmosphere, to this solution dimethyl fomamide was added dropwise. The solution was then quenched and the crude 4-(3-Buten-1-yl)benzaldehyde **19** was purified via column chromatograhy. The method outlined above follows general literature reported aproaches.[77–79] An alternative approach for the formation of **19 step 8** utilises a Grignard reagent[77] rather than a lithium reagent. The final stage in the formation of the HABI monomer is the formation of the heterocyclic core. This was achieved in the same way as discussed above in Figure 3.7.

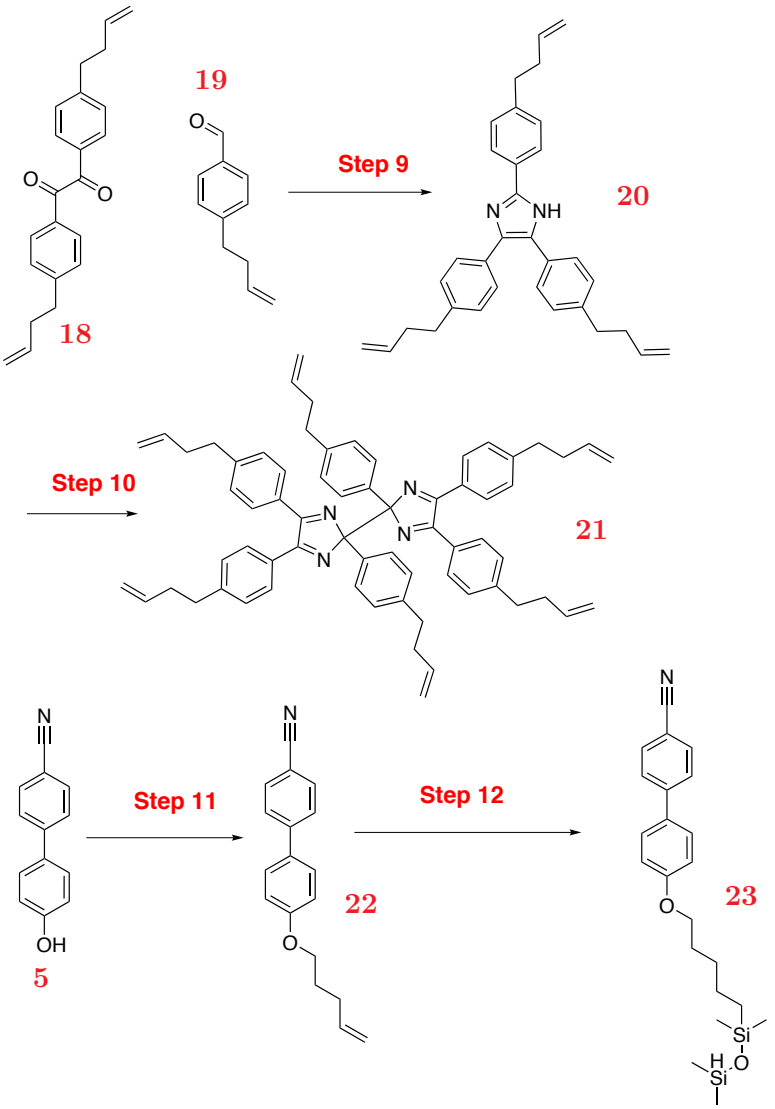

Figure 3.15. Synthetic steps for the formation of the Diketone.

The HABI monomer was formed using ammonium acetate and acetic acid, in a

microwave reactor for at 150°C with a pressure of 827kPa 20 minutes, shown in Figure 3.15 **step 9**. With the HABI monomer formed the synthesis of the HABI dimer can be performed and the completion of the photochromic module. The HABI dimer was formed using the classical method potassium hexacyano ferrate, potassium hydroxide and ethanol to form **21 step 10**. This method was optimised via the use of a microwave which reduced the reaction time from 12hrs to 20 minutes. The final section in the synthesis of **24** shown in Figure 3.17, is the formation of the LC model. The LC mesogen cyanobiphenyl was coupled to 1-bromo-4-pentene **22**, via a Williamson etherification shown in Figure 3.15 **step 11**. The LC mesogen with the attached spacer was then functionalised with the siloxane linking group via a hydrosilation of 1,1,3,3-tetramethyldisiloxane using Karstedt's catalyst, with the terminal alkene of the functionalised LC mesogen **step 12** Figure 3.15.

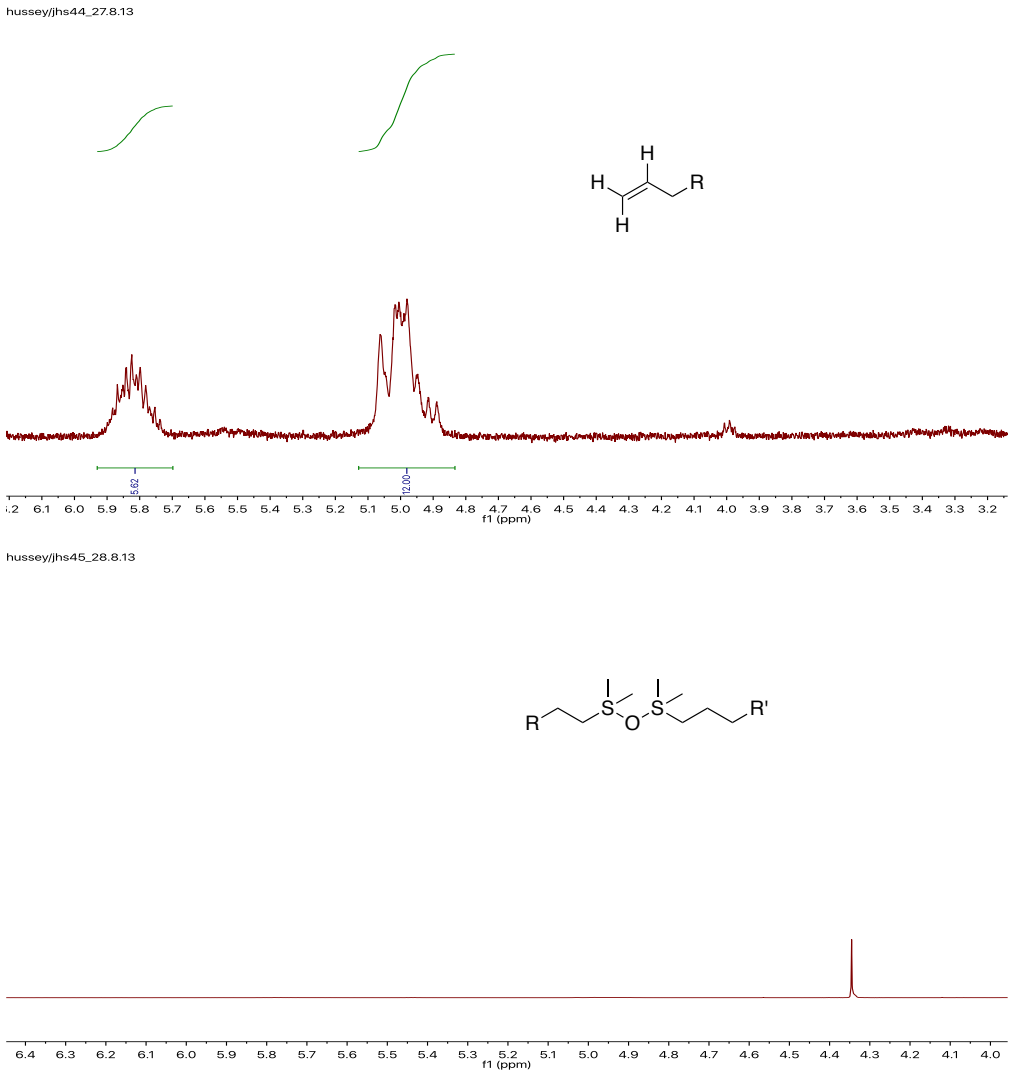

Figure 3.16. ^{1}H NMR of the 6-4ppm range illustrating the before and after hyrosilation and loss of the terminal double bond.

The final step in the formation of **24** seen in Figure 3.17 is the joining of the two modules, the photochromic core and the functionalised liquid crystal mesogen with the linking siloxane group shown in Figure 3.15. The two modules where combined via a hydrosilation of the siloxane functionalised liquid crystal mesogen with the terminal alkene groups on the hydrocarbon spacers of the HABI dimer. The reaction was quenched with water and extracted into dichloromethane, the solvent was removed under reduced pressure and the resulting crude material was purified via recrystalisation form hexane. This resulted in the final compound **24** shown in Figure 3.17.

The full extent of the hydrosilation of the LC mesogen and the photochromic core can be seen from the loss of the multiplet peaks in the 6-4ppm (ppm) range , this is shown in Figure 3.16.

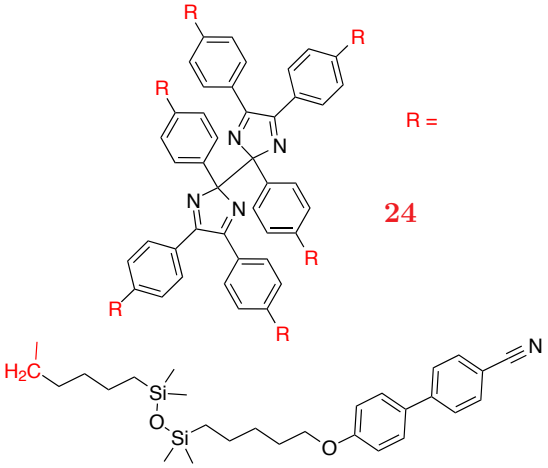

Figure 3.17. Final structure of **24**.

3.4 Synthetic Routes

Scheme 3.7 and Scheme 3.8 where not discussed, in any detail as the steps outlined in Scheme 3.7 did not yield the deired product and alternative routes where utilised. The synthesis of an alternative LC mesogen outlined in Scheme 3.8 was also not discussed as the desired properties where obtained in using the originaly planned LC mesogen shown in Scheme 3.3

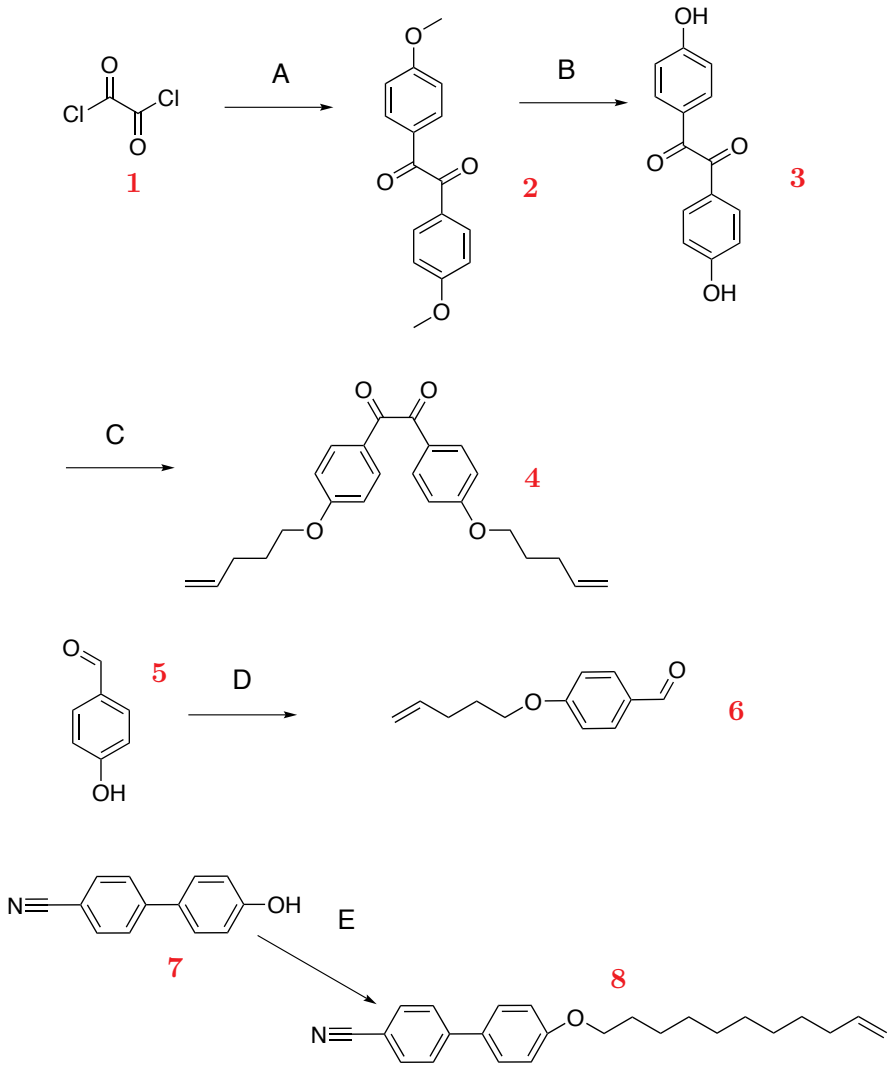

Scheme 3.1. Synthesis of HABI intermediates 4, 6 and LC mesogen 8.

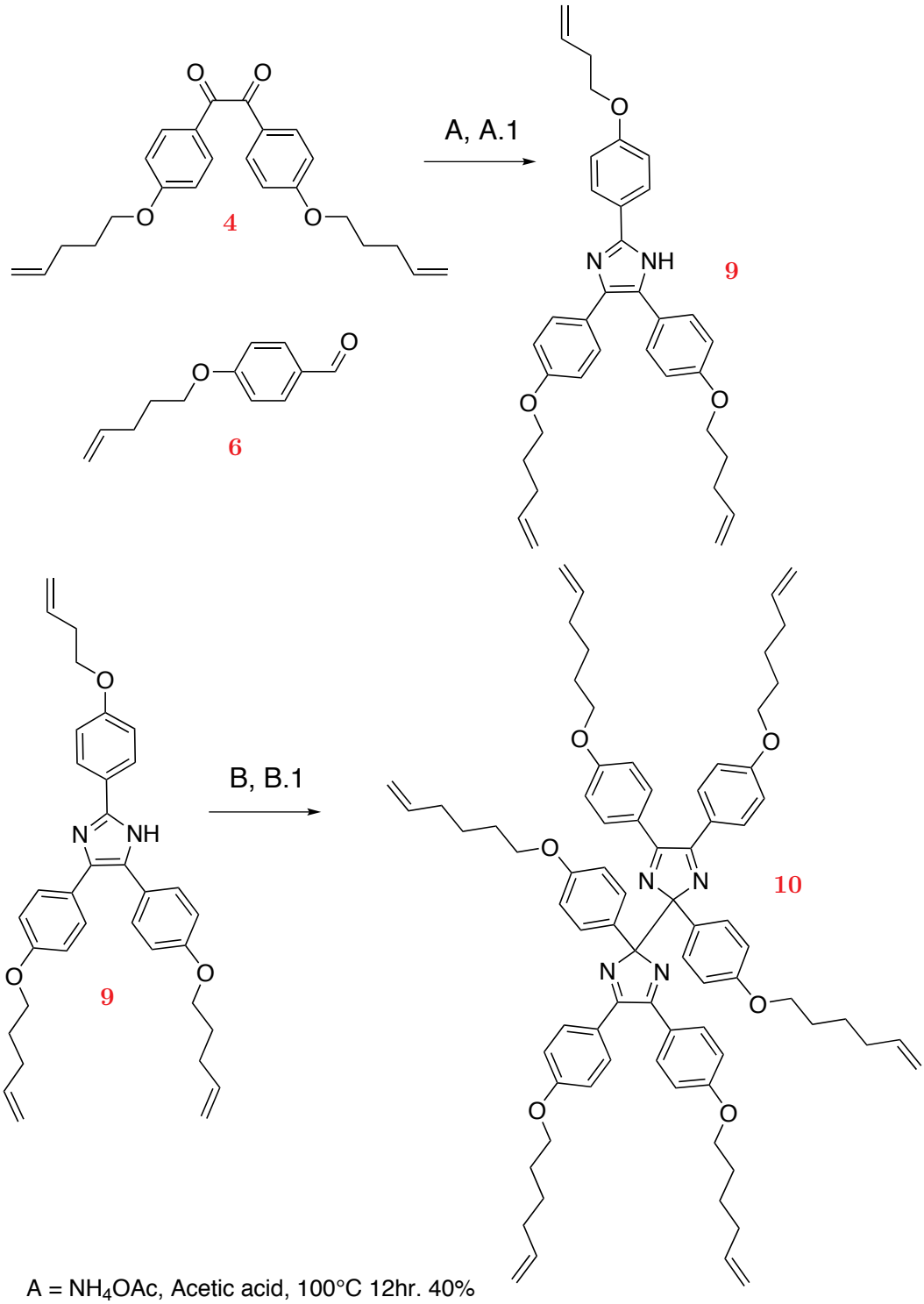

Scheme 3.2. Formation of HABI monomer **9** and the HABI dimer **10**.

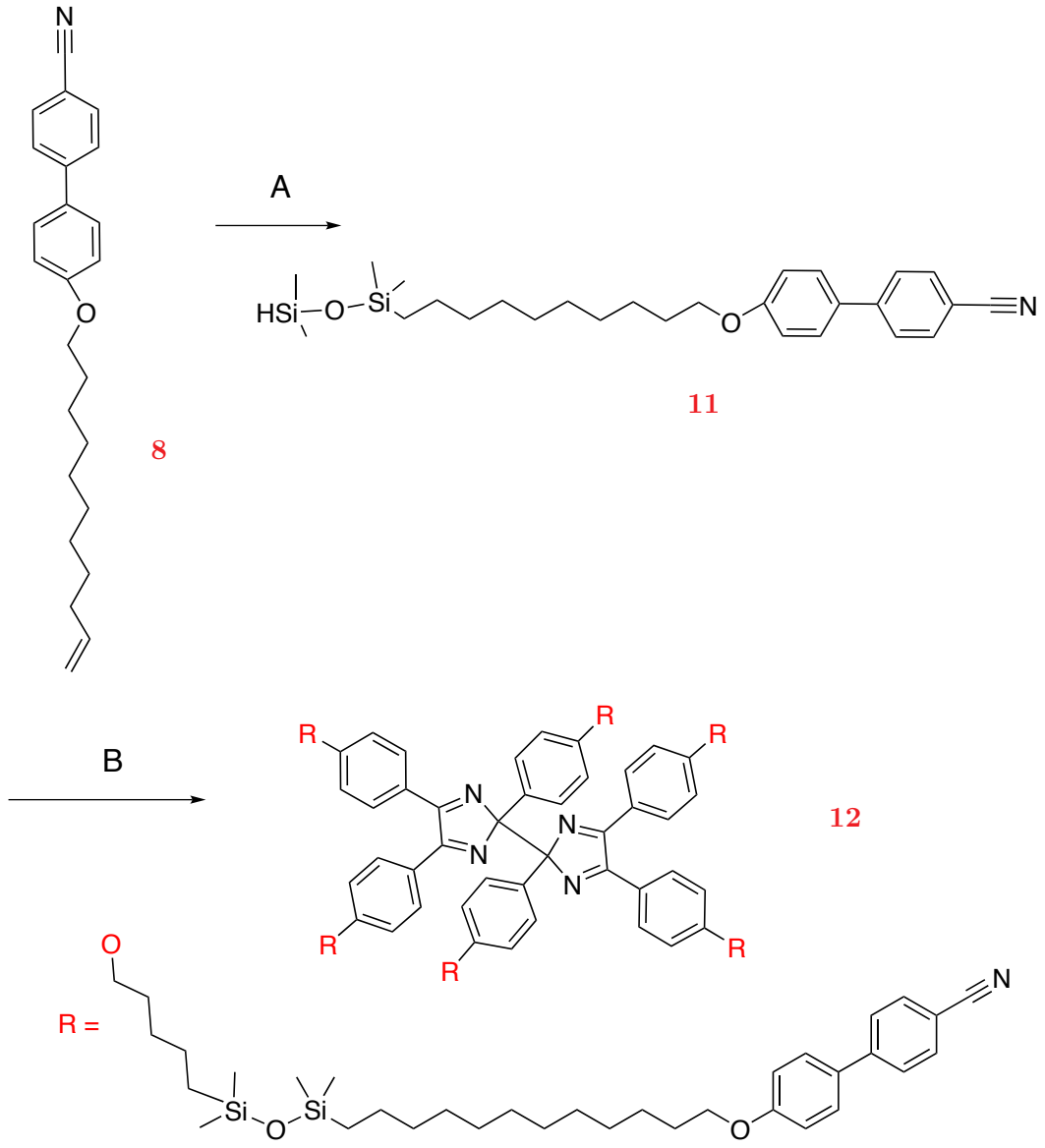

Scheme 3.3. Hydrosilation of the HABI dimer **10** and the siloxane functionalised LC mesogen **11**.

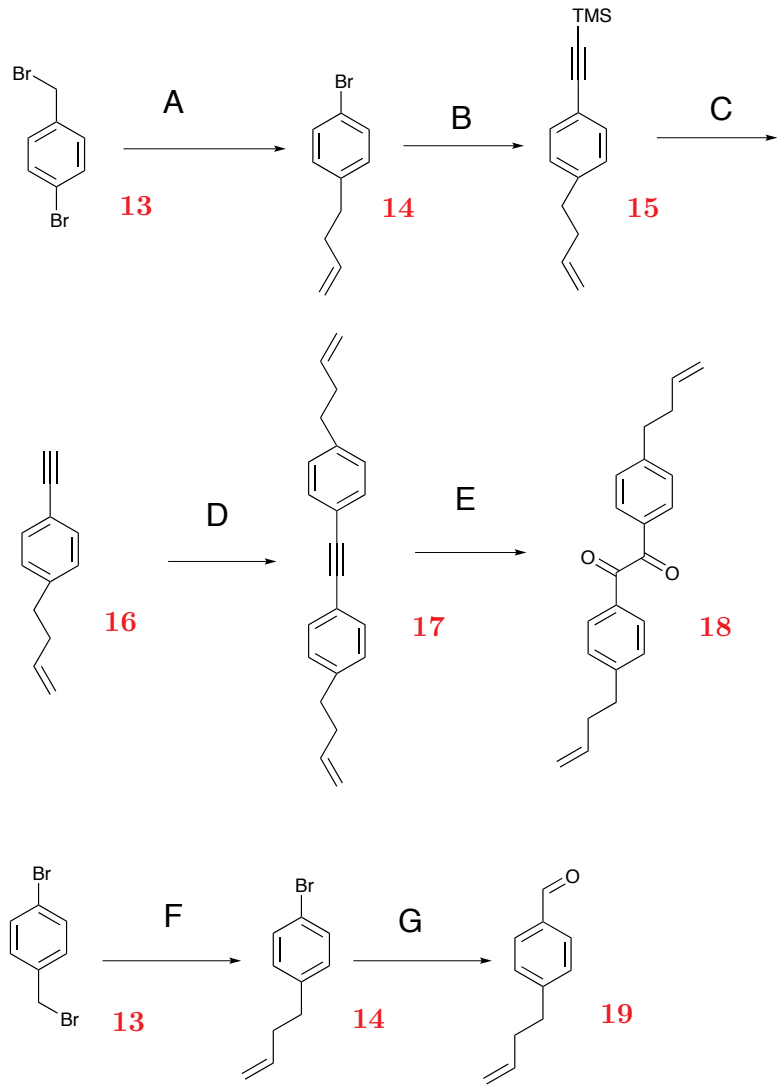

A = Ether,allyl magnesium bromide, RT 90%
B = CuI, NEt_3,TMS-acetylene, $Pd[(C_6H_5)_3P]_4$. 80°C, 12hr 95%
C = KF, DME/water, RT. CuI, NEt_3 80°C, 12hr 85%
D = CuI, NEt_3,$Pd[(C_6H_5)_3P]_4$. 80°C, 12hr 34%
E = DMSO,$Pd(OAc)_2CuBr$, 80°C, 12hr 45%
F = Ether,allyl magnesium bromide, RT 90%
G = n-BuLi THF -78°C, DME, water RT 60%

Scheme 3.4. Modified synthesis of HABI intermediates 18, 19.

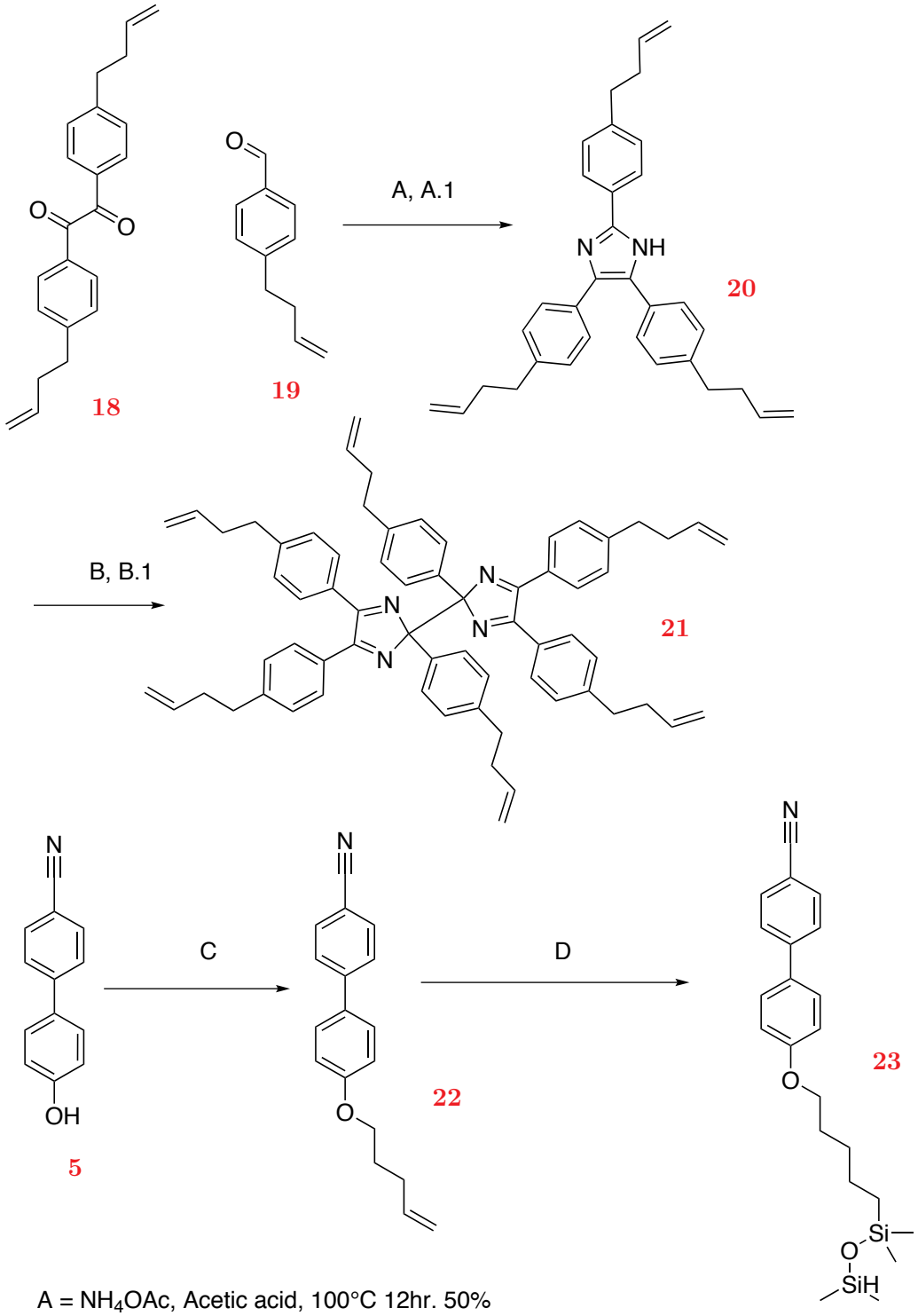

Scheme 3.5. Formation of the HABI monomer **20** dimer **21** and the siloxane functionalised LC mesogen **23**.

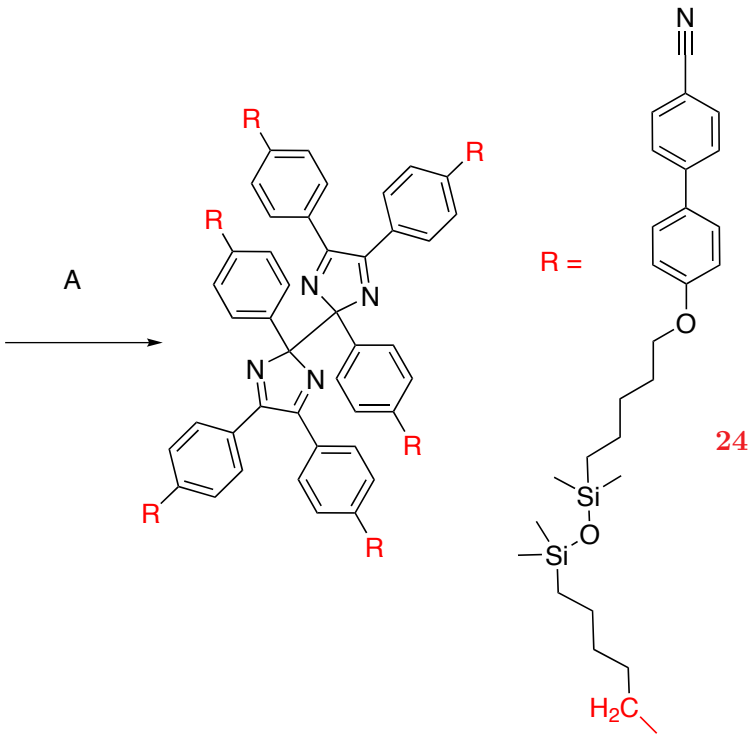

Scheme 3.6. Hydrosilation of the HABI dimer **24** with LC mesogen.

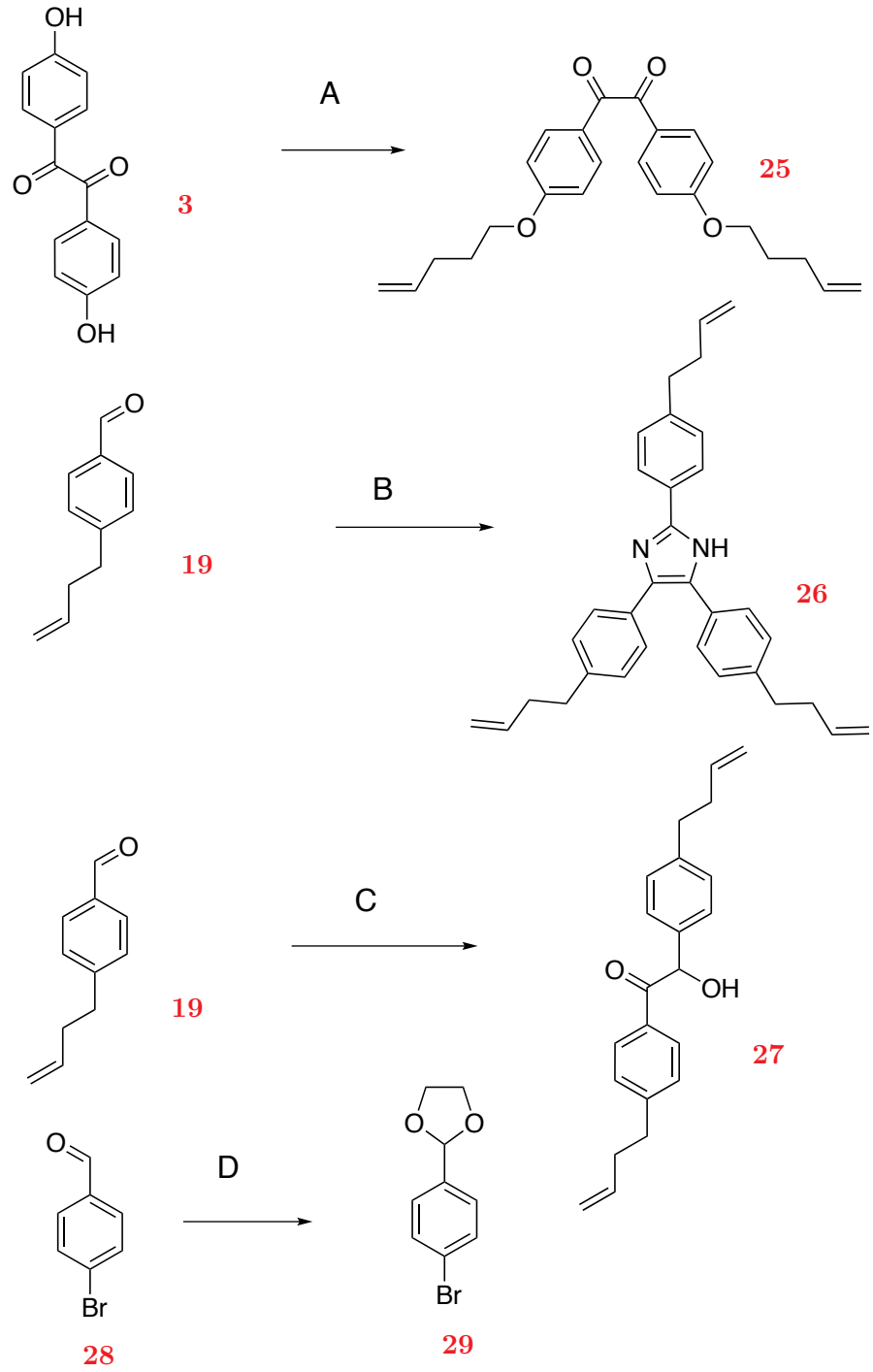

A = DIAD, pentanol, triphenyl phosphine, THF, RT, 16hr, 0%
B = HMDS, iodine, acetonitrile, 100°C, 4hr, 0%
C = potassium cyanide, ethanol/water, 100°C 3hr, 0%
D = bromobenzaldehyde, ethylene glycol, *p*-toluenesulfonic acid, 167°C, 38hr, 0%

Scheme 3.7. Alternative routes for the formation of HABI intermediates.

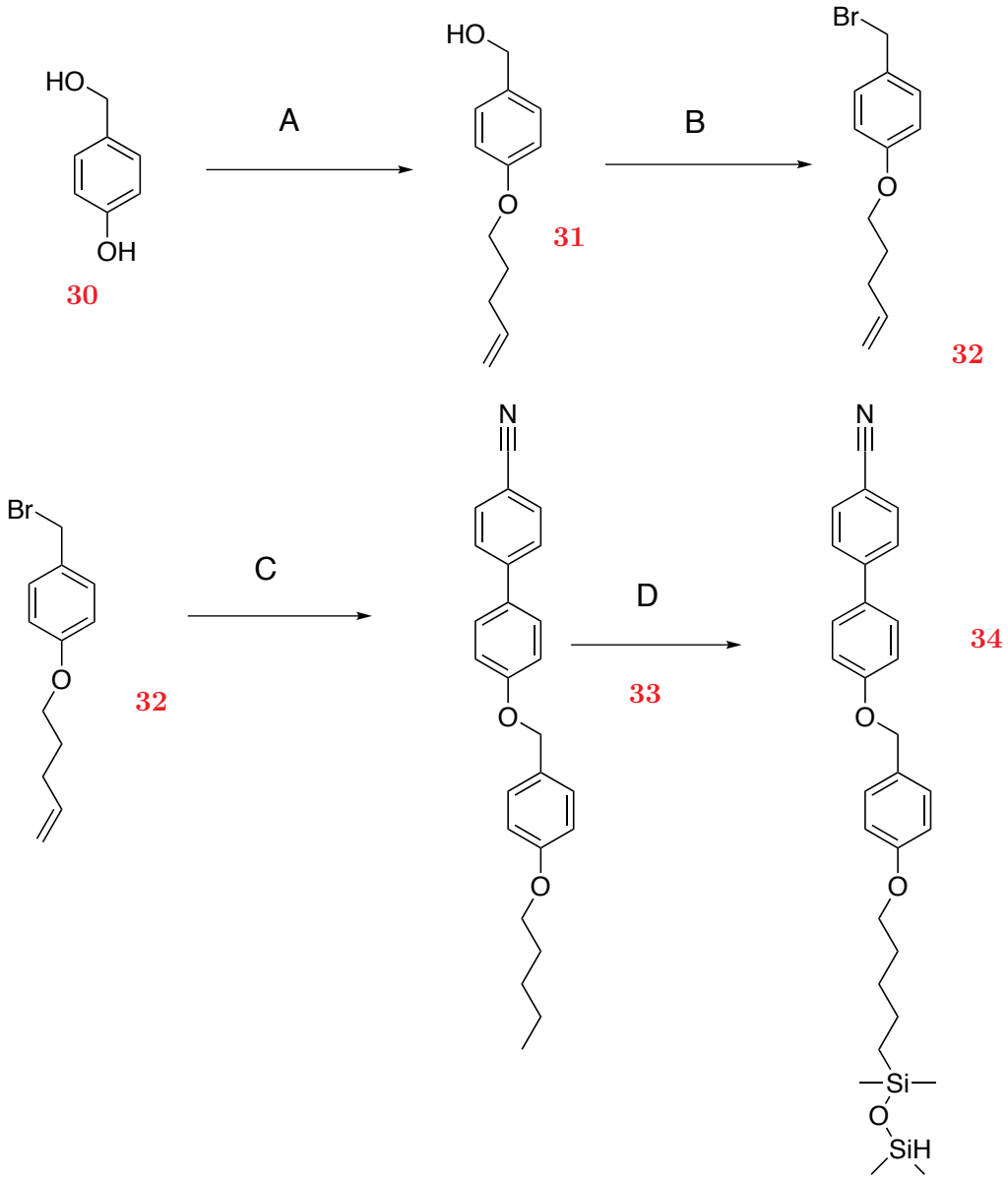

A = 1-bromo-4-pentene, potassium carbonate, potassium iodide, butanone, 100°C, 16hr, 99%
B = THF, phosphorus tribromide, 0°C-RT, 3hr, 40%
C = cyanobiphenyl, potassium carbonate, butanone, 100°C, 16hr, 40%
D = 1,1,3,3-tetramethylsiloxane, Karstedt's catalyst, toluene, RT, 16hr, 90%

Scheme 3.8. Alternative LC mesogen.

3.5 Experimental

Synthesis of 1,2-bis(4-methoxyphenyl)ethane-1,2-dione 2

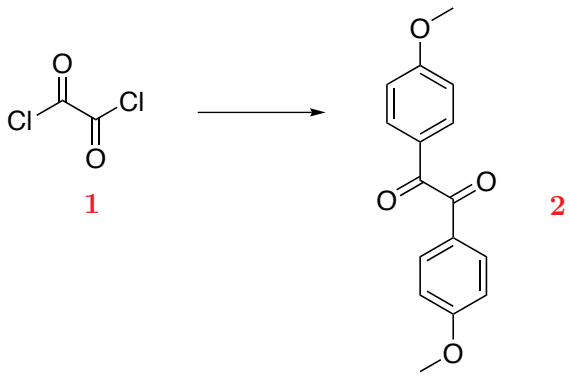

A mixture of anisole (10.8 mL, 100 mmol) and anhydrous aluminum chloride (33.3g, 250 mmol) was cooled to 0°C under nitrogen and to this oxalyl chloride (6.97g, 4.71 mL, 55.2 mmol) was added. Upon addition the solution turned deep red and solid. The mixture was then removed from the ice bath, left to warm to room temperature and then left under nitrogen overnight. To the mixture ice and water was added until the formation of HCl stopped. The mixture was then extracted with dichloromethane and the aqueous layer was removed, the organic layer was then washed with 2M hydrochloric acid and then washed with brine and dried over anhydrous magnesium sulphate. The solvent was removed yielding a red solid, which was recrystallized in the minimum amount of ethanol. The yellow crystals were then filtered off under vacuum and washed with ethanol.

Yield 4.9g, 33%.

^{1}H-NMR (400 MHz, Chloroform-d) δ 7.94 (4 H, d, J 9.0), 6.96 (4 H, d, J 9.0), 3.88 (6 H, s).

^{1}H-NMR matched literature data.[80]

Synthesis of 1,2-bis(4-hydroxyphenyl)ethane-1,2-dione 3

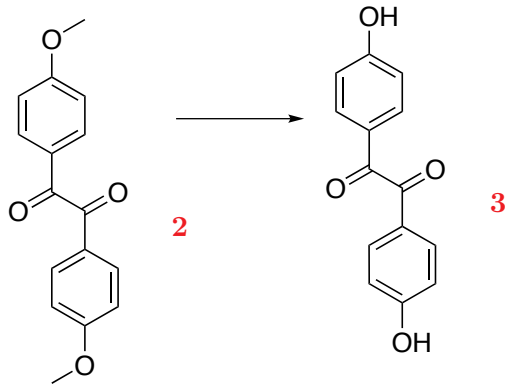

To **2** (4.01g, 0.020 mol) whilst stirred, a solution of HBr (70%) and glacial acetic acid (70 mL) was added. Once the solution had all been added drop-wise, the solution was heated to reflux 155°C for 16 hours. The mixture was then cooled and ethyl acetate was added. The organic layer was extracted then washed with brine twice and then washed with a saturated sodium carbonate solution. The organic layer was dried over anhydrous magnesium sulphate. The solvent was then removed under reduced pressure to yield a light brown solid. Toluene was added in excess to the solid to dissolve the remaining glacial acetic acid, and then removed under reduced pressure.

Yield 3.29g, 68%

^{1}H-NMR (400 MHz, Chloroform-d) δ 7.76 (4 H, d, J 8.9), 6.84 (4 H, d, J 8.9), 2.34 (2 H, s).

^{1}H-NMR matched literature data.[81]

Synthesis of 4'-(undec-10-en-1-yloxy)-[1,1'-biphenyl]-4-carbonitrile 8

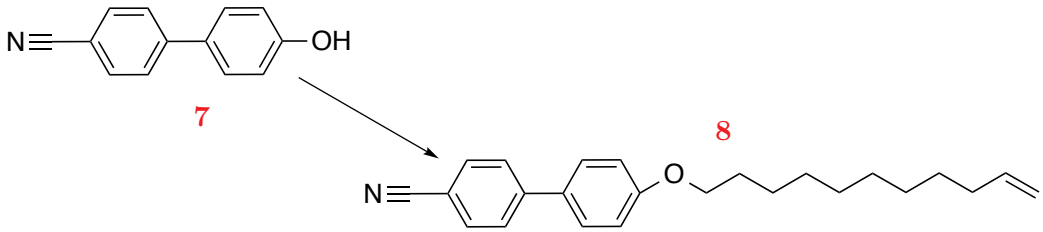

4'-Hydroxy-4-biphenylcarbonitrile 7 (5g, 0.0256 mol) with 11-bromo-1-undecene (18.1g, 17 mL, 0.078 mol) was dissolved in butan-2-one (50 mL) the solution was stirred until complete dissolution of the compounds. To this solution potassium carbonate (7.69g, 0.128 mol) was added and this solution was then heated to reflux for 7 hours (the solution was monitored by TLC in dichloromethane to check the progress, this showed one spot). The solid was filtered off under reduced pressure and the solvent removed for the filtrate under vacuum. The solid was recrystallized from hexane with the precipitate being the clean product

Yield 5.32g, 60%.

^{1}H-NMR (400 MHz, Chloroform-d) δ 7.69 (4 H, d, J 8.7), 7.52 (2 H, d, J 8.9), 6.99 (2 H, d, J 8.9), 5.81 (1 H, dddd, J 17.9, 10.2, 7.2, 6.1), 5.05 – 4.87 (2 H, m), 4.00 (2 H, t, J 6.6), 2.10 – 1.97 (2 H, m), 1.92 – 1.74 (2 H, m), 1.51 – 1.24 (12 H, m).

Synthesis of 1,2-bis(4-(pent-4-en-1-yloxy)phenyl)ethane-1,2-dione 25

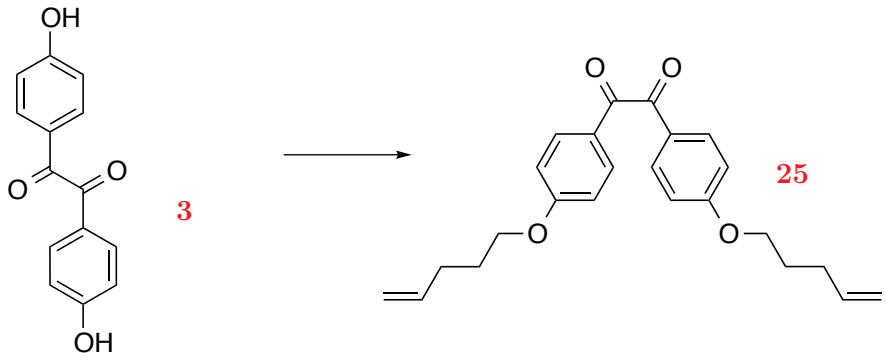

3 (2g , 8.40 mmol), pentanol (2.16g, 3 mL, 0.0253 mol) and triphenylphosphine (6.61g, 0.0253 mol) were dissolved in THF at room temperature. DIAD (Diisopropyl azodicarboxylate) (5.09g, 0.0293 mol) was added slowly. After being stirred at room temperature for 16 hours the solvent was removed under reduced pressure. The crude material was TLC'ed which showed that only the starting material was present and no reaction had occurred. The pathway was abandoned.

Synthesis of 4-(pent-4-en-1-yloxy)benzaldehyde 6

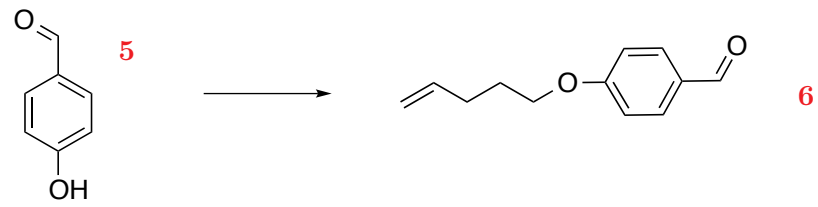

4-Hydroxybenzaldehyde (2g, 0.014 mol) was mixed with bromopentene (7.322g, 5.82 mL, 0.492mol), potassium carbonate (11.33.281g, 0.082 mol) in ethyl methyl ketone (100 mL). This solution was stirred at reflux for 5 hours, the progress of the reaction was monitored via TLC every hour to check the progress. The solution was removed from the heat and the carbonate filtered off. The solvent was removed under vacuum. The crude material was purified using column chromatography using DC : hexane (1:10) as the eluent.

Percentage Yield 1.77g, 90%

^{1}H-NMR (400 MHz, Chloroform-d) δ 9.82 (1 H, s), 7.77 (1 H, d, J 8.9), 6.94 (2 H, d, J 8.8), 5.81 (1 H, ddt, J 16.9, 10.2, 6.7), 5.08 – 4.94 (2 H, m), 4.00 (2 H, t, J 6.4), 2.21 (2 H, q, J 7.4), 1.87 (2 H, dt, J 13.6, 6.5).

^{13}C-NMR (101 MHz, Chloroform-d) δ 190.86, 164.23, 137.52, 132.05, 129.87, 115.55, 114.83, 67.60, 30.04, 28.24.

mass spectrometry- Theoretical: 245, 246, 247, 248. Observed: 245, 246. accurate mass Theoretical: 245.1536, 191.1065 Obeserved: 245.1536, 191.1067. $[M+[M+H+C_4H_6]+]$

Synthesis of 1,2-bis(4-(pent-4-en-1-yloxy)phenyl)ethane-1,2-dione 4

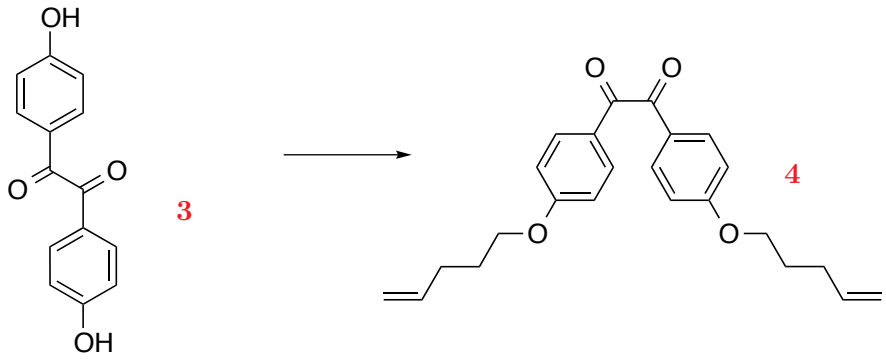

3 (0.5g, 2.1008 mmol) was mixed together in ethyl methyl ketone (20 mL) with bromopentene (1.26g, 1 mL, 0.4033 mmol) and potassium carbonate (1.742g, 0.126 mol). The solution was heated at reflux over night. The solution was removed from the heat and left to cool to room temperature. The carbonate was then filtered off and the solvent removed under vacuum, the crude oil was recrystallization from hexane with an excess of dichloromethane. The solid precipitate that formed when cooled at -4 °C overnight was the starting material **3**; the solid precipitate was filtered of and the filtrate was reduced under vacuum to yield the pure material.

Percentage Yield 0.71g, 90%

^{1}H-NMR (400 MHz, Chloroform-d) δ 7.86 (4 H, d, J 8.9), 6.89 (4 H, d, J 8.9), 5.76 (2 H, ddt, J 16.9, 10.2, 6.6), 5.04 – 4.89 (4 H, m), 3.97 (4 H, t, J 6.4), 2.16 (4 H, q, J 6.9), 1.83 (4 H, p, J 6.6).

^{13}C-NMR (101 MHz, Chloroform-d) δ 193.62, 164.47, 137.47, 132.42, 126.21, 115.59, 114.80, 67.64, 30.02, 28.19.

Masss pectrometry- Theoretical: 379, 380, 381, 382. Observed: 377, 378, 379, 380, 381. accurate mass Theoretical: 379.1904. Obeserved: 379.1905.

Synthesis of 4'-((11-(1,1,3,3-tetramethyldisiloxanyl)undecyl)oxy)-[1,1'-biphenyl]-4-carbonitrile

11

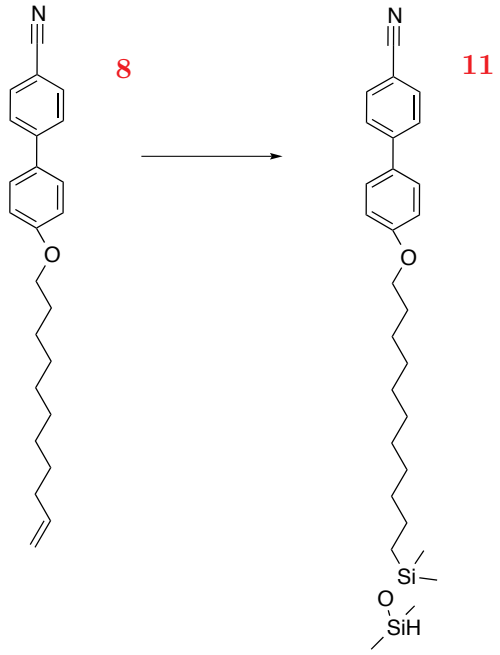

8 (2g, 0.006mol) was dissolved in dry toluene (70 mL), to this the Karstedt's catalyst (40 µL) was added and anhydrous air bubbled through for five minutes, to this solution the 1,1-3,3-tetramethyldisiloxane (32 mL) was added. The solution was stired over night in an inert atmosphere at room temperature. The solvent was removed under vacuum and the resulting solid was purified by column chromatography with DCM : hexane, 1:1 as eluent.

Percentage Yield 2.5g, 90%

^{1}H-NMR (400 MHz, Chloroform-d) δ 7.69 (4 H, d, J 8.6), 7.52 (2 H, d, J 8.8), 6.99 (2 H, d, J 8.8), 4.67 (2 H, q, J 2.8), 4.00 (2 H, t, J 6.6), 1.86 – 1.74 (2 H, m), 1.46 (2 H, q, J 7.1, 6.4), 1.40 – 1.23 (14 H, m), 0.52 (6 H, t, J 7.7), 0.16 (6 H, d, J 2.8), 0.06 (1 H, s).

The results were found to be in line with the previous data.[56] Due to the high reactivity of the siloxane group the material was used with no further analysis.

Synthesis of 2-(4-(but-3-en-1-yloxy)phenyl)-4,5-bis(4-(pent-4-en-1-yloxy)phenyl)-1*H*-imidazole

9

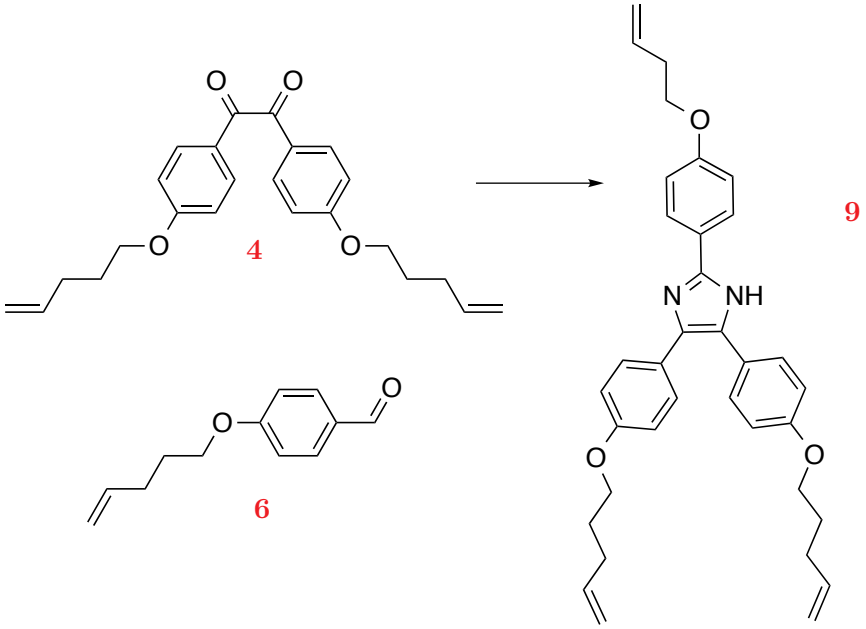

4 (0.9g, 2.625 mmol) with **6** (0.5g, 2.66 mmol) and ammonium acetate (2.2g, 26.25 mmol) was dissolved in glacial acetic acid under sonication. This solution was then transferred to a microwave reactor heated at 150 °C at 827kPa for 20 minutes, then cooled to 40 °C for 5 minutes. The solution was then added drop wise to a concentrated ammonia solution (in excess), the precipitate was removed and dissolved in dichloromethane, a TLC in ethyl acetate: hexane, 1:3 indicated there were impurities. The solvent was removed and then purified by column chromatography with ethyl acetate : heaxane, (1:3) as the eluent.

Percentage Yield 0.57g, 60%

^{1}H-NMR (400 MHz, Acetone-d6) δ 8.02 (4 H, d, J 8.9), 7.49 (2 H, d, J 8.7), 7.00 (4 H, d, J 8.9), 6.95 – 6.86 (2 H, m), 5.90 (3 H, ddt, J 17.0, 10.2, 6.7), 5.07 (3 H, dd, J 17.2, 1.9), 4.98 (3 H, dd, J 10.2, 2.0), 4.04 (6 H, dt, J 12.9, 6.4), 2.25 (6 H, q, J 7.4), 2.05 (3 H, q, J 2.2), 1.93 – 1.82 (6 H, m).

mass spectrometry- Theoretical data: 534, 536. Observed data: 534, 536, 537. [M]

Synthesis of 2,2',4,4',5,5'-hexakis(4-(hex-5-en-1-yloxy)phenyl)-2*H*,2'*H*-2,2'-biimidazole

10

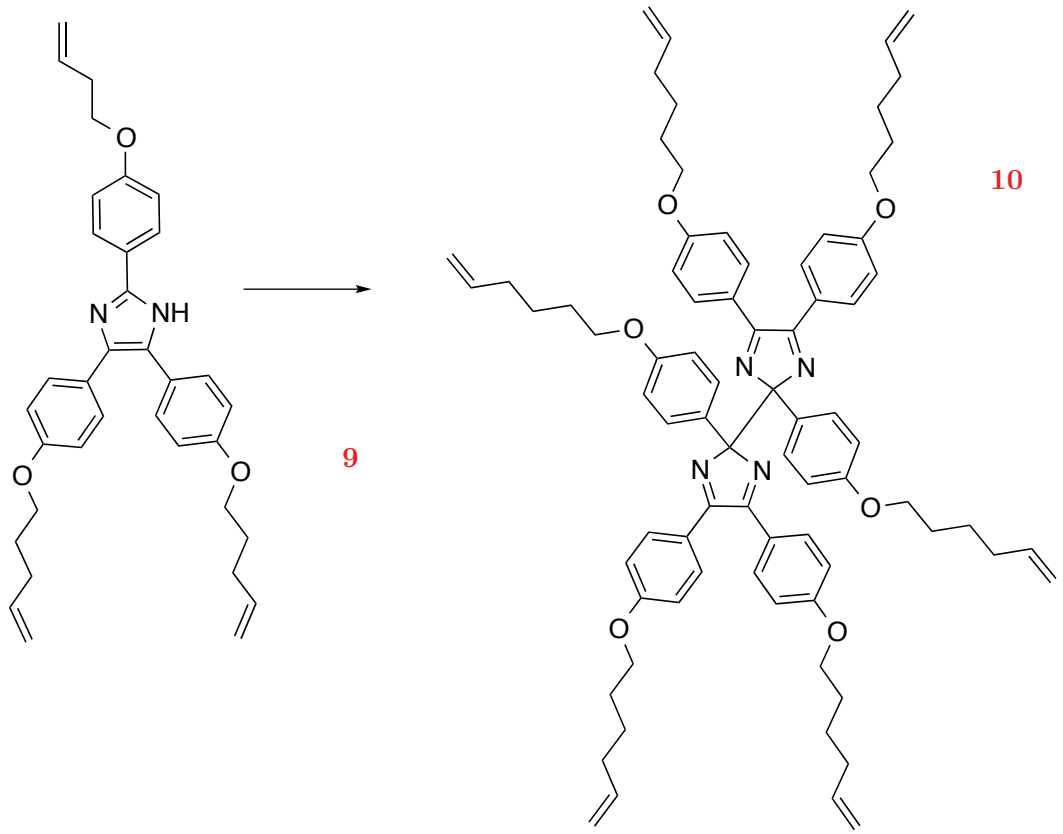

9 (0.051g, 0.0932 mmol) was dissolved in potassium hydroxide (0.40g, 7.28 mmol) solution in ethanol (6 mL). This solution was gently heated, left to cool then added drop wise to a potassium ferricyanide(III) (0.2g, 0.607 mmol) solution in water (30 mL) at 5 °C, not allowing the temperature to rise above 10 °C. The precipitate was removed and washed with cold ethanol: water (50 mL) 1:1 solution. This was then dried under reduced pressure.

Percentage Yield 0.071g, 70%

^{1}H-NMR (400 MHz, Chloroform-d) δ 8.28 (4 H, d, J 8.7), 7.69 (4 H, d, J 8.9), 7.35 (4 H, d, J 8.8), 7.02 (4 H, d, J 8.8), 6.79 (4 H, d, J 8.9), 6.67 (4 H, d, J 8.9), 5.98 – 5.70 (6 H, m), 5.17 – 4.90 (12 H, m), 4.19 – 3.58 (12 H, m), 2.45 – 2.05 (12 H, m), 2.01 – 1.74 (12 H, m), 1.75 – 1.65 (12 H, m).

Synthesis of 12

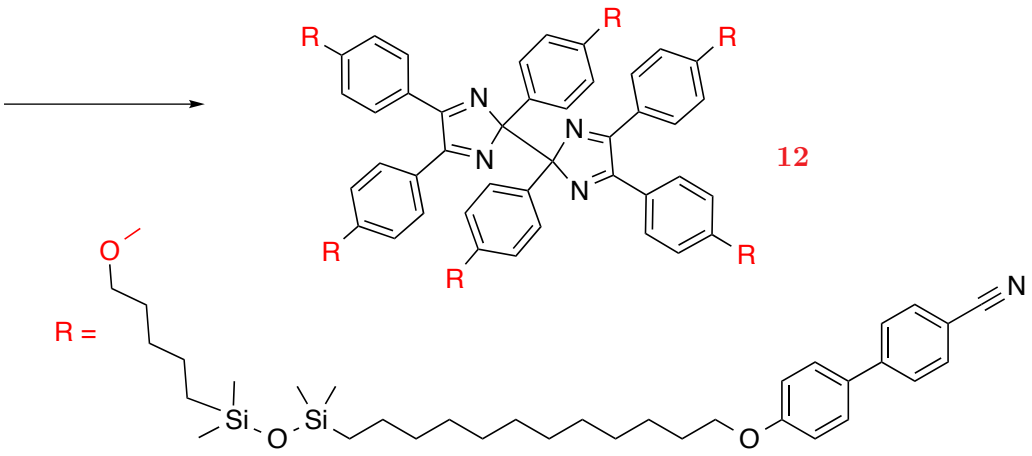

10 (0.0834g, 0.016 mmol) was dissolved with the Karstedt's catalyst (20 µL) in dry toluene (20 mL), air was then bubbled through the solution for five minutes and **11** (0.493g, 0.192 mmol) was added drop wise. After stirring at room temperature for 16 hours the solvent was removed under reduced pressure and the crude product purified by column chromatography in 4:1 (hexane : ethyl acetate). This was followed by recrystallized in neat hexane to give the product.

Percentage Yield 0.045g, 15%

^{1}H-NMR (400 MHz, Acetone-d6) δ 0.07 (19 H, d, J 5.1), 0.35 – 0.95 (10 H, m), 1.38 (28 H, d, J 60.5), 1.76 (8 H, dd, J 14.0, 7.4), 2.86 (11 H, s), 3.65 – 4.30 (8 H, m), 6.89 (3 H, d, J 8.2), 7.00 (5 H, t, J 8.3), 7.49 (0 H, s), 7.64 (4 H, d, J 8.7), 7.78 (5 H, s), 8.05 (1 H, d, J 8.7).

^{13}C-NMR (400 MHz, Acetone-d6) δ 0.15, 18.21, 25.99, 29.15, 33.36, 67.91, 115.13, 127.07, 128.37, 132.66, 205.32.

Elemental analysis- predicted for $C_{246}H_{348}N_{10}O_{18}Si_{12}$ –C-72.53, H-8.22, N-3.52% experimental- C-72.26, H-8.47, N-3.27%

Mass spectrometry - 1994 m/z for the monomer. 4064 m/z for the dimer + ammonium acetate NH_4OAc.

Synthesis of (4-(pent-4-en-1-yloxy)phenyl)methanol 31

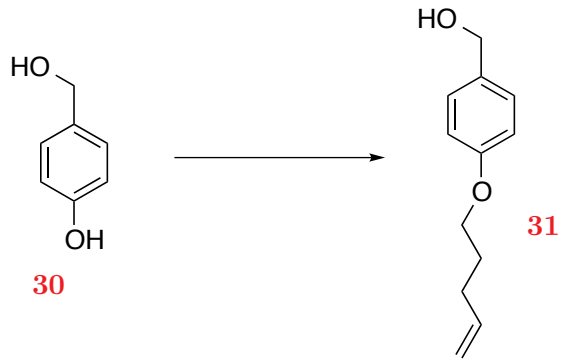

4-Hydroxybenzylalcohol (5.5g, 0.0436 mol), bromopentene (5g, 0.0335 mol), potassium carbonate (23.5g, 0.1675 mol) and potassium iodide (catalytic amount) were dissolved in ethyl methyl ketone and heated to reflux for 16 hours. Once collected, the solid was filtered off and the solvent removed under vacuum. The crude material was purified via columb chromatography using ethanol : hexane (1:100) as the eluent.

Percentage Yield 5.02g, 60%

^{1}H-NMR (400 MHz, Chloroform-d) δ 1.80 (2 H, p, J 6.6), 2.16 (2 H, q, J 6.9), 3.88 (2 H, t, J 6.4), 4.48 (2 H, s), 4.90 – 5.03 (3 H, m), 5.78 (1 H, ddt, J 16.9, 10.2, 6.6), 6.79 (2 H, d, J 8.6), 7.18 (2 H, d, J 8.5).

^{13}C-NMR (101 MHz, Chloroform-d) δ 158.44, 137.88, 133.62, 128.59, 115.25, 114.47, 67.25, 64.42, 30.15, 28.45.

mass spectrometry- Theoretical data: 15, 216, 217, 218. Observed data: 213, 214, 215, 216, 217. $[M + Na]+$.

Synthesis of 1-(bromomethyl)-4-(pent-4-en-1-yloxy)benzene 32

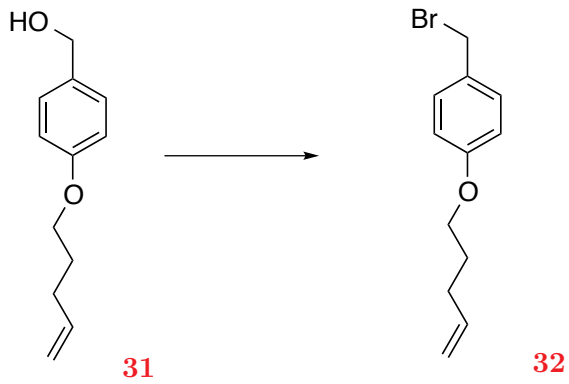

31 32

31 (3g, 0.0156 mol) was dissolved in dry THF (40 mL) and cooled to -5 °C, to this solution phosphorus tribromide (6.21g, 2.2 mL, 0.0234 mol) was added dropwise over 20 minutes, after 5 minutes the solution was left to cool to room temperature. The organics were extracted with DCM and washed with brine and water, then dried over magnesium sulphate. The solvent was removed under vacuum. The crude material was purified via columb chromatography using DCM : hexane (1:10) as the eluent.

Percentage Yield 1.56g, 40%

^{1}H-NMR (400 MHz, Chloroform-d) δ 7.30 (2 H, d, J 8.9), 6.87 (2 H, d, J 9.1), 5.93 – 5.77 (1 H, m), 5.12 – 4.97 (2 H, m), 4.51 (2 H, s), 3.97 (2 H, t, J 6.4), 2.31 – 2.19 (2 H, m), 1.93 – 1.82 (2 H, m).

Synthesis of 4'-((4-(pentyloxy)benzyl)oxy)-[1,1'-biphenyl]-4-carbonitrile 33

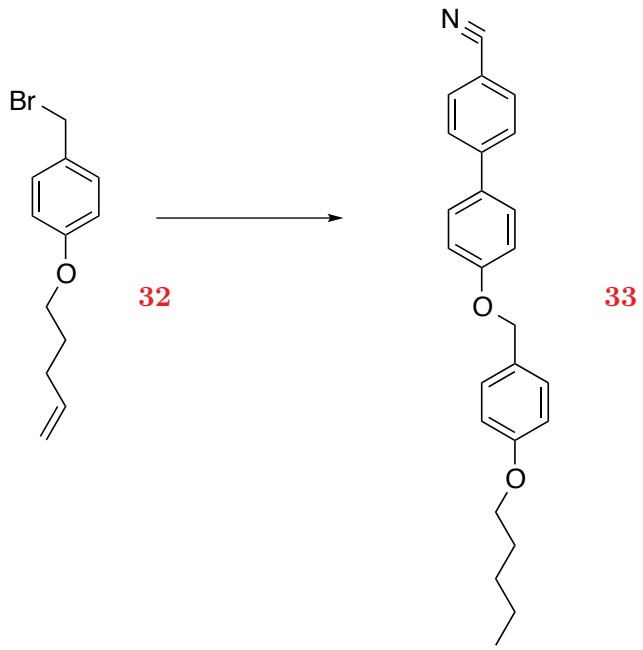

32 (0.54g, 2.11 mmol), cyanobiphenol (0.62g, 3.176 mmol) and potassium carbonate (1.5g, 10.55 mmol) were dissolved in ethyl methyl ketone and heated to reflux for 16 hours, once cooled the solid was filtered off and the solvent removed under vacuum, the resulting crude product was purified via column chromatography with 2:1 hexane: ethyl acetate as the eluent.

Percentage Yield 0.311g, 40%

^{1}H-NMR (400 MHz, Chloroform-d) δ 7.68 (2 H, d, J 8.4), 7.63 (2 H, d, J 8.4), 7.53 (2 H, d, J 8.7), 7.37 (2 H, d, J 8.6), 7.07 (2 H, d, J 8.8), 6.93 (2 H, d, J 8.5), 5.87 (1 H, ddt, J 16.9, 10.2, 6.6), 5.68 – 5.45 (2 H, m), 5.04 (2 H, s), 4.11 – 3.89 (2 H, m), 1.97 – 1.84 (2 H, m), 1.54 – 1.33 (2 H, m).

Synthesis of 4'-((4-((5-(1,1,3,3-tetramethyldisiloxanyl)pentyl)oxy)benzyl)oxy)-[1,1'-biphenyl]-4-carbonitrile

34

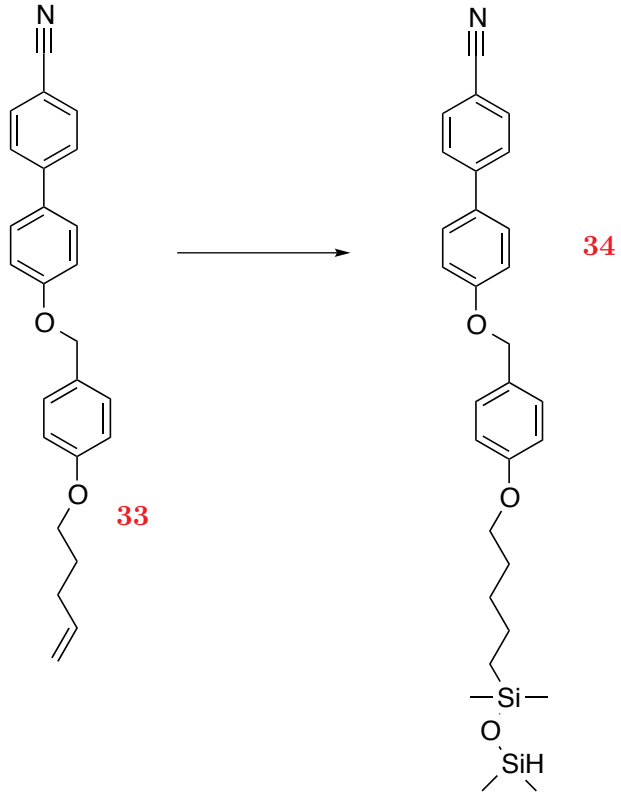

33 (0.2g, 0.54 mmol) was dissolved in dry toluene (70 mL), to this the Karstedt's catalyst (5 µL) was added and anhydrous air was bubbled through for five minutes. To this solution the 1,1,3,3-tetramethyldisiloxane (2.9g, 3.81 mL, 0.021 mol) was added and the solution stirred overnight in an inert atmosphere at room temperature. The solvent was removed under vacuum and the resulting solid was purified by column chromatography using DCM : Hexane, 1:1 as the eluent.

Percentage Yield 0.244g, 90%

^{1}H-NMR (400 MHz, Chloroform-d) δ 7.68 (2 H, d, J 8.2), 7.63 (2 H, d, J 8.3), 7.53 (2 H, d, J 8.6), 7.36 (2 H, d, J 8.5), 7.06 (2 H, d, J 8.7), 6.92 (2 H, d, J 8.5), 5.03 (2 H, s), 3.96 (2 H, t, J 6.6), 1.90 – 1.70 (2 H, m), 1.54 – 1.39 (2 H, m), 1.43 – 1.32 (6 H, m), 0.64 – 0.49 (6 H, m), 0.06 (1 H, s).

The results where found to be in line with the previous data.[56] Due to the high reactivity of the siloxane group the material was used with no further analysis.

Synthesis of 2-(4-bromophenyl)-1,3-dioxolane 29

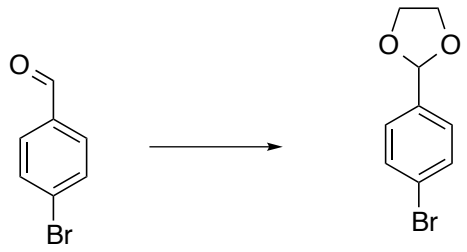

28 29

4-Bromobenzaldehyde (1g, 4.56 mmol), ethylene glycol (3.46g, 3.1 mL, 55.81 mmol) and p-toluenesulfonic acid (catalytic amount) were dissolved in dry toluene (20 mL) heated to 167 °C and the water removed using a Dean Stark trap for 16 hours. Once cooled the organics were extracted into ethyl acetate and washed with water and then sodium bicarbonate and brine. The organic layer was then dried over magnesium sulphate. The magnesium sulphate was filtered off and the solvent removed under reduced pressure. ^{1}H NMR showed that no reaction had occurred. The approach was abandoned.

Synthesis of 1-bromo-4-(but-3-en-1-yl)benzene 14

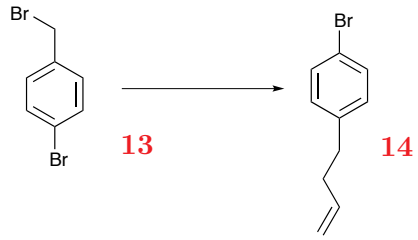

4-Bromobenzyl bromide (2g, 0.008 mol) was dissolved in dry diethyl ether (10 mL). To this solution allyl magnesium bromide (10 mL, 1M, 0.08 mol) was added dropwise under an inert atmosphere. The reaction was stirred for 3-4 hours and then quenched with water. The quenched reaction mixture was extracted with diethyl ether, washed with water and brine and dried over magnesium sulphate. The solvent was removed under vacuum and the crude product was purified using column chromatography, hexane: ethyl acetate, 10:1 as the eluent.

Percentage Yield 1.1g, 65%

^{1}H-NMR (400 MHz, Chloroform-d) δ 7.42 (2 H, d, J 8.3), 7.08 (2 H, d, J 8.5), 5.85 (1 H, ddt, J 16.9, 10.2, 6.6), 5.12 – 4.97 (2 H, m), 2.69 (2 H, t, J 8.2, 7.2), 2.44 – 2.31 (2 H, m).

^{13}C-NMR (101 MHz, Chloroform-d) δ 140.85, 137.69, 131.43, 130.32, 119.65, 115.40, 35.38, 34.85, 1.14.

GC retention time - 7.48

Mass spectrometry- Theoretical: 210, 212, 211, 213, 214. Observed: 207, 210, 212, 210, 213. accurate mass Theoretical: 210.0044, 212.0044. Obeserved: 210.0050, 212.0031. $[M]$

Synthesis of 4-(but-3-en-1-yl)benzaldehyde 19

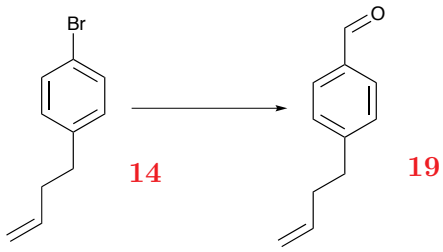

14 (5g, 0.0238 mol) was dissolved in dry THF (90 mL) and cooled to -78 °C in an inert atmosphere. *n*-butyllithium (10.61 mL, 2.5 M) was added over ten minutes and the solution was then stirred for an hour. To this DMF (Dimethylformamide) (2.5 mL) was added drop wise, the solution was then stirred for an hour and the reaction temperature was allowed to rise. Once at room temperature the reaction was quenched with water (70 mL), the organics were extracted with diethyl ether. The organic layer was washed with water and then brine and dried over magnesium sulphate. The solid was filtered off and the solvent removed under vacuum, the crude product was purified via column chromatography using dichloromethane: hexane, 1:1 as the eluent.

Percentage Yield 2.284g, 60%

^{1}H-NMR (400 MHz, Chloroform-d) δ 9.92 (1 H, s), 7.76 (2 H, d, J 8.1), 7.31 (2 H, d, J 8.3), 5.80 (1 H, ddt, J 16.9, 10.2, 6.6), 5.06 – 4.91 (2 H, m), 2.75 (2 H, t, J 7.8, 7.1), 2.37 (2 H, q, J 7.6, 7.3, 6.8).

^{13}C-NMR (101 MHz, Chloroform-d) δ 192.06, 138.09, 137.29, 130.27, 129.96, 129.84, 129.20, 128.61, 128.46, 128.40, 128.32, 125.84, 115.56, 114.93, 35.58, 35.44.

Synthesis of 2,4,5-tris(4-(but-3-en-1-yl)phenyl)-1H-imidazole 26

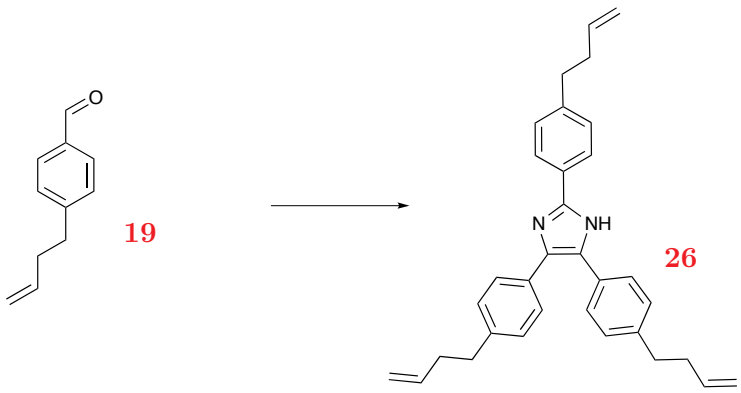

19 (0.16g, 1 mmol) was mixed with (HMDS) Bis(trimethylsilyl)amine (0.1771g, 0.23 mL, 1.1 mmol) and added to a solution of iodine (0.253g, 1.1 mmol) in acetonitrile (3 mL). The solution was heated to reflux for 4 hours. Once cooled to room temperature, the solution was washed with sodium thiosulphate and then extracted with diethyl ether and washed with water and brine, then dried over magnesium sulphate. The solvent was removed under vacuum and the crude product checked by TLC against the starting material, this showed no reaction. The approach was abandoned.

Synthesis of 1,2-bis(4-(but-3-en-1-yl)phenyl)-2-hydroxyethan-1-one 27

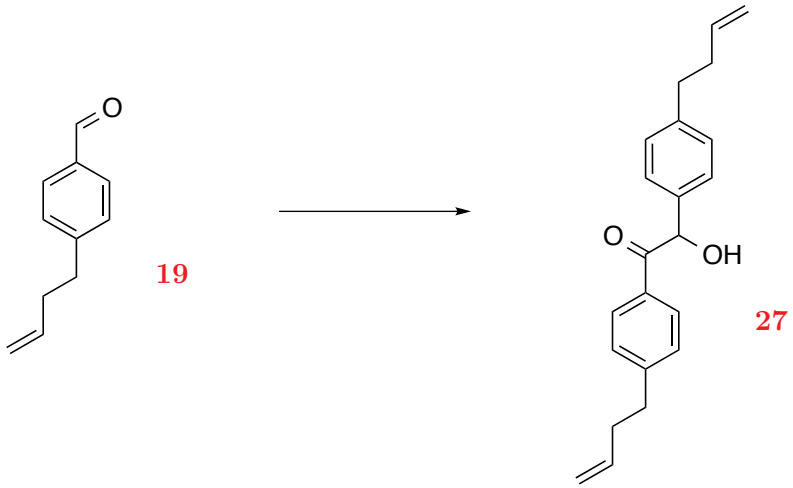

19 (1g, 6.25 mmol), potassium cyanide (0.25g, 3.93 mmol) were dissolved in ethanol: water (15 mL: 15 mL) and heated to reflux for 5 days, once cool the solution was extracted with chloroform and washed with plenty of water and brine, then dried over sodium sulphate. The solvent was removed under vacuum and the crude product was purified via column chromatograpthy using dichloromethane: hexane. ^{1}H-NMR showed no product was formed. The approach was abandoned.

Synthesis of ((4-(but-3-en-1-yl)phenyl)ethynyl)trimethylsilane 15

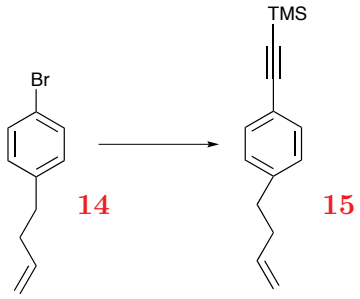

14 (0.5g, 2.369 mmol), copper iodide (0.0134g, 0.071 mmol) and *trans*-dichlorobis triphenylphosphine palladium (II) (0.049g, 0.071 mmol) were placed in a reaction vessel, the atmosphere evacuated and then refilled with dry nitrogen. To this triethylamine (degassed) (12 mL) was added and the solution heated to 50 °C and trimethylsilylacetalene (1.16g, 1.63 mL, 11.845 mmol) was added drop wise and the solution was heated to 70 °C for 16 hours. Once cool the solvent was removed under vacuum and the crude product purified by column chromatography unsing dichrloromethane: hexane (1: 10) as the eluent.

Percentage yield 0.17g, 31%,

^{1}H-NMR (400 MHz, Chloroform-d) δ 7.39 (2 H, d, J 8.0), 7.11 (2 H, d, J 7.9), 5.82 (1 H, ddt, J 16.9, 10.2, 6.6), 5.07 – 4.92 (2 H, m), 2.70 (2 H, t, J 7.6), 2.35 (2 H, q, J 7.0), 0.25 (1 H, s).

^{13}C-NMR (101 MHz, Chloroform-d) δ 142.62, 137.78, 132.04, 128.47, 120.62, 115.31, 105.41, 77.46, 77.14, 76.82, 35.40, 35.34, 0.14.

GC retention time- 9.17

Mass spectrometry- Theoretical: 228, 229, 230, 230, 232. Observed: 228, 229, 230. accurate mass Theoretical: 228.1334. Obeserved: 228.1338. [M]

Synthesis of 1-(but-3-en-1-yl)-4-ethynylbenzene 16

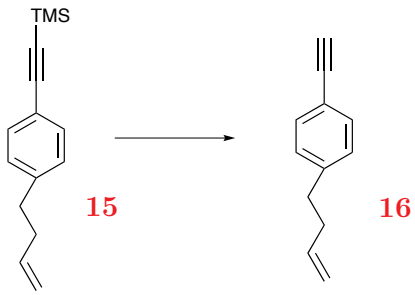

15 (0.1665g, 0.730 mmol) was dissolved in DMF (4 mL) .to this solution potassium flouride in a minimum amount of water (0.169g, 2.921 mmol) was added drop wise and the solution stirred at room temperature for 2 hours. The organics were then extracted with ethyl acetate and washed with water and brine and dried over magnesium sulphate. The solvent was removed under vacuum. The product was used with no further purification.

Percentage yield of 0.11g, 95%

^{1}H-NMR (400 MHz, Chloroform-d) δ 7.35 (2 H, d, J 8.1), 7.09 (2 H, d, J 7.9), 5.77 (1 H, ddt, J 16.9, 10.2, 6.6), 5.02 – 4.88 (2 H, m), 2.97 (1 H, s), 2.66 (2 H, t, J 7.8), 2.36 – 2.26 (2 H, m).

^{13}C-NMR (101 MHz, Chloroform-d) δ 142.95, 137.76, 132.21, 128.59, 119.62, 115.36, 83.90, 77.49, 77.17, 35.37, 35.31.

GC retention time- 6.97

Mass spectrometry- Theoretical: 158, 157, 158, 159. Observed: 158, 157. accurate mass Theoretical: 156.0939. Obeserved: 158.0946. $[M]$

Synthesis of 1,2-bis(4-(but-3-en-1-yl)phenyl)ethyne 17

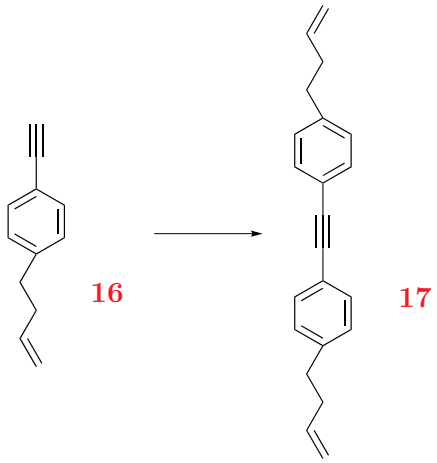

16 (1.06359g, 6.849 mmol) **14** (4.356g, 20.54 mmol), copper iodide (0.093g, 0.205 mmol) and *trans*-dichlorobis(triphenylphosphine palladium (II) (0.1452g, 0.205 mmol) were placed in a reaction vessel and the atmosphere evacuated and then refilled with dry nitrogen, to this triethylamine (degassed) (24 mL) was added and the solution was heated to 70 °C for 16 hours. Once cooled to room temperature the solvent was removed under vacuum and the crude product purified by column chromatography using dichloromethane: hexane (1:10) as the eluent.

Percentage yield 0.66g, 34%

^{1}H-NMR (400 MHz, Chloroform-d) δ 7.48 (4 H, d, J 8.0), 7.19 (4 H, d, J 7.9), 5.88 (2 H, ddt, J 16.9, 10.2, 6.6), 5.14 – 4.99 (4 H, m), 2.79 – 2.70 (4 H, m), 2.46 – 2.37 (4 H, m).

^{13}C-NMR (101 MHz, Chloroform-d) δ 140.88, 137.71, 131.47, 130.36, 128.63, 119.70, 115.45, 89.17, 35.42, 34.88.

Mass spectrometry- Theoretical: 287, 288, 289, 290. Observed: 286, 287,288,289. [$M+H$]

Synthesis of 1,2-bis(4-(but-3-en-1-yl)phenyl)ethane-1,2-dione 18

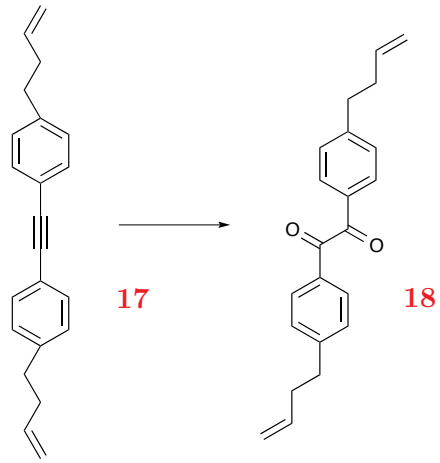

17 18

17 (0.79g, 2.79 mmol) was dissolved in DMSO (3 mL) with palladium (II) acetate $Pd(OAc)_2$ (0.1877g, 0.279 mmol) and copper bromide CuBr (Copper bromide) (0.06g, 0.297 mmol) and heated to 120 °C for 20 hours. Once the reaction had cooled to room temperature the solution was extracted with ethyl acetate and washed with water, then brine, and dried over anhydrous sodium sulphate. The solvent was removed under vacuum and the crude product purified by column chromatography using hexane: dichloromethane (10: 1) as the eluent.

Percentage Yield 0.34g, 45%

^{1}H-NMR (400 MHz, Chloroform-d) δ 7.89 (4 H, d, J 8.1), 7.39 – 7.29 (4 H, m), 5.82 (2 H, ddt, J 16.9, 10.2, 6.6), 5.12 – 4.91 (4 H, m), 2.84 – 2.68 (4 H, m), 2.39 (4 H, q, J 7.9, 7.1).

^{13}C-NMR (100 MHz, Chloroform-d) δ 194, 149, 137, 131, 130, 129, 115, 77, 76, 35, 34.

Mass spectrometry- Theoretical: 319, 320, 321, 322. Observed: 311, 319, 320, 321. accurate mass Theoretical: 319.1698. Obeserved: 319.1697. $[M + H]$

synthesis of 4'-(pent-4-en-1-yloxy)-[1,1'-biphenyl]-4-carbonitrile 22

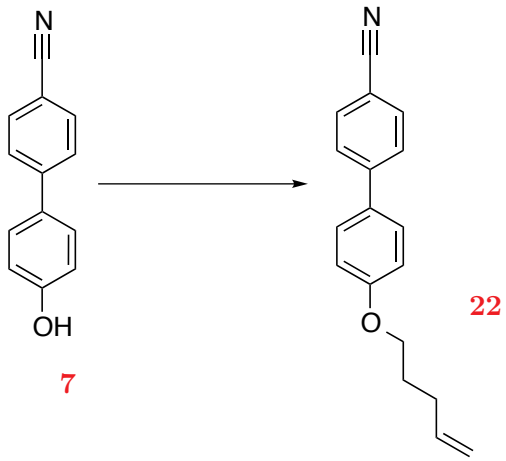

4'-Cyano-4-biphenol (5.5g, 0.0436 mol), bromopentene (5g, 0.0335 mol), potassium carbonate (23.5g, 0.1675 mol) and potassium iodide (catalytic amount) were dissolved in ethyl methyl ketone and heated to reflux for 16 hours. Once cooled the solid was filtered off and the solvent removed under vacuum. The crube material as purified via column chromatography using dichloromethane : hexane (1:1) as the eluent.

Percentage Yield 5.02g, 60%

^{1}H-NMR (400 MHz, Chloroform-d) δ 1.92 (2 H, p, J 6.9), 2.27 (2 H, q, J 7.3), 4.02 (2 H, t, J 6.4), 4.98 – 5.15 (2 H, m), 5.87 (1 H, ddt, J 16.9, 10.2, 6.6), 6.99 (2 H, d, J 8.7), 7.52 (2 H, d, J 8.6), 7.60 – 7.71 (4 H, m).

^{13}C-NMR (101 MHz, Chloroform-d) δ 159.81, 145.36, 137.78, 132.66, 131.44, 128.43, 127.17, 119.21, 115.43, 115.20, 110.15, 67.41, 30.18, 28.46.

Mass spectrometry- Theoretical: 281, 282, 283, 284. Observed: 281, 282, 283. accurate mass Theoretical: 281.1654. Obeserved: 281.1650. $[M + NH_4+]$

Synthesis of 4'-((5-(1,1,3,3-tetramethyldisiloxanyl)pentyl)oxy)-[1,1'-biphenyl]-4-carbonitrile

23

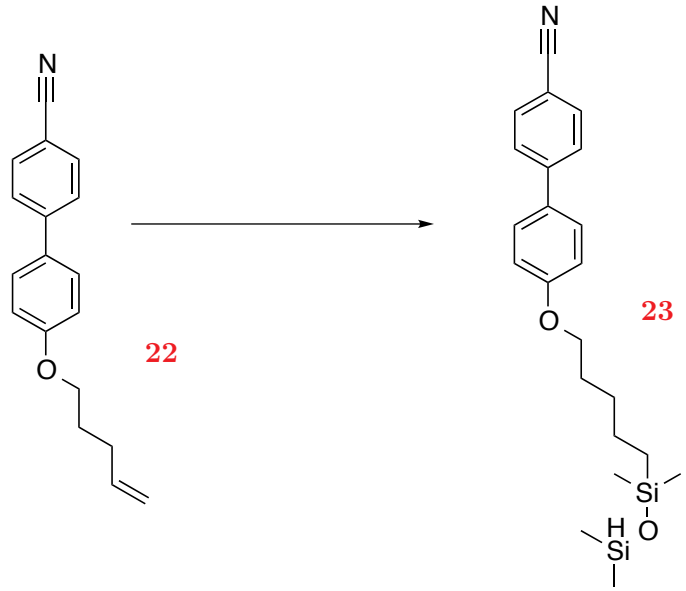

22 (2g, 7.604mmol) and Kastedt's catalyst (in xylene, Pt 2%) (40µL) was dissolved in toluene (70mL). Air was bubbled through the solution for 5 mins, to this solution 1,1,3,3-tetramethyldisiloxane (53mL, 0.3041mmol) was added and the solution was heated to 40°C for 16 hours. The solvent was removed under reduced pressure and used with no further purification.

Percentage Yield 7.3g, 95%

^{1}H-NMR (400 MHz, Chloroform-d) δ 7.65 (dd, J = 13.4, 8.4 Hz, 4H), 7.52 (d, J = 8.9 Hz, 2H), 6.98 (d, J = 8.5 Hz, 2H), 3.99 (t, J = 6.1 Hz, 2H), 1.93 – 1.72 (m, 2H), 1.54 – 1.34 (m, 2H), 0.94 (t, J = 7.0 Hz, 6H), 0.65 – 0.46 (m, 6H), 0.07 (s, 1H).

The results were found to be in line with the previous data.[56] Due to the high reactivity of the siloxane group the material was used with no further analysis.

Synthesis of 2,4,5-tris(4-(but-3-en-1-yl)phenyl)-*1H*-imidazole 20

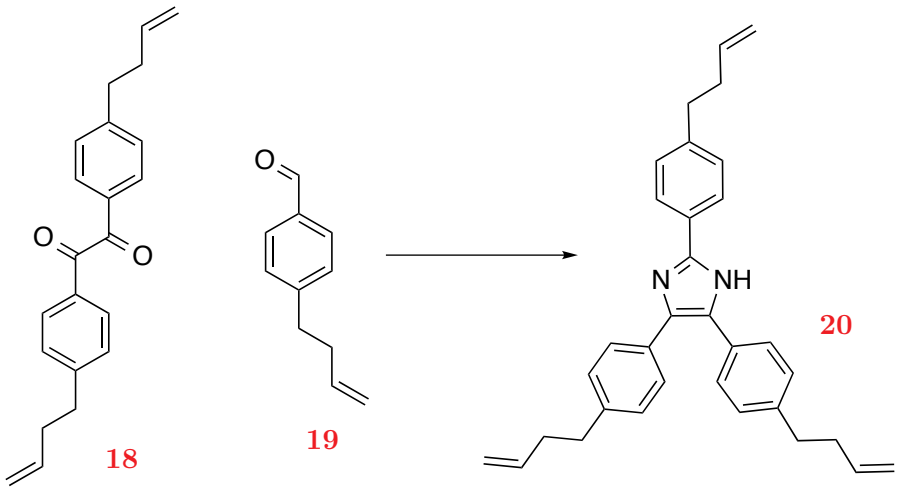

18 (0.1907g, 0.59 mmol) with **19** (0.095g, 0.59 mmol) and ammonium acetate (0.129g, 5.9 mmol) were dissolved in glacial acetic acid (5 mL) under sonication. This solution was then transferred to a microwave reactor and heated at 150°C at 827kPa for 20 minutes, then cooled to 40°C for a further 5 minutes. The solution was then added drop wise to a concentrated ammonia solution (in excess), the precipitate was removed and dissolved in DCM, a TLC in ethyl acetate: Hexane, 1:3 indicated there were impurities. The solvent was removed and then purified by column chromatography using DCM and the eluent, then the product was flushed off using methanol and recrystallised from methanol to yield the product.

Percentage yield 21.8%

^{1}H-NMR (400 MHz, Chloroform-d) δ 7.82 (2 H, d, J 8.1), 7.47 (6 H, d, J 7.4), 7.16 (4 H, d, J 7.8), 5.86 (3 H, ddd, J 16.6, 10.4, 6.1), 5.13 – 4.94 (6 H, m), 2.78 – 2.64 (6 H, m), 2.44 – 2.34 (6 H, m).

^{13}C NMR (101 MHz, Chloroform-d) δ 171.32, 149.91, 137.25, 130.30, 130.16, 129.24, 115.68, 35.61, 34.92.

Mass spectrometry- Theoretical: 459, 460, 461. Observed: 459, 460, 461. $[M+H]$

Synthesis of 2,2',4,4',5,5'-hexakis(4-(but-3-en-1-yl)phenyl)-2*H*,2'*H*-2,2'-biimidazole

21

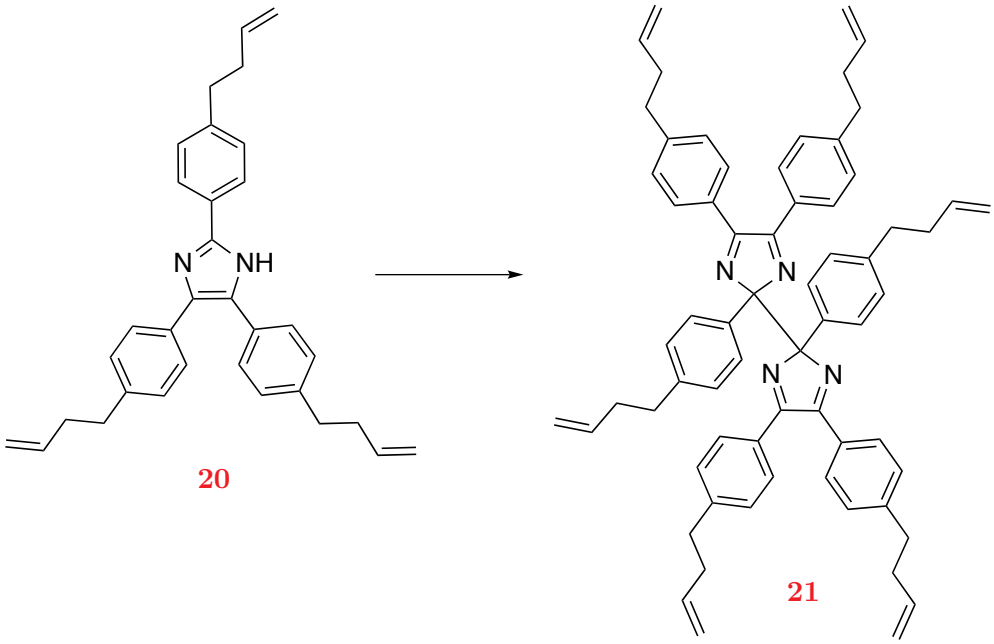

20 (0.1091g, 0.0238 mmol), potassium hydroxide (1.586g, 28 mmol), (potassium hexacyano ferrate) $K_3Fe(CN)_6$ (2.34g, 7.14 mmol) were dissolved in benzene (11 mL) and water (11 mL) the solution was stirred for 2 hours. The cooled solution was extracted with ethyl acetate and washed with water (2x) then brine (2x). The solvent was then removed under vacuum to yield a solid. The solid was then crystalised from hot hexane, the product was used with no further purification.

^{1}H-NMR (400 MHz, Chloroform-d) δ 7.14 (20 H, dd, J 20.7, 6.0), 6.70 (4 H, d, J 7.7), 5.81 (6 H, dd, J 16.9, 6.6), 5.10 – 4.86 (12 H, m), 2.66 – 2.52 (12 H, m), 2.49 (12 H, t, J 8.0, 7.5).

Confirmed by Mass spectrometry - 460 $[M + 2H^+]$, 916 $[M]$.

Synthesis of LC substituted HABI compound 24

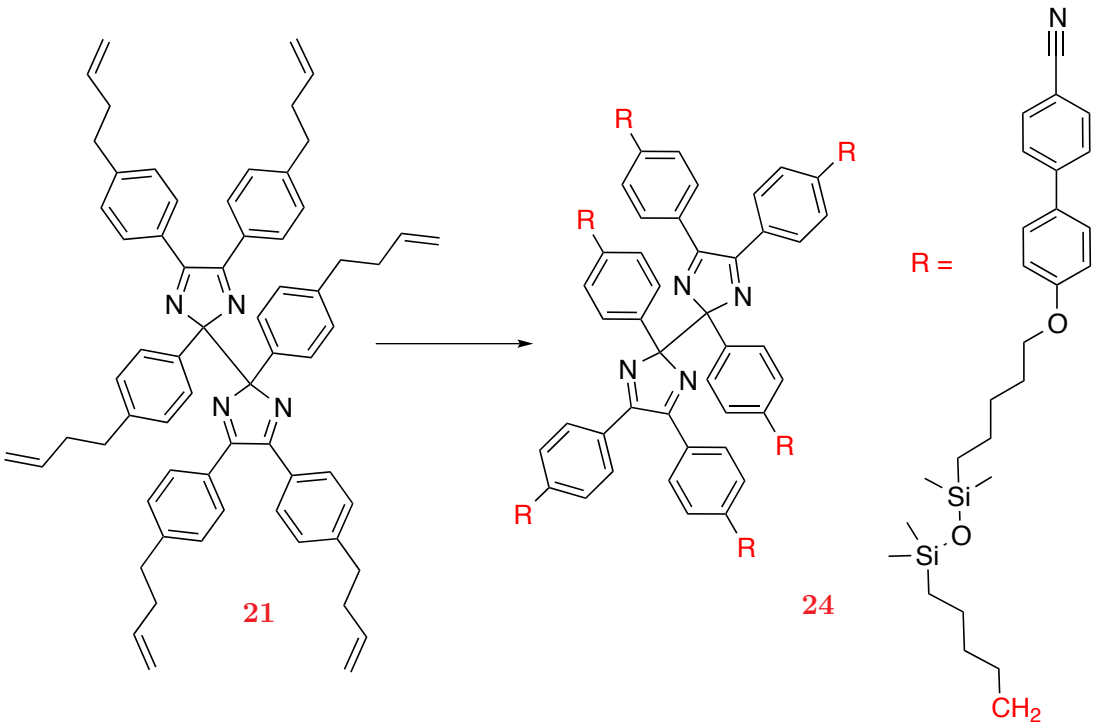

21 (0.0828g, 0.0903 mmol) was dissolved with the Karsted's catalyst (5 µL) in dry toluene (20 mL), air was then bubbled through the solution for five minutes and to this solution **23** (0.7081g, 1.807 mmol) was added drop wise. After stirring at room temperature for 16 hours the solvent was removed under reduced pressure and the crude product purified by column chromatography using 4:1 (hexane : ethyl acetate) as the eluent, this was followed by recrystallized in neat hexane to give the product.

Percentage Yield 0.1g 20%

^{1}H-NMR (400 MHz, Acetone-d6) δ 7.84 – 7.74 (24 H, m), 7.74 – 7.62 (24 H, m), 7.27 – 7.10 (16 H, m), 7.08 – 6.99 (8 H, m), 4.08 – 4.00 (12 H, m), 2.52 – 2.48 (12 H, m), 1.85 – 1.74 (12 H, m), 1.58 – 1.34 (12 H, m), 0.96 – 0.89 (18 H, m), 0.68 – 0.56 (18 H, m), 0.11 (12 H, t, J 2.3), 0.08 (72 H, s). (overlapping due to oligomeric type structure.)

^{13}C-NMR (101 MHz, Acetone-d6) δ 205.37, 132.69, 128.40, 127.11, 115.14, 67.89, 29.62, 29.42, 29.23, 29.04, 28.85, 28.66, 28.46, 0.59. (overlapping carbon peakes)

Mass spectrometry- observed: 3297, 3300, 3305. $[M + H]$

(half the molecular weight due to splitting during the analysis)

Mass spectrometry- Theoretical: 1589, 1590, 1591. Observed: 1589, 15890, 1591. $[1/2M + H]$

3.6 HABI Results

Two novel LC photochromic single molecule materials were synthesised and the properties of the materials were optimised. An LC phase was introduced and the photochromic properties were improved. The siloxane linking the mesogen and the HABI core was introduced to lower the melting point, it is well known in the literature that siloxanes have this effect. The lengthening of the hydrocarbon spacer was also increased to lower the melting point. The LC mesogen that was chosen was a cyanobiphenyl group, this was chosen as it has good LC phase inducing behaviour. The molecule was found to be liquid crystal at 48.3 °C exhibiting a SmA phase, see Figure 3.18. **12** is the first reported liquid crystal photochromic compound based on the HABI core show in Figure 3.18, with a fine but typical smetic A texture and this assignment is confirmed by the differential scanning calorimetry data. The DSC plot also shows that there is no crystal phase present and that a **SmA** phase at 48.3°C is formed with a transition to the isotropic phase at 60°C with an enthalpy value of 5.43 $\mathrm{J\,g^{-1}}$. The DSC trace shows a broad transition peak, shown in Figure 3.18, this is due to the large polymeric, oligomeric structure of the molecule. This broad transition on the the DSC is typical for oligomeric structures.

From the optical polarising micrograph recorded at 48.3°C using crossed polarisers shown in Figure 3.18 the typical focal conic defect textures of the smectic A phase can be seen with areas which are non birefringent, they are indicative of a homeotropic alignment under cross polarisers. They are indicative of areas where on average the moleculare long axis of the mesogens are parralel to the beam of light.

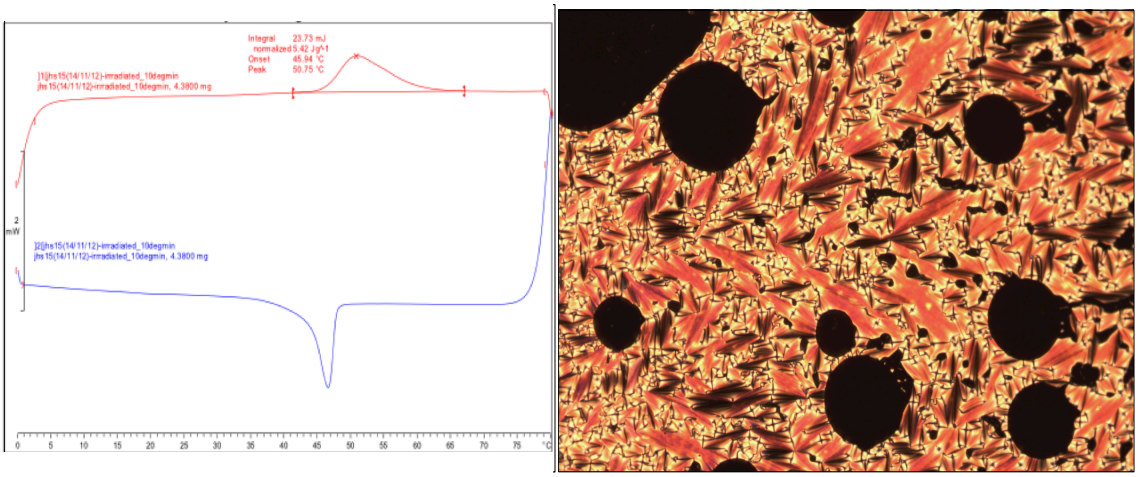

Figure 3.18. Right : DSC trace of **12** ΔH 1.68 J g^{-1}, area 23 78mJ, onset 44.54°C, peak 52.38°C , Left : OPM image of the LC phase, Smectic A, 48.3°C, 100x magnification.

The OPM images of **12** are in accord with the XRD data. The XRD data was collected from samples in capillaries (0.8µm) and alligned by an external magnet with a field strengh of 0.5T. The strength of the standard permanent cobalt-selenium magnets that are used to align liquid crystal samples, has a strong enough field to align nematic phases but typically not a smectic phase. The samples are in a micro furnace and the temperature is controlled with an accuracy of 0.5°C.[82,83] The data collection is carried out using a 2D image plate. A typical diffractogram is shown in Figure 3.19. The external magnetic field applied to the sample is vertical. The data shows that the sample is poorly aligned and this is attributed to the viscosity of the sample. The 2D allows us to calculate a pseudo 1D plot, this is shown in Figure 3.20.

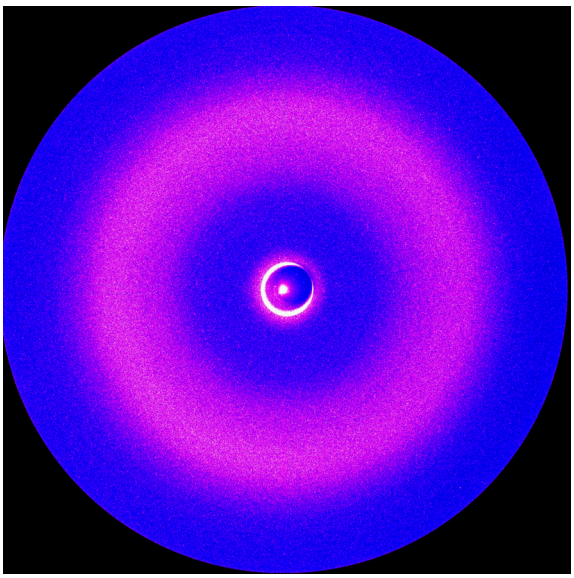

Figure 3.19. 2D XRD plot of **12**, taken at 48°C.

The 1D plot of **12** gives rise to three diffraction intensities, see Figure 3.20. In the small angle one reflection (A) can be seen, which is associated with the layer spacing of 31.2Å. In the wide angle the second intensity is seen (B), this can be attributed to the siloxane linker of 6Å. The siloxane group diffracts because of the higher electron density of the groups, than the hydrocarbon chains a microphase separation occurs. The broad pireodisity that can be seen in the wide angle region has a value of 4.6Å, which is associated with the intermolecular lateral distance of the molecules.

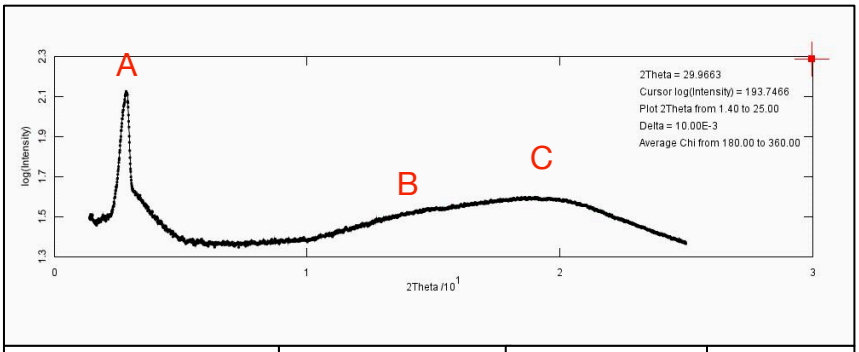

A	B	C	unit
31.2	6.0	4.6	Å
Smectic layer	Siloxane group	Intermolecular distance	

Figure 3.20. 1D XRD plot and table of **12**, taken at 48°C.

The photochromic properties of **12** were analyzed using UV-vis spectroscopy. The data was collected using a Varian Cary 50 UV-Vis spectrometer, and the sample was irradiated perpendicular to the sample via a mercury vapour light source monochromated to the desired wavelength. The red trace on see Figure 3.21, is pre-irradiation and has a strong absorption in the 330-360nm region, post-irradiation the green trace shows the appearance of the absorption at 430nm region and the reduction of the 350nm peak.

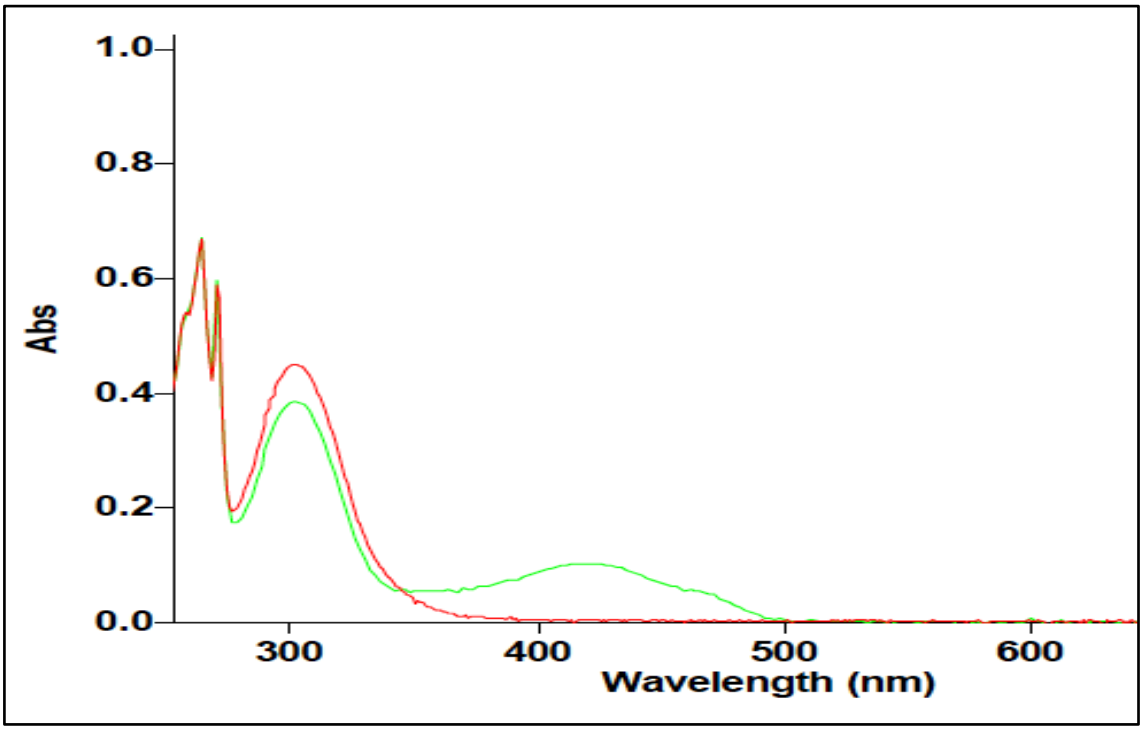

Figure 3.21. UV-Vis plot, **red** trace before irradiation, **green** after irradiation with 365nm light (mercury vapor lamp).

The structure of **24** was altered. This is shown in Figure 3.22 to improve the LC phase behavior and photochromic properties. The removal of the oxygen linking the hydrocarbon spacer to the HABI core resulted in an alteration to the photochromic properties, which can be seen by a red shift in the absorption spectrum post-irradiation.

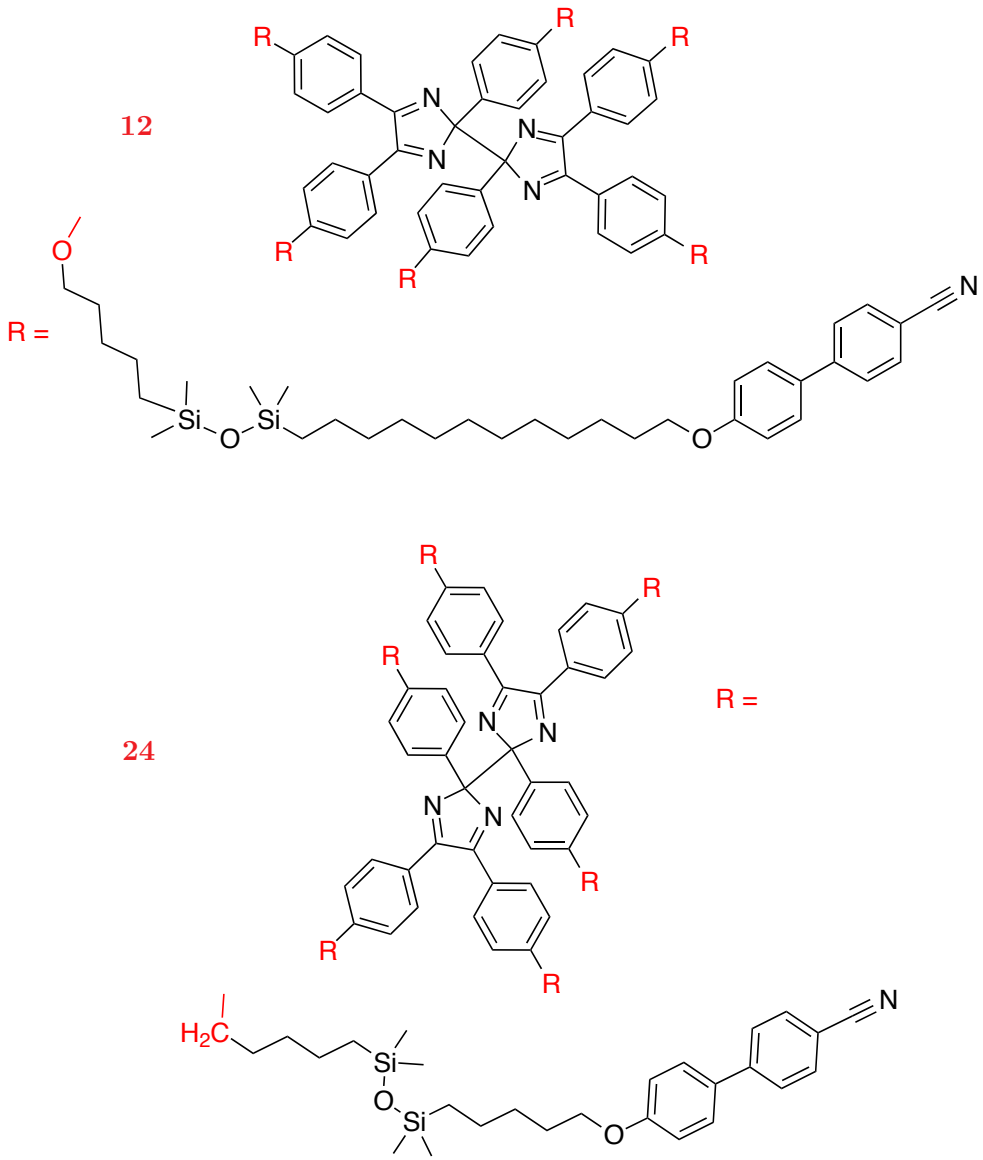

Figure 3.22. Structures of **12** and **24**.

This effect of the alteration of the absorption spectra and the association speed, of the radical species back to the dimer HABI. It is well reported in the literature that the alteration of the structure of HABI can greatly alter the photochromic properties as well as the absorption spectra.

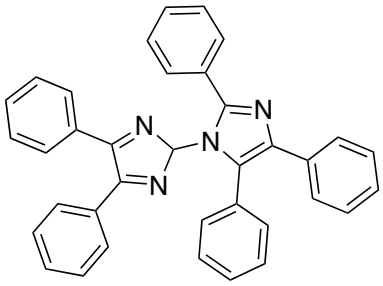

HABI refernce
absorption 325nm
$t_{1/2}$ 12hr+

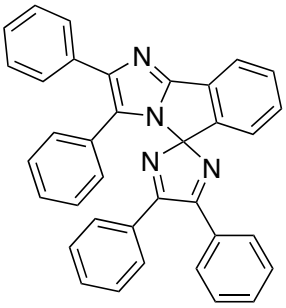

PABI1 absorption 750nm
$t_{1/2}$ 2x10^{-4}s

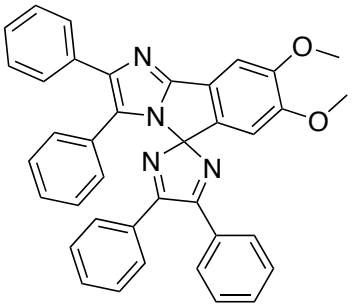

PABI2 absorption 780nm
$t_{1/2}$ 10.1x10^{-3}s

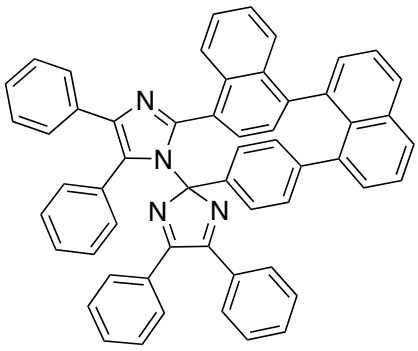

1,8-NDPI-TPI absorption 450nm
$t_{1/2}$ 260x10^{-3}s

Figure 3.23. Some examples of the affect of altering the structure of HABI, and this effect of the absorption spectra and speed of association of the radical species.1,8-NDPI-TPI,[27] PABI 1-2.[84]

This can be seen in Figure 3.23 with the alteration of the structure from the reference

HABI with a $t^1/2$ of more than 12 hours to the 1,8-NDPI-TPI,[27] where the $t^1/2$ has been dramatically reduced to 2.6x10^{-5}s. This reduction in the association speed is due to the alteration of the structure with the introduction of a naphthalene bridge. The second affect as shown in Figure 3.23 is the introduction of electron donating groups like the oxy group in PABI 2.[84] The introducion of the electron donating oxy group has a visible effect on the association speeds between PABI 1 and PABI 2, PABI 1 has a $t^1/2$ of 10x10^{-}3s the induction effect of the oxy group is stabilising the radical species. **12** shows an absorption at 430nm, with the changes to the structure the absorption of the radical species shifted to 550nm **red** trace shown in Figure 3.24.

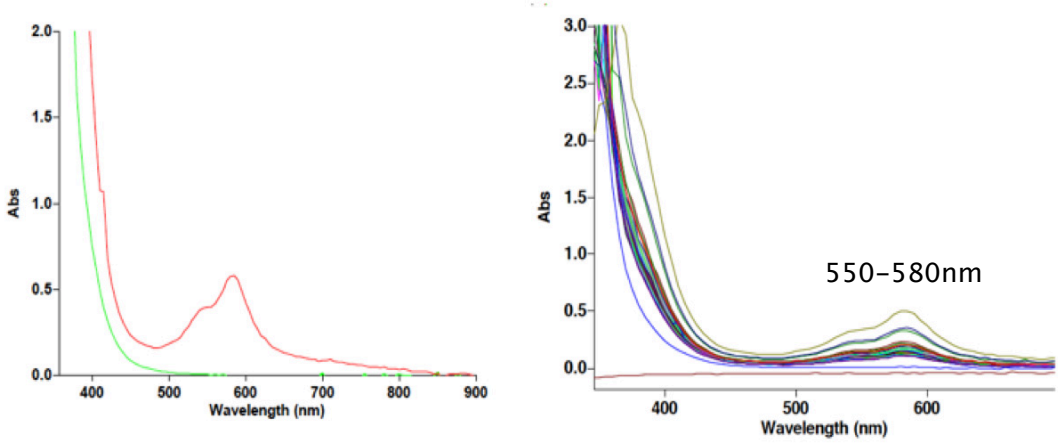

Figure 3.24. UV-Vis plot, of **63** **green** trace before irradiation, **red** after irradiation with 365nm light (mercury vapor lamp).

The alterations in the structure from **12** to **63** shown in Figure 3.22 also changed the LC properties. There was a change in the transition temperature from the LC phase to the isotropic phase from 48.3°C **12** to 51 °C in **24**. The **24** still exhibits a **smectic A phase** phase structure, see Figure 3.25. The DSC plot still exhibits the broad transition due to the polymeric type structure with enthalpy values of 1.67 J g^{-1}.

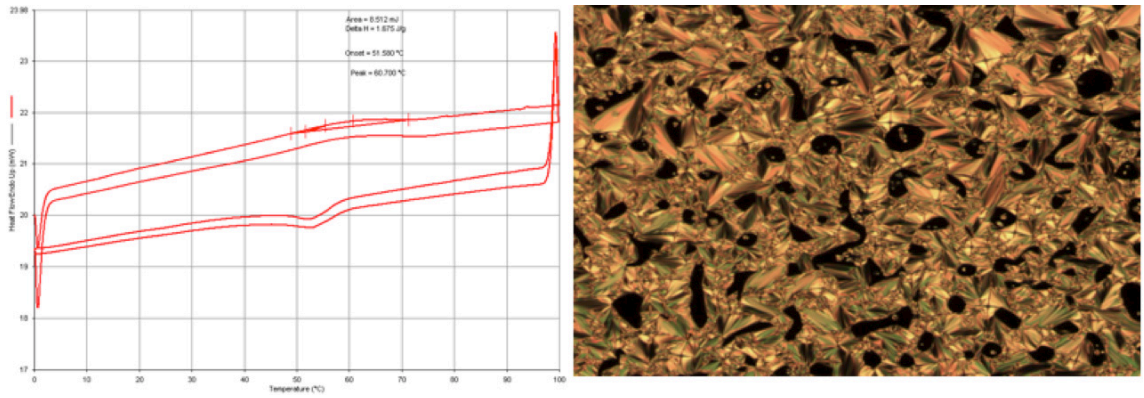

Figure 3.25. Right : DSC plot of **24**, Left : OPM image smectic A, 43 °C, 100x magnification.

The OPM image, shown in Figure 3.25, of a smectic A phase shows the same typical focal conic fans with areas of non birefringent which are due to homeotropic alignment. This texture, unlike **12**, is much finer. The textures shown in the OPM images are backed up by the XRD plots. For magnetically aligned samples there is no tilt of the mesogen relative to the layer normal director. This confirms the Smectic A phase structure. Figure 3.28 shows the layers that are formed in a smectic phase, the value is different to the estimated molecular length of 38.4 Å, as there is some interdigitation of the cyanobiphenyl mesogens occurs. The second value see Figure 3.28 at 20.5 Å, is associated with the length of the anti parallel cyanobiphenyl mesogens, this distance is related to the siloxane group linking the hydrocarbon spacer chains at 7.2 Å. Finally, from the plot one can also see that the distance between the molecules is on average 4.7 Å. This repeat distance of **24** is similar to the lengths found for **12**. With the irradiation of **12** and **24**, there was no alteration of the liquid crystal phase upon irradiation. The formation of the radicals does not induce such an alteration of the structure, therefore there is no increase or decrease in the order of the system. In contrast to that, the destabilisation of liquid crystal phase behaviour has in the literature been reported for diarylethenes. The increased rigidity of the system alters the liquid crystalline behaviour, this can be seen in Table 3.1.[56]

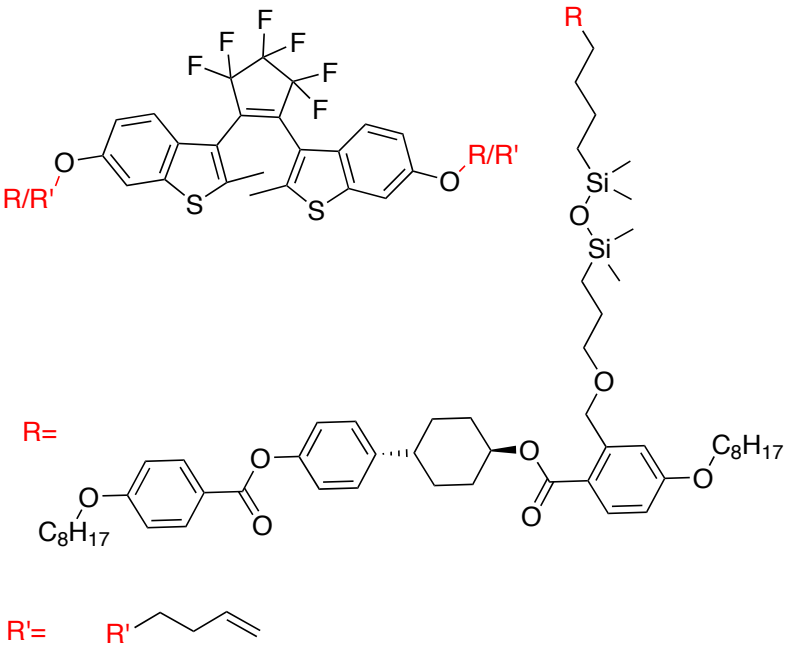

[An example of a LC dierylethene.]

Figure 3.26. An example of a LC diarylethene.[56]

Table 3.1. The effect of structure change in diarylethenes through electrocyclisation on the liquid crystal transition temperatures.[56]

Compound	R,R'	Transition Temperatures °C
I	R,R'	Tg -10.4 [N 14.2] Iso
II	R,R	Tg 2.6 [N 54.3] Iso
Ips	R,R'	Tg -1.9 (N 14.3) Iso
IIps	R,R	Tg 7.4 (N 51.3) Iso

Upon irradiation there was a bulk change in the colour of the material in the liquid crystal phase. The irradiation of the HABI dimer and the formation of the radical species of **12** and **24** did not show an alteration in the transition temperatures. This could be attributed to the fact that there is a change in the rigidity of the material which would alter the packing of the molecules in the liquid crystal phase. It was not possible to measure the irradiated form by XRD studies due to the use of UV to irradiate the material.

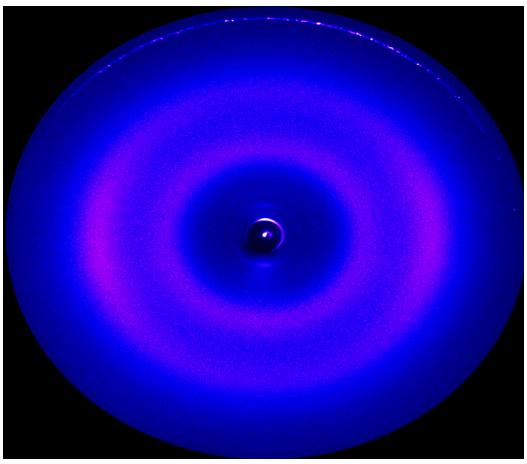

Figure 3.27. XRD date for alligned sample of **24**.

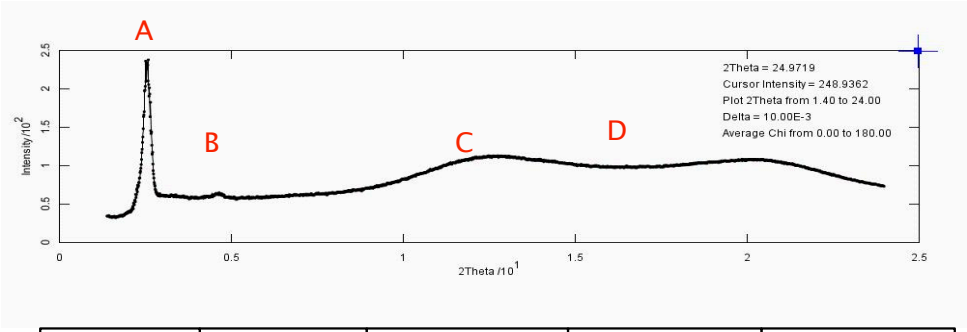

A	B	C	D	unit
38.4	20.5	7.2	4.7	Å
smectic layer	anti parallel mesogens	siloxane group	intermolecular distance	

Figure 3.28. 1D plot and table of detected intensitis of **24**.

3.7 HABI 12 and 24 isomer predictions

The HABI dimer structure has been determined through ^{13}C NMR investigation reported by S. Delbaere *et al.*[22] The six possible isomers are shown in Figure 3.29.

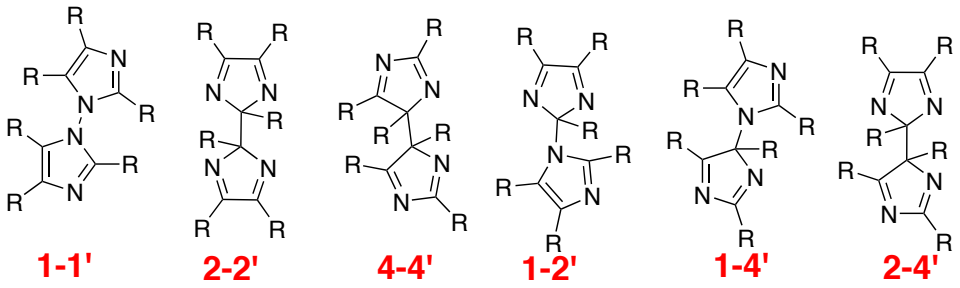

Figure 3.29. The six possible isomers of the HABI dimer reported by S. Delbaere *et al.*[22]

The work carried out by S. Delbaere *et al*, confirmed the six possible structures of the HABI dimer. This was achieved using alterations of the ^{13}C ppm values of the carbons in the hetrocyclic core of the HABI. The shift in the peaks from the ^{13}C spectra shows the point of connection of the dimers. this is shown in Table 3.2

Table 3.2. ^{13}C NMR chemical shifts of the stable HABI isomers (n.o - not observed).[22]

HABI Isomer	C2-C2'	C4-C4'	C5-C5'
1-2'	149.0, 112.6	138.4, 166.2	132.2, 166.2
2-2'	110.7, 111.1	168.6, 168.6	168.6, 168.6
4-4'	171.3, 171.3	n.o	194.1, 194.1

The work showed that there was a large difference in the ppm value between the 1,2'-, 2,2'- and 4,4'- isomers shown in Table 3.2. It is known that the 1,2'- isomer is the dominant form for the HABI; this isomer is known to be the most stable form.

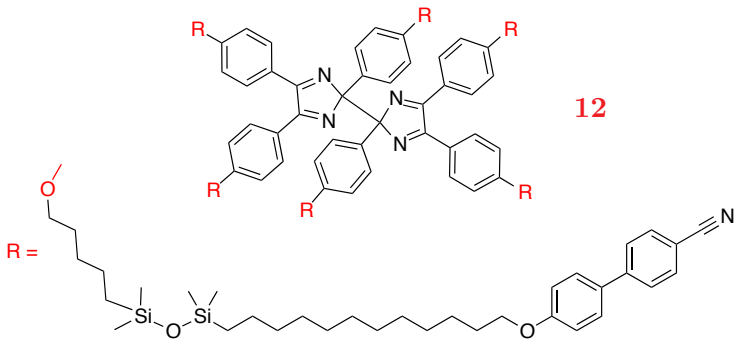

Figure 3.30. Structue of **12**.

Using the ^{13}C data and the XRD data, see Figure 3.20, the structure of **12** shown in Figure 3.30 is hypothesised to be 4,4'- isomer. This fits the XRD data with the hydrocarbon spacers compressing to give the smectic layer distance of 31.6Å. The XRD data does not show any interdigitation, see Figure 3.20, this is in line with the argument that only the 2,2'- isomer is present. The ^{13}C NMR shows the 160 ppm and 109 ppm peaks which could correlate to the 2,2'- isomer shown in Figure 3.31. This model would also account for the lack of interdigitation which is seen in the XRD spectra of **12**.

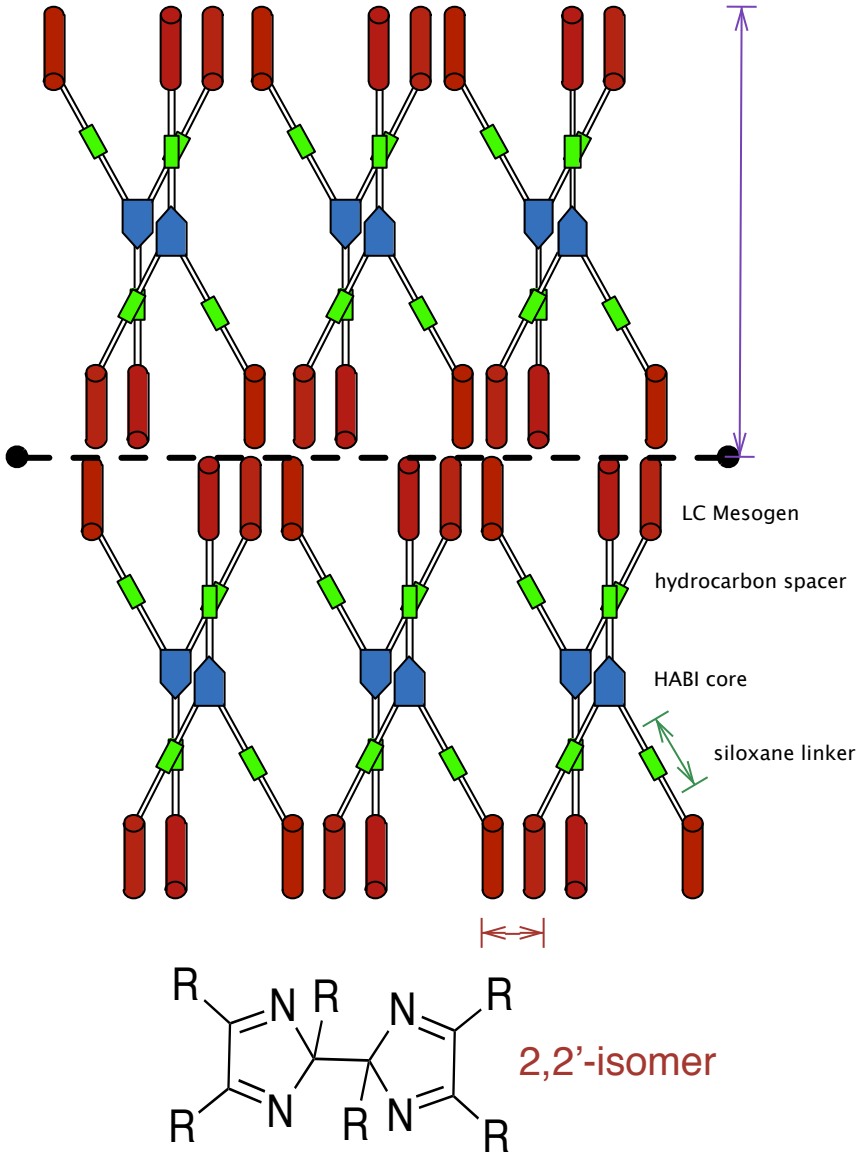

Figure 3.31. Representation of the liquid crystal packing of **12** based on the XRD data, black line - smectic layer boundary, purple - smectic layer length 31.2Å, green line - length of the siloxane linker 6Å, red line - intermolecular distance 4.6Å

The model for the packing of **24** differs from **12** as there is a second reflection for the smectic layer. This is associated with the interdigitation of the LC mesogens see Figure 3.33. The differences in the packing structure is shown in the XRD values shown in Table 4.1.

Table 3.3. XRD defraction values comparison for **12** and **24** (n.o - not observed).

	Compound	
assigned spacing	**12**	**24**
smectic layer	31.2 Å	38.4 Å
local anti-parallel mesogens	n.o	20.5 Å
sioxane group	6.0 Å	7.2 Å
intermolecular distance	4.6 Å	4.3 Å

The XRD data shows the overall smectic layering is similar to that found for **12**. The occurance of reflection relating to a lattice of 20 Å, for **24** is indicative of interdigitated species, see Figure 3.33. The formation could be rationalised due to the occurnce of 1,2'- and 2,2'- isomers of **24** which would account for the interdigitation isomers shown in Figure 3.33. The presence of this is also seen in the ^{13}C NMR, the peaks at 160 ppm and 110 ppm can be attributed to the 2,2'- isomer which is in line with the literature values.[22]

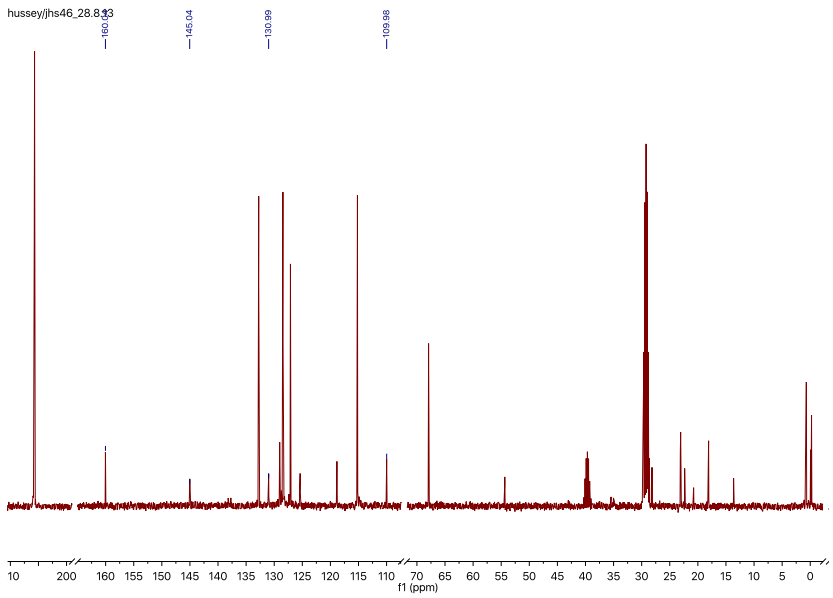

Figure 3.32. ^{13}C NMR spectrum of **24**

The 1,2'- isomer can be seen from the presence of 145ppm and 130ppm peaks. The presence of both of these isomers could be due to partial irradiation of the sample

before the NMR causing a partial radicalisation and recombination, giving the 2,2'-isomer and the 1,2'- isomer. The reduction in the length of the hydrocarbon spacer could also contribute to the 1,2' and the 2,2'- isomers being stabilised through the reduction of the steric interaction of the siloxane linkers. This would also support the explanation of why the system **12** is only showing the 2,2'- isomer and no interdigitation.

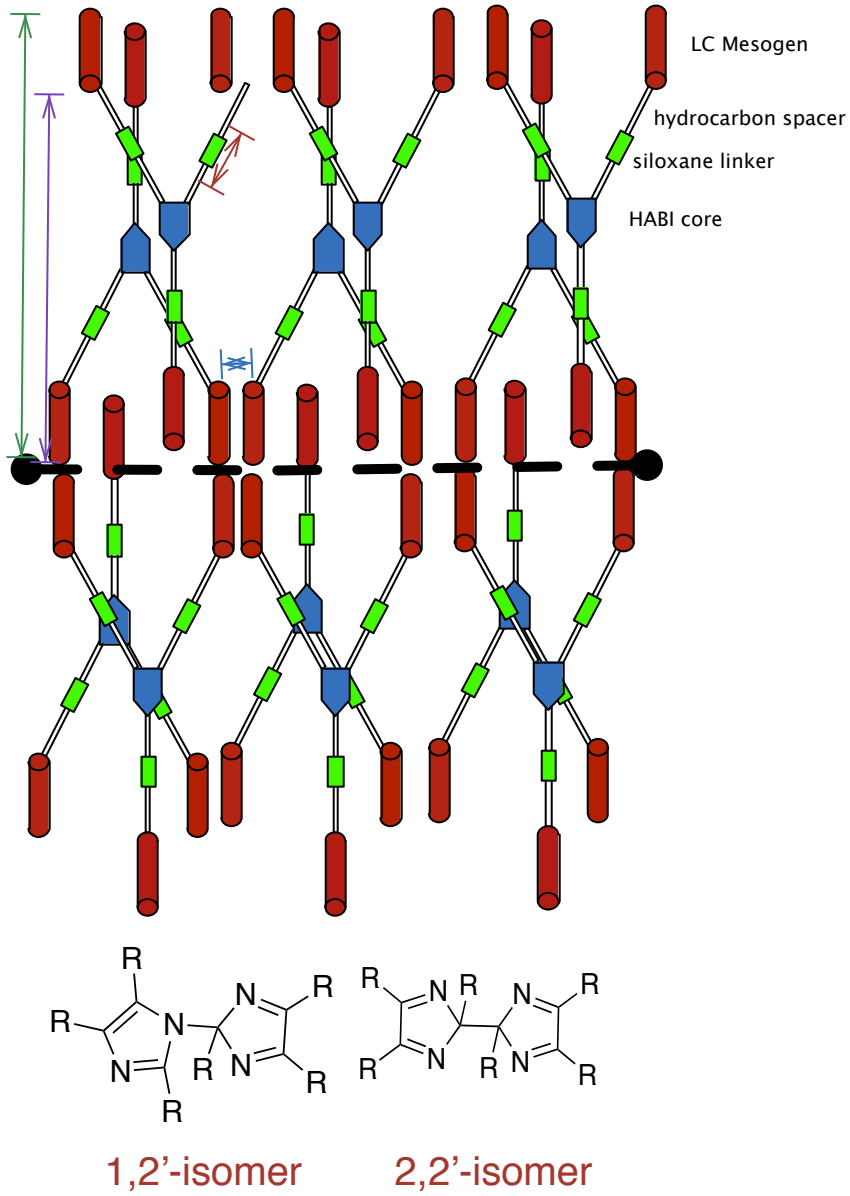

Figure 3.33. Representation of the packing of **24** based on the XRD data, black line - smectic layer boundary, purple - smectic layer length 20.5Å, green line - total smectic layer length 38.6Å, red line - length of the siloxane linker 7.2Å, blue line - intermolecular distance 4.3Å.

3.8 Summary

Two novel photochromic liquid crystal compounds utilising HABI group were designed, synthesised, investigated, and optimised. The construction is based on the optimisation of the liquid crystal properties from earlier work. This was achieved through the reduction of the length of the hydrocarbon spacer and the addition of a siloxane linker. The photochromic properties were optimised through the removal of electron donating oxy group attached to the HABI core. The changes are shown in Figure 3.34

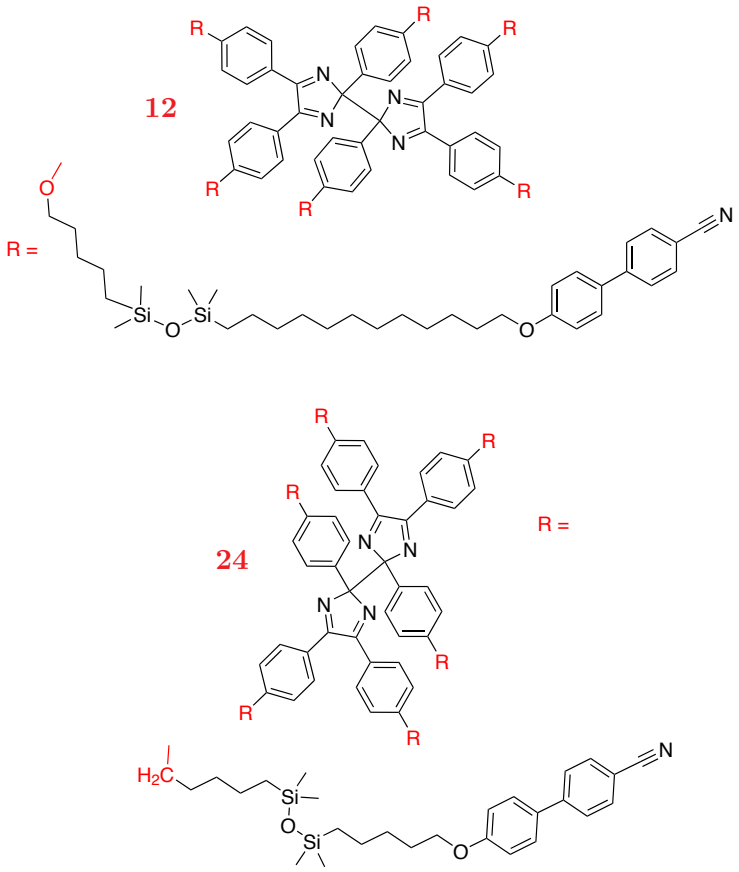

Figure 3.34. Final compounds **12** and **24**.

The first final material **12** showed room temperature liquid crystal phase behaviour exhibiting a Smectic A phase with an isotropisation temperature of 44.5°C with and enthalpy value of 1.68 $J\,g^{-1}$, with a wide transition range to the isotropic due to the oligomeric type structure. The packing structure in the liquid crystal phase was

determind using XRD diffraction. This gave a smectic layer spacing of 31.2 Å and intermolecular distance of 4.6 Å, the siloxane link due to the high electron density also gave a diffraction pattern and length of 6.0 Å. The XRD pattern showed there was no interdigitation and this combined with the ^{13}C NMR data the 2,2'-HABI isomer can be predicted to be the predominant isomer. The absorption spectra showed a red shift compaired to the reference material HABI with the λ max at 430nm. The conclusion of **12** as a photochromic-LC material was a bulk colour change in the material with no effect to the liquid crystal properties and an increase in the recombintion time compaired to the HABI referance material (The inrease in the recombination time was observed but not calculated). The structure of **12** was altered to **66**.

Material **24** was altered, as shown in Figure 3.34, to optimise the photochromic properties. This was achieved through the removal of the oxy group linking the hydrocarbon spacer to the HABI core, the oxygen was acting as an electron donor and stabilising the radical monomer. This also caused a further red shift in the absorption spectrum and altered the absorption maximum from 430nm for **12** to 580nm for **24**. The removal of the oxy linking group, the hydrocarbon spacer and the reduction of the length of the hydrocarbon specer between the HABI core and the LC mesogen from **12** to **24**, increased the liquid crystal phase range from 44°C to 55°C. Compound **24** still exhibits a Smectic A phase with transition enthalpy to the isotropic of 1.68J g^{-1} with a wide transition range similar to compund **12**. The packing structure of the liquid crystal phase was determined using XRD diffraction, the scattering pattern of **24** was roud to be similar to **12** with a smectic layer seperation of 38.4 Å, siloxane group lenght of 7.2 Å and a lateral molecular distance of 4.3 Å. The difference betwen compounds **12** and **24** is the appearance of another scattering intensity with a value of 20.5 Å, this was attributed to local anti-parallel mesogens. This length of 20.5 Å shows that there is interdigitation of the liquid crystal mesogens and end-on-end stacking of the mesogens giving rise to the 20.5 Å length. The presence of the interdigitation could be associated with the presence of a second isomer of the HABI dimer, the ^{13}C NMR data shown in Figure 3.32 shows the presence of the 2,2'-isomer and the possible presence of the 1,2'-isomer due to the occurance of peaks at the 145ppm and 130ppm peaks in the ^{13}C NMR spectrum. This along with the presence of interdigitation points to the presence of the both the isomers. The appearance of the second isomer could be attributed to the reduction

of the hydrocarbon spacer between the HABI core and the LC mesogen, which could have an affect on the association of the radicals formed after association.

References

(1) P. J. Collings and M. Hird, *Introduction to liquid crystals: chemistry and physics*, 1997.

(11) S. Delbaere, G. Vermeersch, M. Frigoli and G. H. Mehl, *Org Lett*, 2010, **12**, 4090–4093.

(14) S. Delbaere, G. Vermeersch, M. Frigoli and G. H. Mehl, *Org. Lett.*, 2006, **8**, 4931–4934.

(17) G. R. Coraor, L. A. Cescon, R. Dessauer, E. F. Silversmith and E. J. Urban, *J. Org. Chem.*, 1971, **36**, 2262–2267.

(22) S. Delbaere, M. Orio, J. Berthet, M. Sliwa, S. Hatano and J. Abe, *Chem. Commun.*, 2013, **49**, 5841–5843.

(23) Y. Harada, S. Hatano, A. Kimoto and J. Abe, *J. Phys. Chem. Lett.*, 2010, **1**, 1112–1115.

(27) K. Fujita, S. Hatano, D. Kato and J. Abe, *Org Lett*, 2008, **10**, 3105–3108.

(52) M. Frigoli and G. H. Mehl, *Chem. Commun. (Camb.)*, 2004, 2040–2041.

(53) M. Frigoli and G. H. Mehl, *Chem. Commun. (Camb.)*, 2004, 818–819.

(54) T. Kosa, L. Sukhomlinova, L. Su, B. Taheri, T. J. White and T. J. Bunning, *Nature*, 2012, **485**, 347–349.

(56) M. Frigoli and G. H. Mehl, *Eur. J. Org. Chem.*, 2004, **2004**, 636–642.

(57) S. Delbaere, J. C. Micheau, M. Frigoli, G. H. Mehl and G. Vermeersch, *J. Phys. Org. Chem.*, 2007, **20**, 929–935.

(58) M. Frigoli and G. H. Mehl, *Angew. Chem. Int. Ed.*, 2005, **44**, 5048–5052.

(59) K. Arai, Y. Kobayashi and J. Abe, *Chem. Commun. (Camb.)*, 2015, **51**, 3057–3060.

(60) J. Hussey, *Photochromic Liquid Crystals.* MChem Dissertation, University of Hull, UK, 2012.

(61) B. Atorf, A. Hoischen, M. B. Ros, N. Gimeno, C. Tschierske, G. Dantlgraber and H. Kitzerow, *Applied Physics Letters*, 2012, **100**, 223301.

(62) S. D. Lepore and Y. He, *J. Org. Chem.*, 2003, **68**, 8261–8263.

(63) C. J. Moody and L. M. Harwood, *Experimental organic chemistry: principles and practice*, 1989.

(64) K. Bahrami, M. M. Khodaei and A. Nejati, *Monatsh Chem*, 2011, **142**, 159–162.

(65) K. C. Majumdar, D. Ghosh and S. Ponra, *Synthesis*, 2013, **45**, 2983–2988.

(66) H. Veisi, A. Khazaei, L. Heshmati and S. Hemmati, *Bull. Mater. Sci.*, 2012, **33**, 1231–1234.

(67) A. Sedrpoushan, Z. Joshani and L. Fatollahi, *Lett. Org. Chem.*, 2014, **11**, 287–292.

(68) A. Y. Usyatinsky and Y. L. Khmelnitsky, *Tetrahedron Lett*, June 2000, **41**, 5031–5034.

(69) C. O. Kappe, *Angew. Chem. Int. Ed.*, 2004, **43**, 6250–6284.

(70) C. M. Sousa, J. Berthet, S. Delbaere and P. J. Coelho, *J. Org. Chem.*, 2012, **77**, 3959–3968.

(71) C. M. Sousa, J. Berthet, S. Delbaere, A. Polónia and P. J. Coelho, *J. Org. Chem.*, 2015, **80**, 12177–12181.

(72) R. Adams and C. S. Marvel, *Benzoin*, John Wiley & Sons, Inc., Hoboken, NJ, USA, 1941.

(73) R. Chen, Z. An, F. Li, X. Chen and P. Chen, *Liq. Cryst.*, 2016, **43**, 564–572.

(74) N. Marion, R. S. Ramón and S. P. Nolan, *J Am Chem Soc*, 2009, **131**, 448–449.

(75) N. Xu, D.-W. Gu, Y.-S. Dong, F.-P. Yi, L. Cai, X.-Y. Wu and X.-X. Guo, *Tetrahedron Lett*, 2015, **56**, 1517–1519.

(76) A. Gao, F. Yang, J. Li and Y. Wu, *Tetrahedron*, 2012, **68**, 4950–4954.

(77) M. D. Greenhalgh and S. P. Thomas, *Chem. Commun.*, 2013, **49**, 11230–11233.

(78) J. M. Bakker, S. J. Langford, M. J. Latter, K. A. Lee and C. P. Woodward, *Aust. J. Chem.*, 2005, **58**, 757–755.

(79) A. R. Mulholland, C. P. Woodward and S. J. Langford, *Chem. Commun.*, 2011, **47**, 1494–1496.

(80) L. Ruan, M. Shi, N. Li, X. Ding, F. Yang and J. Tang, *Org. Lett.*, 2014, **16**, 733–735.

(81) C. Giansante, P. Ceroni, V. Balzani, M. Maestri, S.-K. Lee and F. Vögtle, *New J. Chem.*, 2007, **31**, 1250–1259.

(82) E. Ramou, Z. Ahmed, C. Welch, P. K. Karahaliou and G. H. Mehl, *Soft Matter*, 2015, **12**, 888–899.

(83) Z. Ahmed, C. Welch and G. H. Mehl, *RSC Adv.*, 2015, **5**, 93513–93521.

(84) H. Yamashita and J. Abe, *Chem. Commun.*, 2014, **50**, 8468–8465.

Chapter 4 Diazocine

4.1 Diazocine - previous work and background

H. Duval *et al* discovered in 1910 the diazocine molecule shown in Figure 4.1 (compound 58), but it was not until 2009 that Herges, *et al*[47] investigated the photochromic properties and then, in later work, the effects of substitution on these properties.[48] The effect of substitution was also studied through non-symmetrical substitution.[49] The effect of substituting the fundamental core azocine molecule with amines resulted in a red shift on the absorption of the molecule. This is also seen in the non-symmetrical substitution of the core material. There has been some investigation into the synthesis of the diazocine molecule and the formation of the restricted azo link. The methods outlined by Herges, *et al* and Wang, *et al* of new mild conditions for the synthesis of symmetrical and non-symmetrical azobenzenes,[39,48] the effectiveness of these methods was demonstrated on the diazocine molecule.

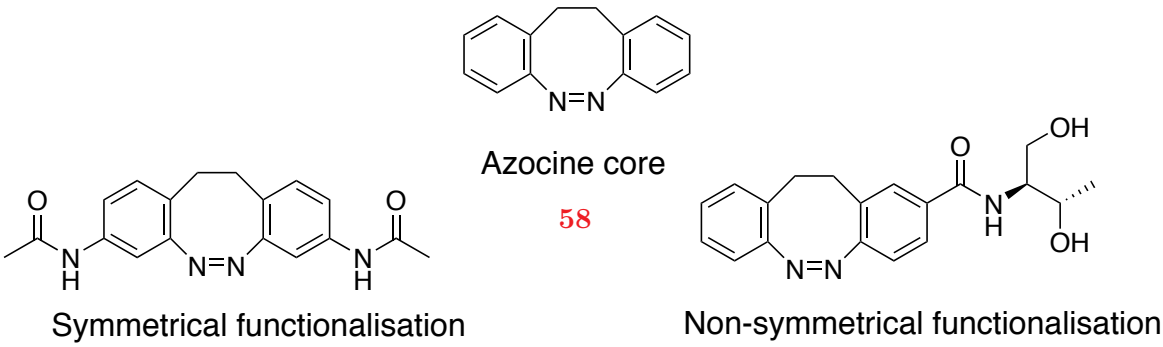

Figure 4.1. 58 Original material,[48] 60 Symmetrical substitution,[48] 59 non-symmetrical substitution.[49]

The interest in this molecule for the synthesis of single molecule photochromic LC mesogens arises from the isomerisation of the stable ground state *cis* isomer to the *trans* isomer in the excited irradiated form. With this switch from the *cis* to *trans* form there is an increase in the order of the compound as the molecule adopts a

more rod like structure. This in turn will help stabilise the LC phase or introduce a LC phase from the isotropic. With the aim to synthesise a molecule to exhibit LC properties, the symmetrical compounds shown in Figure 4.1 were altered at the point of substitution to the diazocine central core, the *meta* amine groups were removed and replaced with halogens. The removal of the *meta* amines on the diazocine central core was carried out so that the attachment of the LC mesogen could be done directly and was the final planned step in the synthesis. The removal of the amine groups and the direct attachment will increase the possibility of inducing a liquid crystal phase throught the attachment of the LC mesogen. The aim of the removal of two nitrogens in the final compound and the direct attachment of the LC mesogen is to reduce the melting point of the material and increase the stability over multiple heat-cool cycles.

4.2 Synthesis discussion

The standard method for the formation of azo containing mesogens is via diazonium salt formation[85,86] or the formation of nitrosobenzene derivative, and the reaction with *N*-hydroxyaniline (see Scheme 4.1) through the synthesis of a hydrazine and then the dehydrogenation to the azo group.[87] A selection of the traditional methods are illistrated in Scheme 4.1. There are many more methods reported in the literature, a comprehensive review of the methods for the formation of the azo link was carried out by E. Merino.[88] An issue with these methods are the harsh conditions, if they are to be applied to the synthesis of diazocines. The strong acids could cause problems with halogen groups present in **37** as the halogens can be removed from the aromatic ring by the strong acid.

Througout the synthesis of **39** many problems were encountered. The formation of **36** followed the traditional nitration method.[48] It started with heating 4,4'-ethylenedianiline in conc. sulfuric acid with the slow addition of sodium nitrite. This reaction works in a quantitative yield and an orange solid is formed. A problem occurs when the acidic solution is over neutralised and made basic through the addition of ammonia. Many side reactions were found to occur. A large number of routes where explored to complete the synthesis of **39**

The main problem with the aim of direct attachment of the LC mesogen to a diazocine core lies in the reactivity of the halogen group. With this in mind, the formation of a diazonium salt for the closure of the center ring system (see Figure 4.7) was eliminated as the process of forming the salt would remove the halogen group because of its reactivity. To overcome this problem different routes were attempted. The formation of the central ring system (see Figure 4.7) was carried out using D-glucose and potassium hydroxide **49**. Then the halogen groups were attached through the formation of a di-diazonium salt and quenched with iodine solution **50**. This was unsuccessful as during the salt formation the azo link was destroyed.

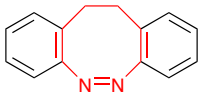

58

Figure 4.2. Red indicating center ring system

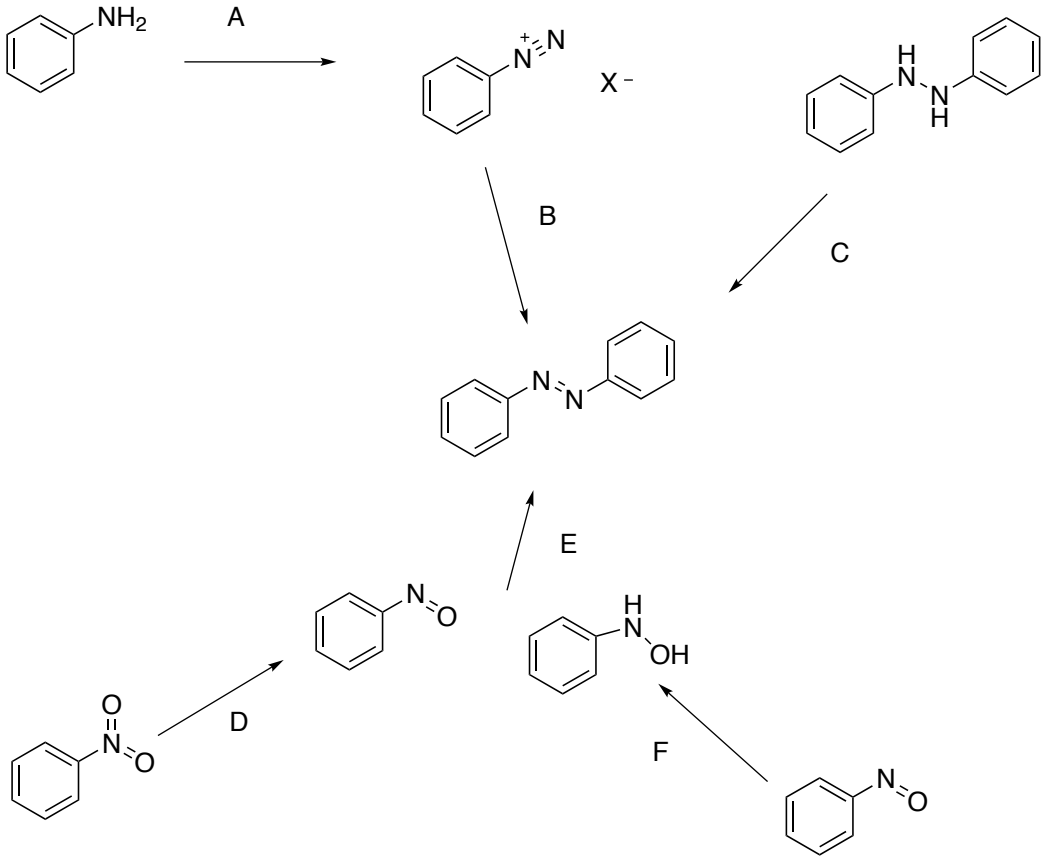

A = diazonium salt formation, conc. sulfuric acid, KI, sodium nitrite.
B = azo formation, acetic acid, water, conc. sulfuric acid.
C = dehydrogonation, KF, aluminium oxide.
D = nitroso formation, molybdenum salt, peroxide.
E,F = zinc, ammonium chloride. Degradation of the nitroso group.

Scheme 4.1. An overview of some of the traditional method for the synthesis of azobenzene

With the traditional methods used to form azo links removed as a synthetic option, a new synthetic scheme was derived with milder conditions used following the nitration step **36** shown in Scheme 4.2. This new route was used, instead of the formation of the azo link via a diazonium salt at the point of ring closure, or the formation of the diazonim salt for halogen subsitution after the formation of the azo link, which is known to be sensitive to strong acids or bases. The first step in the new method was the removal of the amines in the 4 positions, which were replaced with iodines using the formation of a diazonium salt.[89] The only other substitutions in the 1 and 2 positions were not effected by this method. After the iodination on the 1,2-bis(4-iodo-2-nitrophenyl)ethane, the next hurdle was the formation of the center ring and azo link. This was explored through many different methods. One was the classic hydrogenation using palladium on carbon and a gaseous hydrogen in a hydrogenator, but this led to the removal of the iodines[90–92] which is often observed.

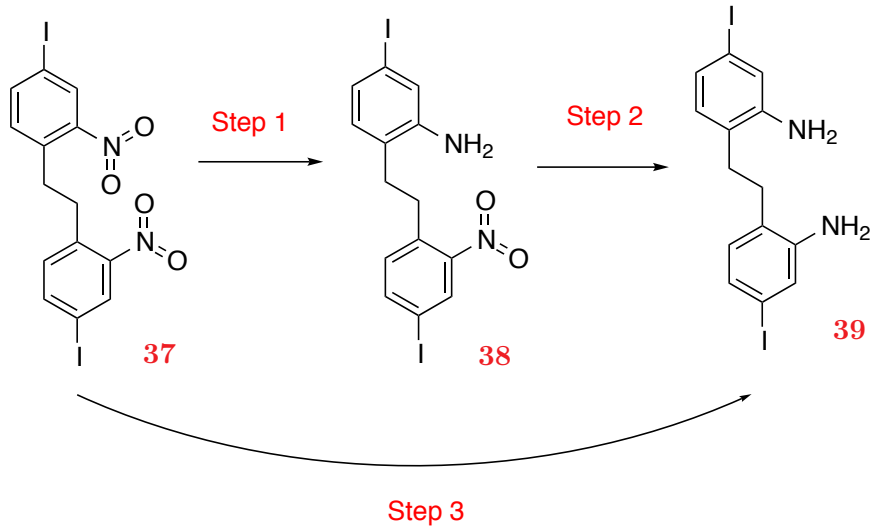

Figure 4.3. Routes for the formation of the amine groups.

The most successful route was by the hydrogenation of the nitro group on compound **37** using platinum on carbon (5%) and ammonium formate as the hydrogen donor[93] shown in Figure 4.3 step 1. Formic acid can also be used as the hydrogen donor, but this was found to result in lower yields. This was found to be a successful method for the reduction of the nitro groups to amine groups. The problem that was detected was that only a single reduction took place as shown in Figure 4.3 step 1 **38**. A consequence was that the reaction mixture had to be worked up and purified before

the singly reduced compound could be reduced again using the same method as seen in Figure 4.3 step 1-2 to produce **39**. The need for the two reactions to reduce both of the nitro groups resulted in a significant loss in the yields as the conversion would only go up to 50% completion which resulted in a net yield of 25%. The initial hypothesis was that the ammonium formate was not soluble in the chosen solvent THF so the reaction was tried in ethanol EtOH, this led to no product formation. Following this result, a ratio of methanol and THF 2:3 was used and this increased the reaction yields slightly. The method was further modified; the equivalents of the ammonium formate where increased by a factor of 3, and the platinum on carbon component was increased by a factor of 1.5, the ratio of methanol increased almost to 1:1, as did the overall volume of the solution. It was found that reducing the reaction temperature from 100 °C to 75 °C eliminated the build up of aqueous soluble salt on the condenser, which is suspected to be ammonium formate and some byproduct of the reaction. With all of these changes the reaction was optimised towards the original intention of full reduction of the nitros shown in Figure 4.3 step 3 with the elimination of steps 1-2 and a direct route to compound **39** with a yield of 50%.

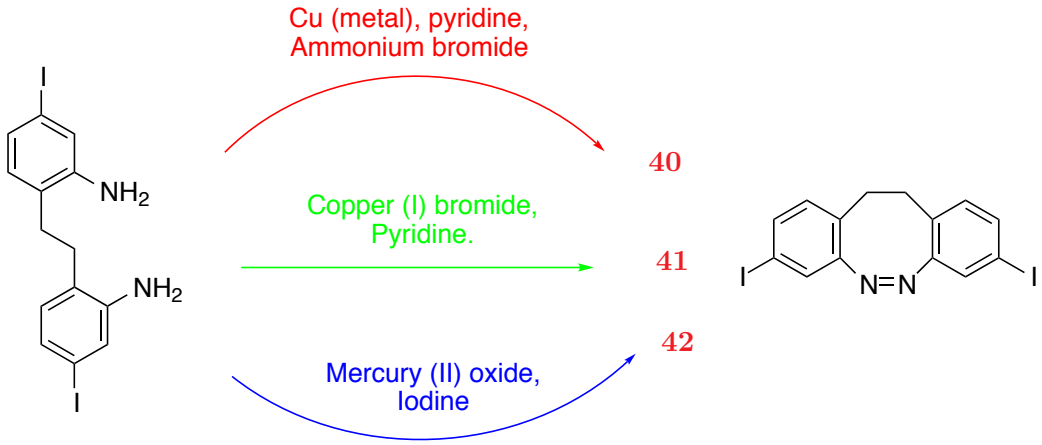

Figure 4.4. Atempted routes for the formation of the cental ring

Following the synthesis of 6,6'-(ethane-1,2-diyl)bis(3-iodoaniline) **39**, the next hurdle was the closure of the central ring. This was approched initally using two methods, the first employing CuBr, this can be formed in situ **41**[39] shown in Figure 4.4 red route or CuBr can be added directly **42**[94] seen in Figure 4.4 green route. These two methods both have the disadvantage of being low yielding and the products were found to be difficult to work up. The second method has the advantage of a shorter

reaction time and improved yields, however it requires the use of mercury oxide and elemental iodine to form the azo link.[95] Even with the advantages of an easier work up and reaction time this route did not yield the product.

The aim for the future is that following the closure of the central ring, see Figure 4.7, the attachment of the LC mesogen can be formed directly through a substitution reaction at the site of the halogen, in this case iodine. The LC mesogen was attached using a classical Suzuki coupling. Due to the problems with the formation of the halogenated diazocine shown in Figure 4.4.

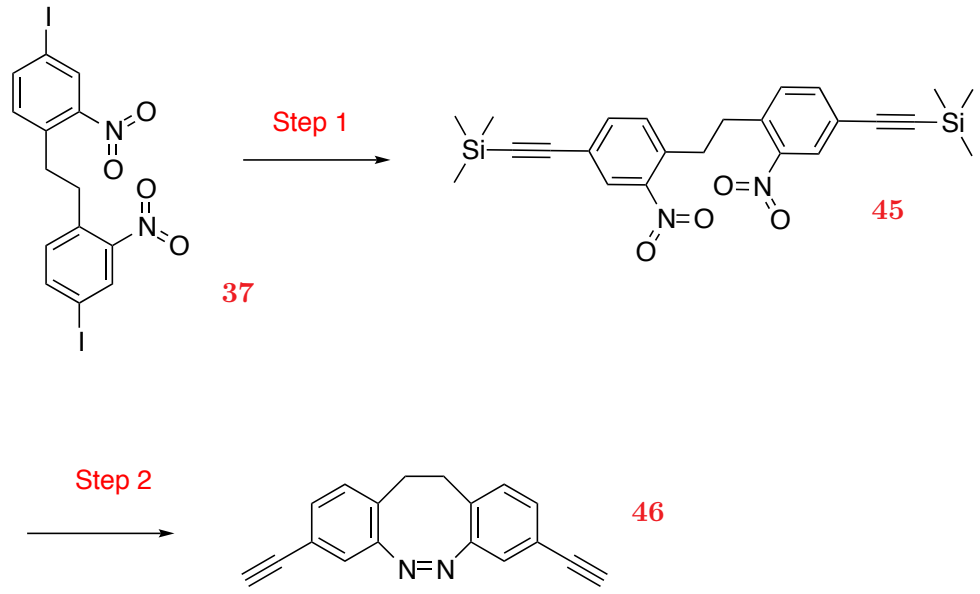

Figure 4.5. Alternative route for the formation of a functionalisable diazocine.[96]

An alternative route was followed, outlined by Herges *et al.*[96] The first step to yield **37** shown in Figure 4.5 follows the original route with the replacement of the amine groups positioned para to the ethylene bridge with iodo groups to form **37**. The halogens in the para position are substituted in the second step shown in Figure 4.5 step 2, via the attachment of trimethylsilylacetlene via a Sonogashira coupling for form **45**. As the reactive position on the aromatic centers are now protected a ring closure is now possible. This is achieved via reduction of the nitro groups using barium hydroxide and zinc metal. This method closes the ring and at the same time removes the trimethylsilyl protecting groups, as seen in Figure 4.5 step 3 to form **46**. The final step is the addition of the LC mesogen via a Sonogashira coupling to

produce **48**. This final step was unsucessful and only produced homocoupled **46** in a polymeric like structure. This was assumed to be due to the activation of both of the alkyne protons in the copper cycle.

4.3 Synthetic route

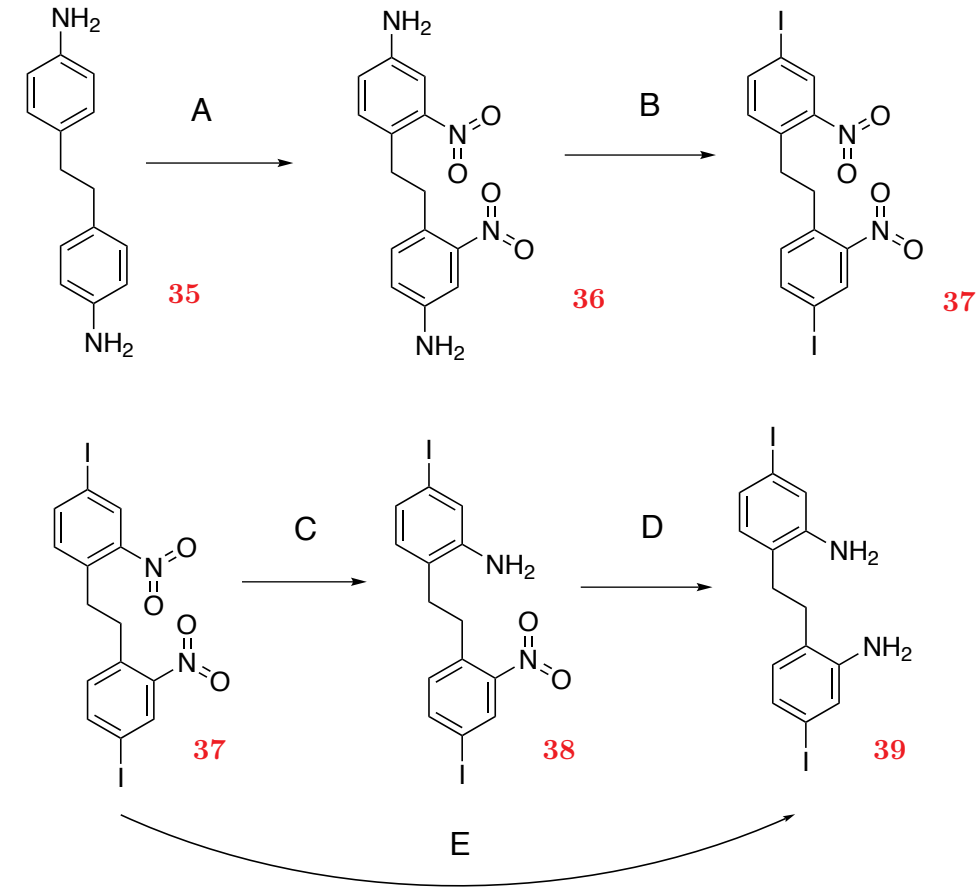

A = sulfuric acid, sodium nitrate, 80°C, 5hr. 99%
B = 16:1 water : sulfuric acid, sodium nitrite, coppper (elemental powder), KI. 6hr 23%
C = methanol , THF, ammonium formate,platinum on carbon 5%, 100°C. 3 days 20- 50%
D = methanol , THF, ammonium formate,platinum on carbon 5%, 100°C. 3 days 20-50%
E = 2 :3 methanol : THF, ammonium formate,Platinum on carbon 5%, 75°C. 3days 50%

Scheme 4.2. Synthesis of diazocine intermediates **64**.

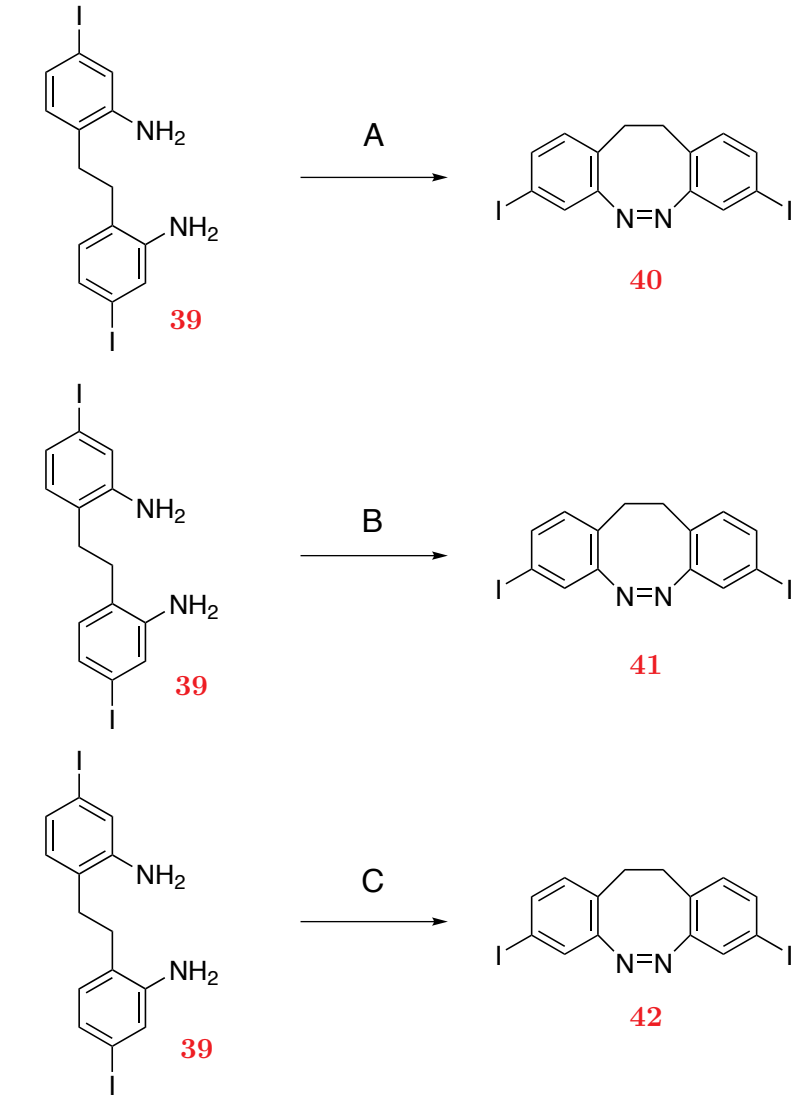

A = copper metal, pyridine, ammonium bromide, toluene, 100°C, 24hr 0%
B = copper (I) bromide, pyridine, toluene, 60°, 24hr 0%
C = mercury (II) oxide, toluene, iodine, RT 1-5hr 0%

Scheme 4.3. Atempted routes for the central ring closure and LC attachment **65**.

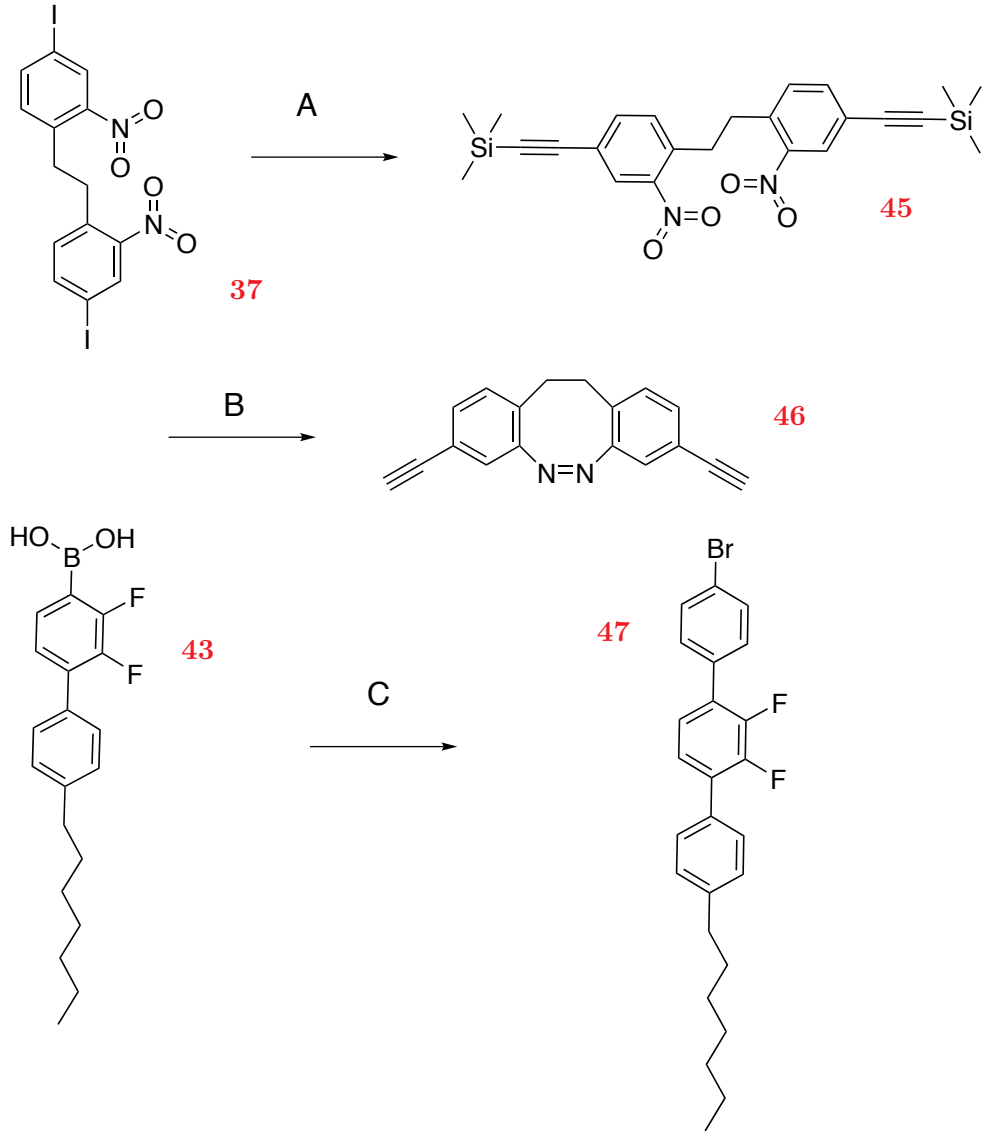

A = CuI, Et_3N, bis(triphenyl phosphine) palladium (II) chloride, toluene, trimethylsilylacetylene 40°C, 5hr, RT, 16hr 75%
B = barium hydroxide octahydrate, zinc, 110°C, 3hr 18%
C = tetrakis triphenyl phosphine palladium (0), DME, water, K_2CO_3 , 60°C.12hr 80%

Scheme 4.4. Revised method for the formation and functionalisation diazocine LC synthesis 46.

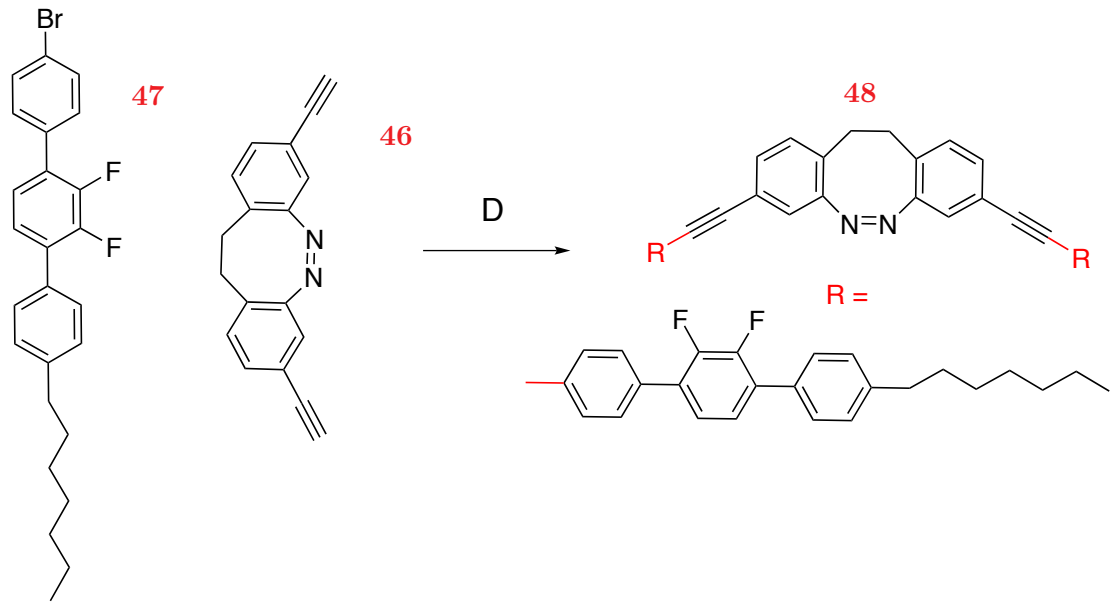

D = CuI, Et_3N, bis(triphenyl phosphine) palladium (II) chloride, toluene, trimethylsilylactylene
40°C, 5hr, RT, 16hr 0%

Scheme 4.5. Revised method for the formation of the halogenated diazocine final step.

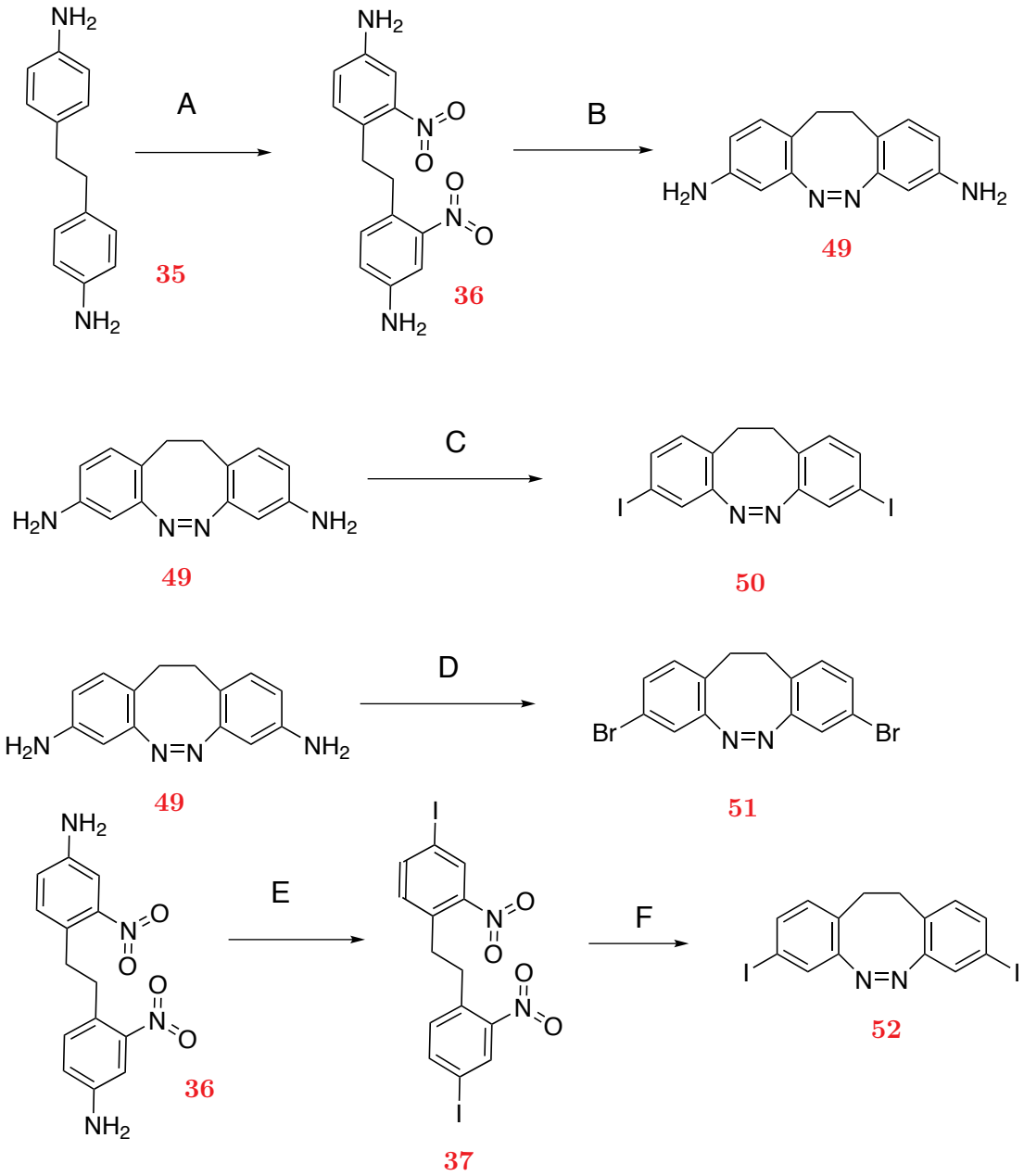

A = sulfuric acid, sodium nitrate, 80°C, 5hr. 99%
B = D-glucose, potassium hydroxide, ethanol, water, 80°C. 30%
C = sulfuric acid, sodium nitrite, potassium iodide, copper (elemental powdered), 6hr, 0%
D = sodium nitrite, HBr in water (30%), copper bromide, 3hr, room temperature, 0%
E = sulfuric acid, sodium nitrite, potassium iodide, copper (elemental powdered), 6hr, 20%
F = D-glucose, potassium hydroxide, ethanol, water, 80°C. 0%

Scheme 4.6. Original method for the formation of the halogenated diazocine.

4.4 Experimental

Synthesis of 4,4'-(ethane-1,2-diyl)bis(3-nitroaniline) 36.

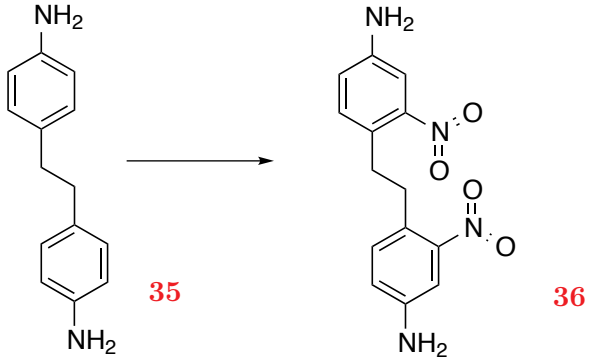

4,4-Ethylenedianiline **67** (10g, 48mmol), was stirred in sulfuric acid (80mL) the solution was heated to 60°C, to this sodium nitrate (8.8g, 102mmol) in sulfuric acid 90mL, was added drop wise. The solution was stirred for 6 hours, once cooled the solution was poured onto ice water and neutralised using conc ammonia solution (37%). The orange precipitate was filtered off under vacuum and washed with plenty of water and dried in a dessicator over calcium hydroxide overnight. **36** was used with no further purification.

Percentage Yield 14g, 99%

^{1}H-NMR (400 MHz, DMSO-d6) δ 7.06 (2 H, d, J 6.2, 2.0), 6.99 (2H, d, J 3.2, 8.3), 6.78 (2H, dd, J 2.3, 8.3, J 2.6, 2.1), 5.58 (4H, s), 2.86 (4H, s)

^{13}C NMR (101 MHz, DMSO-d6) δ 149.90, 148.58, 132.85, 121.85, 119.21, 108.48, 33.25

Synthesis of 1,2-bis(4-iodo-2-nitrophenyl)ethane 37

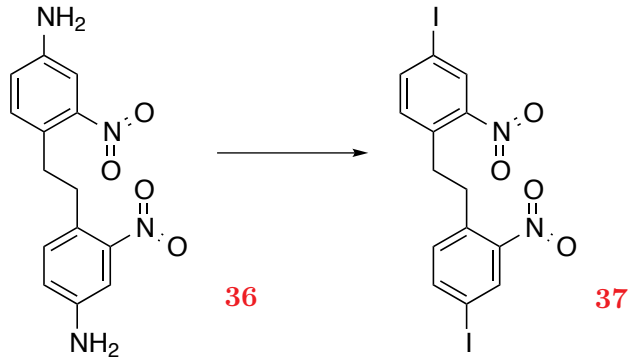

36 (10.93g, 36mmol) was mixed with water (250mL), conc sulfuric acid (20mL), the solution was cooled and sodium nitrite (4.9g, 72.11mmol) in conc sulfuric acid (50mL) was added drop wise. Once added, the solution was stirred at room temperature for 1.5 hours and then added to potassium iodide (18g, 108.1mmol) in water (100mL). To this solution copper powder (0.136g, 2.16mmol) was added and the solution stirred. The solution was slowly heated to 80°C for 20 minutes. The cooled solution was then extracted with DCM (3x), the combined organic phase was then washed with sodium thiosulphate (saturated solution). The organic phase was then dried over magnesium sulphate and filtered under a vacuum and the solvent was removed by reduced pressure. The crude product was purified using column chromatography using DCM as the eluent.

Percentage Yield 6g, 23%

^{1}H-NMR (400 MHz, tetrahydrofuran-d8) δ 2.49 – 2.71 (6 H, m), 6.23 (1 H, dd, J 8.1, 1.1), 6.97 (1 H, dt, J 8.1, 1.5), 7.33 (1 H, t, J 1.5).

^{13}C-NMR (101 MHz, Chloroform-d) δ 142.19, 133.87, 133.31, 77.45, 33.71.

mass spectrometry- Theoretical: 562, 563, 564. Observed data: 562, 563, 564. accurate mass Theoretical: 541.9058 Obeserved: 541.9057. $[M + K^{+}]+$

Synthesis of 5-iodo-2-(4-iodo-2-nitrophenethyl)aniline 68

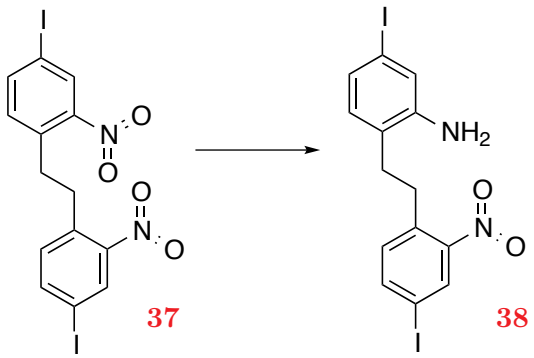

37 (6.5g, 11.56mmol), platinum on carbon (5% on carbon) (0.8g) was dissolved in THF (100mL). The solution was stirred and ammonium formate (2.2g, 34.9mmol) in methanol (20mL) the solution was heated to 100°C for 3 days. Once the solution was cooled the platinum on carbon was filtered off through celite and washed with THF. The organics were extracted with DCM (3x), the organics were then washed with water and brine. The solution was dried over magnesium sulphate and filtered under vacuum, the solvent was then removed under reduced pressure. The crude product was purified using column chromatography using DCM as the eluent.

Percentage Yield 2.5g, 50%

^{1}H-NMR (400 MHz, tetrahydrofuran-d8) δ 1.79 (2 H, dd, J 9.4, 6.6), 2.07 (2 H, dd, J 9.4, 6.6), 3.59 (1 H, s), 5.68 (1 H, d, J 7.9), 5.89 (1 H, dd, J 7.9, 1.7), 6.03 (1 H, d, J 1.7), 6.14 (1 H, d, J 8.2), 6.87 (1 H, dd, J 8.1, 1.8), 7.27 (1 H, d, J 1.8)

Synthesis of 6,6'-(ethane-1,2-diyl)bis(3-iodoaniline) 39

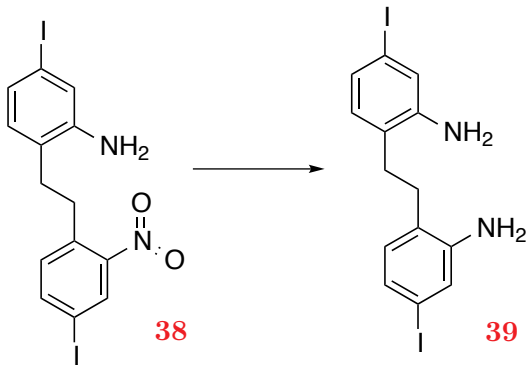

38 (0.44g, 0.8827mmol), platinum on carbon (5% weighting) (0.07g) was dissolved in THF (20mL). The solution was stirred and ammonium formate (0.3g, 4.761mmol) in methanol (4mL) was added to the solution was heated to 100°C for 3 days. Once the solution was cooled the platinum on carbon was filtered off through celite and washed with THF. The organics were extracted with DCM (3x) and were then washed with water and then brine. The solvent was dried over magnesium sulphate and filtered under vacuum, the solvent was then removed under reduced pressure. The crude product was purified using column chromatography using DCM as the eluent.

Percentage Yield 80mg, 50%

^{1}H-NMR (400 MHz, tetrahydrofuran-d8) δ 2.62 (4 H, s), 5.72 (2 H, d, J 7.9), 5.88 (2 H, dd, J 7.9, 1.7), 6.00 (2 H, d, J 1.7).

^{13}C-NMR (101 MHz, Chloroform-d) δ 142.19, 135.07, 133.87, 133.31, 77.77, 33.71.

mass spectrometry- Theoretical: 464, 465, 466. Observed: 463, 464, 465. $[M+H]+$

Modified synthesis of 6,6'-(ethane-1,2-diyl)bis(3-iodoaniline) 39

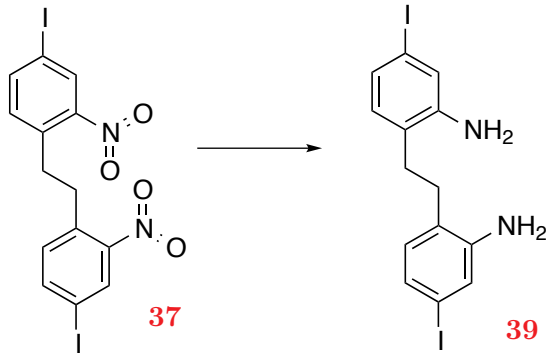

37 (6.5g, 11.56mmol), platinum on carbon (5% weighting) (0.8g) was dissolved in THF (100mL). The solution was stirred and ammonium formate (2.2g, 34.9mmol) in methanol (60mL), The solution was sealed and the atmosphere evacuated. The solution was then heated to 75°C for 5 hours, the pressure was vented and the reaction was left to stir at 75°C for 10 hours. The cooled solution was then filtered through celite and washed with DCM, the organics were extracted with DCM and washed with water and then brine. The solution was dried over magnesium sulphate and filtered under vacuum and the solvent removed under reduced pressure. The crude product was purified using column chromatography using DCM as the eluent.

Percentage Yield 3.67g, 50%

^{1}H-NMR (400 MHz, tetrahydrofuran-d8) δ 2.62 (4 H, s), 5.72 (2 H, d, J 7.9), 5.88 (2 H, dd, J 7.9, 1.7), 6.00 (2 H, d, J 1.7).

^{13}C-NMR (101 MHz, chloroform-d) δ 142.19, 135.07, 133.87, 133.31, 77.77, 33.71.

mass spectrometry- Theoretical: 464, 465, 466. Observed: 463, 464, 465. $[M+H]+$

Synthesis of (Z)-3,8-diiodo-11,12-dihydrodibenzo[*c*,*g*][1,2]diazocine 40

Route one

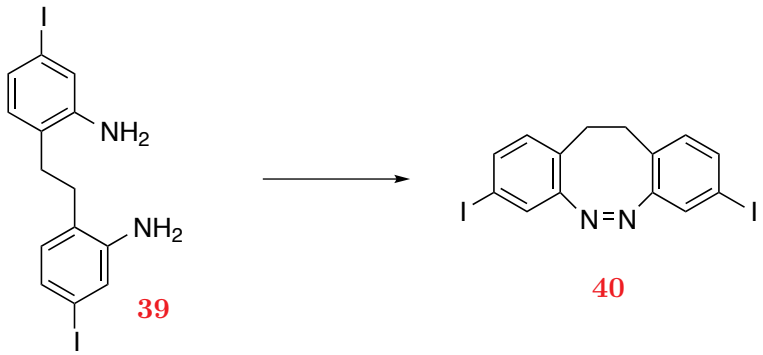

39 40

39 (0.11g, 0.2263mmol), ammonium bromide (0.022g, 0.2263mmol), copper (I) bromide (0.039g, 0.216mmol) were mixed in dry toluene (2mL). The atmosphere was evacuated and flushed with O_2 (3x), the solution was then filled with O_2 and heated to 100°C. To this pyridine (0.0107g, 10.8µL, 0.138mmol) was added dropwise and left to stir for 24 hours. Once cooled the organics were extracted with DCM and washed with water and then brine, the solution was dried over magnesium sulphate and filtered under vacuum, the solvent was removed under reduced pressure. The crude product was purified using column chromatography DCM. No product was yielded and thus not persued any further.

Synthesis of (*Z*)-3,8-diiodo-11,12-dihydrodibenzo[*c*,*g*][1,2]diazocine 40

Route two

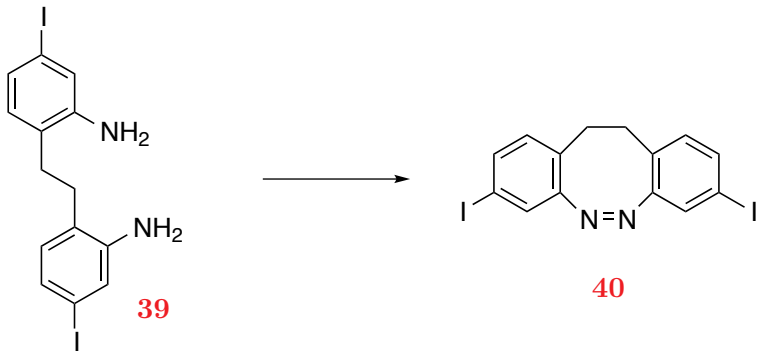

39 (0.1g, 0.00022mmol), mercury oxide (I) (0.7128g, 0.00033mmol) and iodine (0.08349g, 0.0003mmol) were all disolved in THF (5mL) under an oxygen environment, the solution was stirred for 16 hours at room temperature. The organics were extrated with DCM and washed with sodium thiosulphate, water, and brine. The organics were dried over magnesium sulphate and filtered under vacuum, the solvent was removed under reduced pressure. The ^{1}H-NMR spectrum showed that no reaction had occurd.

Synthesis of (*Z*)-3,8-diiodo-11,12-dihydrodibenzo[*c*,*g*][1,2]diazocine 40

Route three

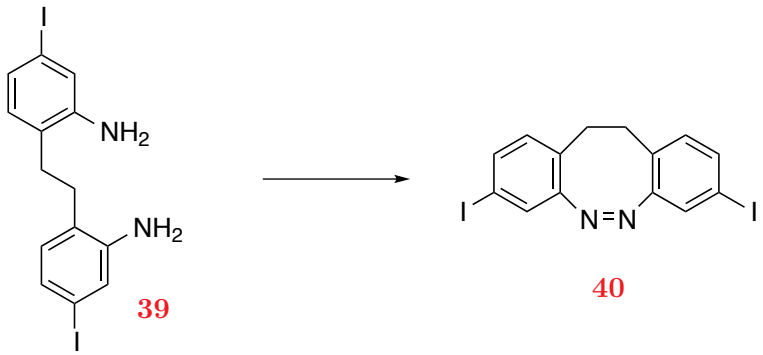

39 (0.11g, 0.2263mmol), ammonium bromide (0.022g, 0.2263mmol), copper metal (2.2mg) were all dissolved in dry toluene (2mL). The atmosphere was evacuated and flushed with oxygen (3x), the solution was then filled with oxygen and heated to 100°C, to this pyridine (0.011g, 10.8µL, 0.138mmol) was added dropwise and left to stir for 24 hours. Once cooled the organics were extracted with DCM and washed with water and then brine, the solution was dried over magnesium sulphate and filtered under a vacuum, the solvent was removed under reduced pressure. The crude product was purified using column chromatography, using DCM as the eluent. The analysis of the isolated materials showed that no product had been formed.

Synthesis of 1,2-bis(2-nitro-4-((trimethylsilyl)ethynyl)phenyl)ethane 45

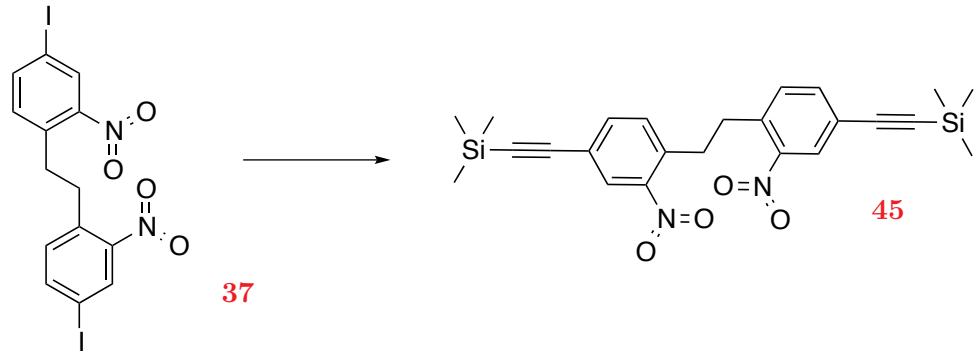

37 (2.48g, 4.732mmol), copper iodide CuI (Copper iodide) (49mg, 0.25mmol) and bistriphenylphosphine palladium dichloride (0) (134mg, 0.1911mmol), was disolved in degassed NEt_3 (100mL) and THF (20mL) the solution was evacuated and the atmosphere replaced with nitrogen (3x). To this solution trimethylsilyl acetylene (0.973g, 1.4mL, 9.93mmol) was added dropwise. The solution was stirred at 40°C for 5 hours and then at room temperature for 16 hours. The solvent was removed under reduced pressure and then dissolved in DCM:Hexane (1:1) and flushed through a silica plug. the filtrate was combined and the solvent removed under reduced pressure and the resulting solid recyrstalised from methanol. The precipitate was filtered under vacumm and dried overnight.

Percentage Yield 2.56g, 66%

^{1}H-NMR (400 MHz, Methylene chloride d2) δ 0.26 (18 H, s), 3.22 (4 H, s), 7.29 (2 H, d, J 8.0), 7.58 (2 H, dd, J 8.0, 1.7), 8.01 (2 H, d, J 1.7).

The data matched literature values.[96]

Synthesis of (*Z*)-3,8-diethynyl-11,12-dihydrodibenzo[*c*,*g*][1,2]diazocine 46

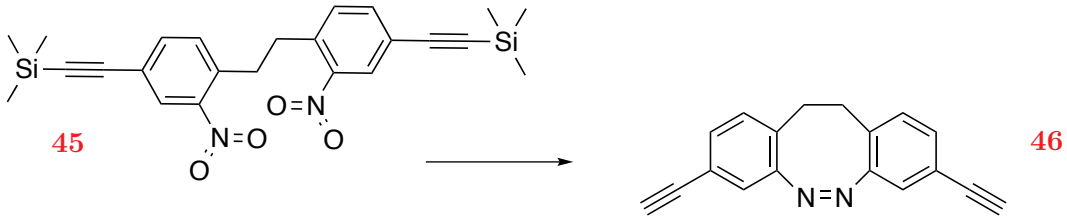

45 (226mg, 0.243mmol), barium hydroxide octahydrate (600mg in water (100mL), 0.952mmol) and zinc powder (500mg, 9.23mmol) were all added together and ethanol (300mL) was added and the solution was heated to reflux for 3 hours, whilst hot the solution was filted through a plug of celite. The filtrate was extracted with DCM and dried over magnesium sulphate and filtered under vacuum. The solvent was removed under reduced pressure and the crude product was purified via column chromatography using DCM as the eluent.

Percentage Yield 10mg, 18%

^{1}H-NMR (400 MHz, Methylene chloride d2) δ 7.14 (dd, J = 7.8, 1.7 Hz, 2H), 7.02 – 6.85 (m, 4H), 3.04 (s, 2H), 3.01 – 2.92 (m, 2H), 2.84 – 2.69 (m, 2H).

The data matched literature values[96]

Synthesis of (*Z*)-3,8-diethynyl-11,12-dihydrodibenzo[*c*,*g*][1,2]diazocine functionalised with 2',3'-difluoro-4-heptyl-1,1':4',1''-terphenyl 48

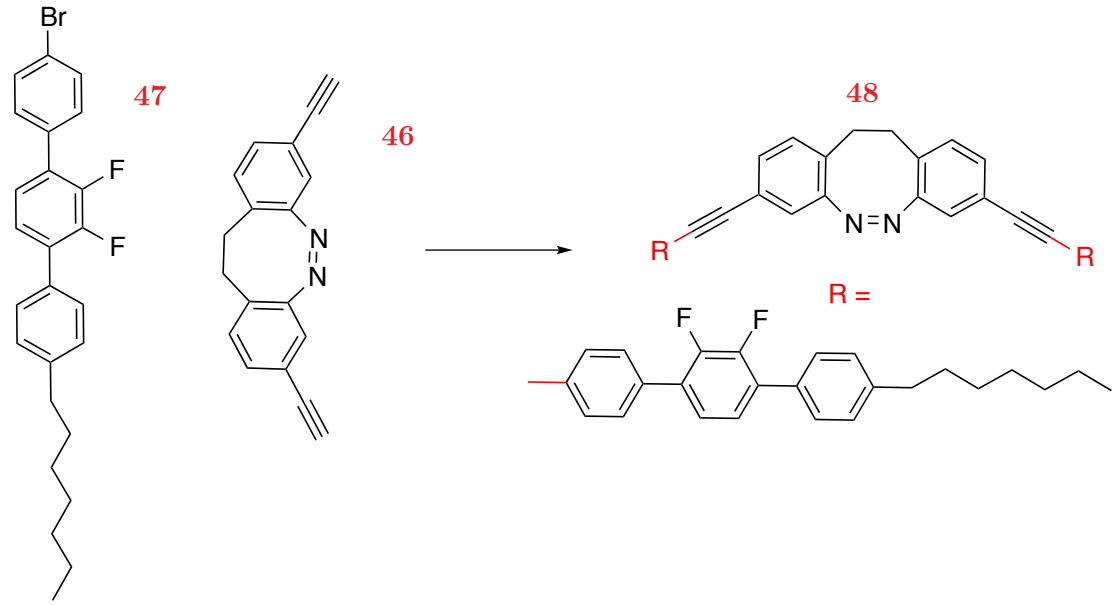

46 (0.0219mg, 0.0855mmol), copper iodide (0.00488g, 0.0257mmol) and bistriphenlyphosphine palladium dichloride (0) (0.018g, 0.025mmol) was dissolved in degassed triethylamine (2mL) and THF (1mL). The atmophere was evacuated and replaced with nitrogen (3x). To this solution **47** (0.115g, 0.2565mmol) in THF (1mL) was added dropwise and then the solution heated to 80°C for 16 hours. Once cooled the solvent was removed under reduced pressure and the crude product purified using column chromatography DCM. The ^{1}H-NMR spectrum showed that no product formation had occurd. The presence of a polymeric film in the reaction vessel suggests that polymerisation of **46** had taken place.

Synthesis of (*Z*)-11,12-dihydrodibenzo[*c*,*g*][1,2]diazocine-3,8-diamine 49

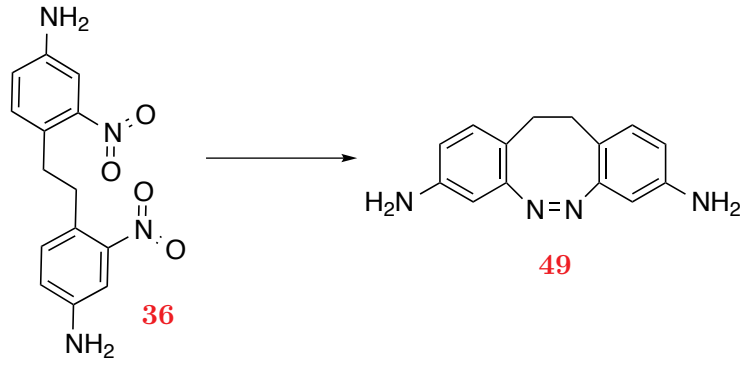

36 (5.96g, 0.0797mol), D-Glucose (36g, 0.197mol) in water (110mL) was mixed with ethanol (800mL) and heated to 80°C. To this solution potassium hydroxide (49g, 1.24mol) in water (100mL). The solution was heated at 80°C for 16 hours, once cooled the solution was added to water and ice (500mL). The reaction mixture was extracted into ethyl acetate and washed with water. The solution was then dried over magnesium sulphate and filtered under a vacuum. The solvent was removed under reduced pressure. The crude material was purified via column chromatography using hexane : DCM (1:1) as the eluent. Yielding a pale yellow crystalline solid.

Percentage Yield 1.5g, 30%

^{1}H-NMR (400 MHz, DMSO-d6) δ 6.67 (2H, d, J 6.5, 8.2), 6.24 (2H, dd, J 6.5, 8.2, J 5.3, 2.3), 5.97 (2H, d, J 3.5, 2.3), 5.15 (4H, br.s), 2.63 (4H, m)

^{13}C-NMR (101 MHz, DMSO-d6) δ 155.87, 146.76, 130.15, 115.18, 112.88, 103.11, 30.44

Synthesis of (*Z*)-3,8-diiodo-11,12-dihydrodibenzo[*c*,*g*][1,2]diazocine 50

49 50

49 (2.47g, 0.07mol) was mixed with water (250mL), conc sulfuric acid (29mL), the solution was cooled and sodium nitrite (2.72g, 40mmol) in conc sulfuric acid (10mL) was added droppwise, once added the solution was stirred at room temperature for 1.5hr and then added to potassium iodide (12.113g, 73mmol) in water (10mL. To this solution copper powder (0.136g, 2.16mmol) was added and the solution stirred. The solution was slowly heated to 80°C for 20 minutes. The cooled solution was then extracted with DCM (3x), the combined organic phase was then washed with sodium thiosulphate (saturated solution). The organic phase was then dried over magnesium sulphate and filtered under a vacuum and the solvent removed by reduced pressure. The crude product was purified using column chromatography in DCM. The ^{1}H-NMR spectrum showed degradation of the material and no product formation.

Synthesis of (*Z*)-3,8-dibromo-11,12-dihydrodibenzo[*c*,*g*][1,2]diazocine 51

49 51

49 (0.1325g, 0.556mmol) was stirred with HBr 30% in water (2mL) to this solution sodium nitrite (0.153g, 2.2mmol) in water (5mL) was added dropwise. To this solution coppper bromide (0.159g, 0.6mmol) was added and HBr (3mL) was added dropwise and the solution stirred for 3 hours at room temperature. The organics were extracted with DCM and washed with water and sodium thiosulphate (conc) solution. The organics were dried over magnesium sulphate and filtered under vacuum. The solvent was removed under reduced pressure and the crude product was purfied via column chromatography DCM. The ^{1}H-NMR showed that the reaction did not work. The ^{1}H-NMR data did not corrolate with expected values see Figure 4.6

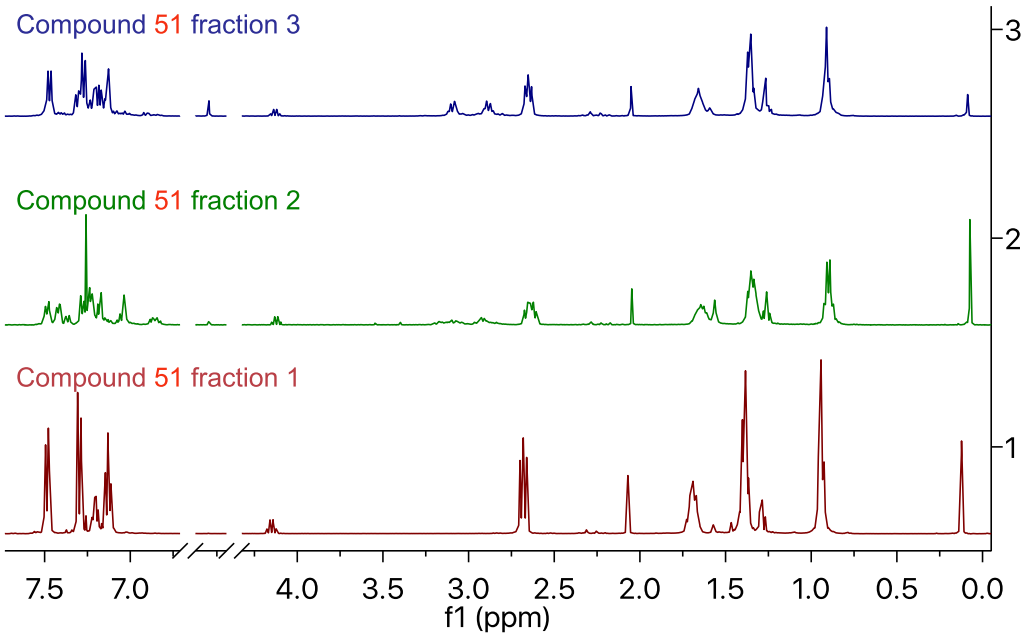

Figure 4.6. ^{1}H-NMR spectrum of the columned fractions.

Synthesis of (*Z*)-3,8-diiodo-11,12-dihydrodibenzo[*c*,*g*][1,2]diazocine 52

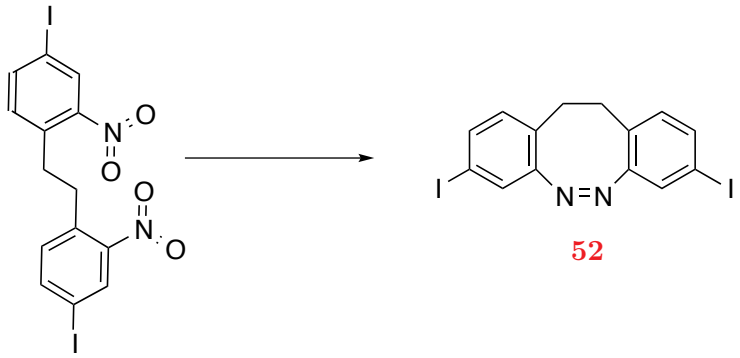

37 52

37 (3.41g, 0.0713mol), D-Glucose (16g, 0.087mol) in water (110mL) was mixed with ethanol (450mL) and heated to 80°C. To this solution, KOH (26g, 0.0499mol) in water (100mL) was added. The solution was heated at 80°C for 16 hours, once cooled the solution was added to water and ice (500mL). The organics were extracted with ethyl acetate and washed with water. The organics were dried over magnesium sulphate and filtered under a vacuum. The solvent was removed under reduced pressure. The crude material was seperated via column chromatography hexane : DCM (1:1). The ^{1}H-NMR showed that the product had degraded in the reaction.

4.5 Results

The synthesis of a novel iodinated diazocine **49** was attempted, see Scheme 4.2 and Scheme 4.3. The problem with the chosen route is in the formation of the central ring, see Figure 4.7.

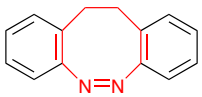

58

Figure 4.7. Red indicating center ring system

The methods tried did not yield any of the target material. The formation of the azo link befor the reduction and iodination of the nitro groups, proved to degrade the previously formed azo link. The alternative approach uesd was the conversion of the nitro groups to halgens, then form the azo link. This approache did not yield the desired material. The original method for the formation of the central ring Figure 4.7, that was tried was taken from previous work by Herges.[48] This used glucose as the reducing agent of the nitro groups and the source of hydrogen. The glucose, when in strong, hot, basic conditions, degrades to form hydrogen and lactate, formate and other compounds.[97,98] It is also used in the reduction of aromatic nitro compounds to their amines[98] or azoxy compounds. The proposal for the mechanism of the reduction of 1,2-bis(2-nitro-4-aminophenyl) ethane **36** follows the reduction of one of the nitro groups to a nitroso and the other to a hydroxyamine. With the formation of these two groups the azoxy compound is formed, then the final reduction and removal of the negatively charged oxygen takes place to form the final azo product, see Scheme 4.7. This would support the low yield of the reaction due to the stability of the intermediates and over-reduction of the nitro groups to amine groups, see Scheme 4.7. The formation of the azo link from the di-amino di-iodo intermediate proved to be very low yielding **40** or did not yield product at all. This could be due to the stability of the iodo groups in the 2 position of **37** withdrawing the electron density, which could be the reason for the low reactivity of the amines in the 4 position. To overcome the problem with the low reactivity a different approach was taken, this followed a method used by Herges.[96] **37** was functionalised

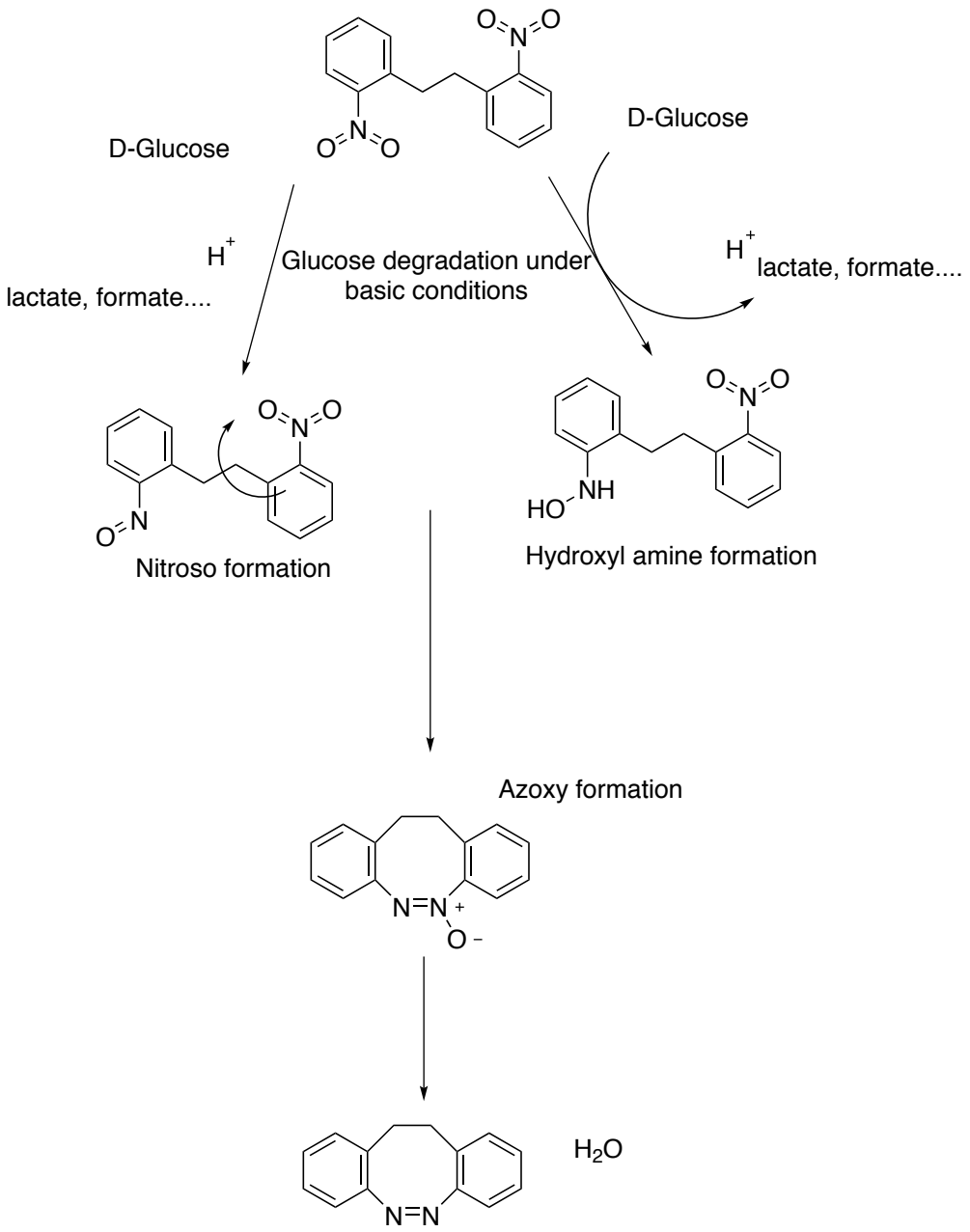

Scheme 4.7. Proposed mechanism for the formation of diazocine using D-Glucose as the H source and the reducing agent.

with trimethylsilylacetylene using a modified Sonogashira method. Once functionalised the central ring was formed using barium hydroxide and zinc **46**, due to the basic conditions this also de-protected the alkyne groups. With the formation of the diazocine functionalised with alkynes, the next step was the attachment of the LC mesogen via a Sonogashira coupling. This proved to be a problem, the reaction was unsuccessful. Compound **46** homocoupled and there was no reaction with the LC mesogen **47**. The reason for this are illustrated in the reaction mechanism at the formation of the copper complex highlighted in red with the alkyne see Figure 4.8. At this point in the cycle, if there is too much copper iodide present the formation of the copper complex could occur on both the alkynes. This means that both are reactive and can take part in the rest of the cycle.

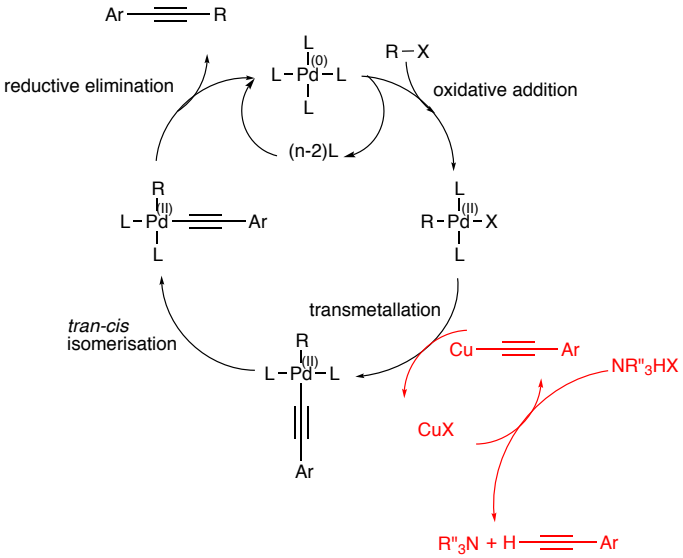

Figure 4.8. Sonogashira reaction mechanism. Red highlighted the copper cycle.

With this in mind, the mol % of the copper iodide should be reduced with the aim of the formation of a single alkyne copper complex and the reduction of the homocoupling.

4.6 Photochromic properties of 62

The UV-Vis spectra depicted in Figure 4.9 show the isomerisation of the diazocine when irradiated with a 365nm LED diode (13V, 1A). The *cis* state absorbed in the 390nm region, with the irradiation and the isomerisation the absorption peak at 390nm reduces and the apperance of an absorption at 480nm is observed. This change is seen in the solution of yellow to red, this can be seen in Figure 4.10. With the exclusion of light the compound returned back to the cis isomer.

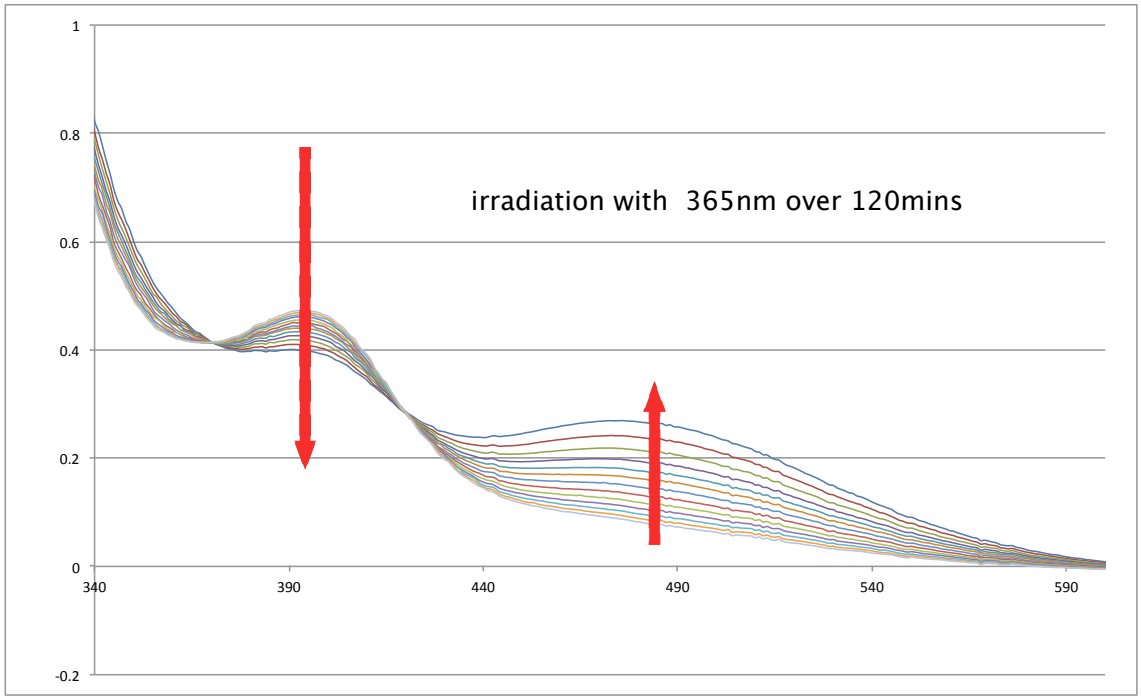

Figure 4.9. UV-Vis spectra of 46 irradiated at 365nm for 120 minutes with scans every 8 minuets

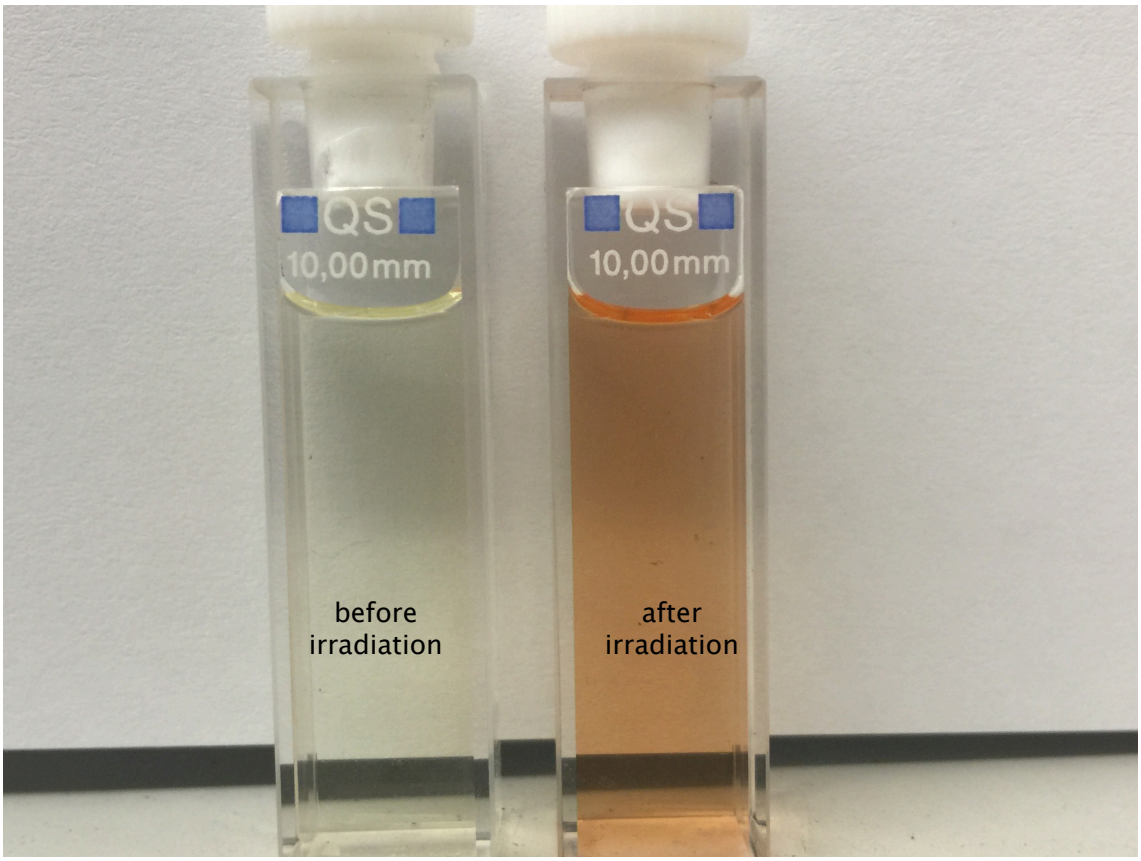

Figure 4.10. Solutions of **46** $8x10^{-4}$mol dm^{-3} in acetonitrile before and after irradiation at 365nm

The half life was calculated for **46**. the equation used was as follows

$$t_{\frac{1}{2}} = \frac{ln2}{k}$$

this equals

$$t_{\frac{1}{2}} = \frac{0.693}{k}$$

K is derived form the ln of the difference in the absorption over time

$$k = \frac{ln(^{2.78}/_{2.653})}{378}$$

when the K value of 1.23x10^{-4} s^{-1} is inserted back into the first equation the $t_{\frac{1}{2}}$ is calculated.

$$t_{\frac{1}{2}} = \frac{ln2}{1.23x10^{-4}}$$

$$t_{\frac{1}{2}} = 5601\,\mathrm{s}$$

The values for the K calculation are obtained for Figure 4.11 plot. The natural log of λ max is plotted against time. The values for k are taken form the line of best fit highlighted in red.

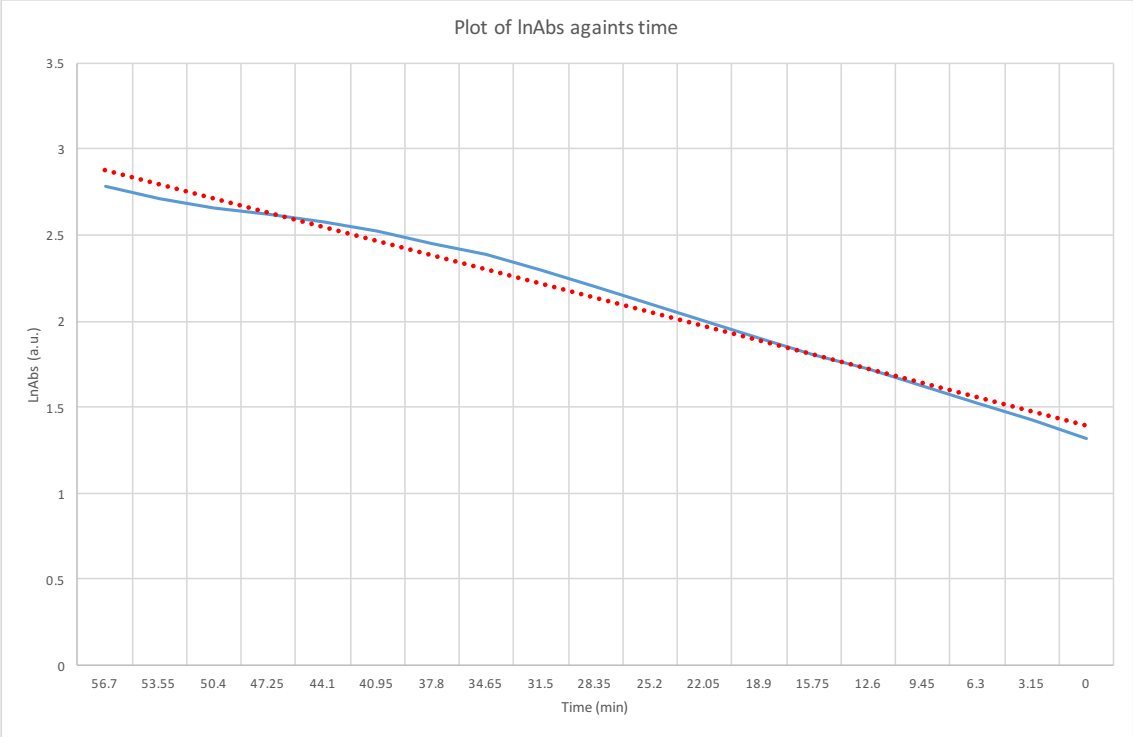

Figure 4.11. $t_{\frac{1}{2}}$ of **46** ln of the λ max against time.

Table 4.1. Data for the $t_{\frac{1}{2}}$ calculation of **46**.

Compound		
Absorption (a.u.)	|lnAbs|	Time (min)
0.269	2.780	56.70
0.241	2.710	53.55
0.217	2.653	50.40
0.197	2.616	47.25
0.179	2.572	44.10
0.165	2.518	40.59
0.150	2.453	37.80
0.135	2.386	34.65
0.122	2.295	31.50
0.111	2.200	28.35
0.101	2.103	25.20
0.092	2.000	22.05
0.086	1.109	18.90
0.081	1.801	15.75
0.076	1.718	12.60
0.073	1.625	9.45
0.070	1.528	6.30
0.067	1.423	3.15
0.062	1.314	0.00

The calculated $t_{\frac{1}{2}}$ for **46** is 7.78 hours, this is different to the reported $t_{\frac{1}{2}}$ of 19.6 hours by Herges *et al.*[96] This could be due to the irradiation wave length **46** was irradiated with 365 nm light, where as the literature uses light of 385 nm. This could account for the difference in the $t_{\frac{1}{2}}$ of the same material.

4.7 Diazocine conclusion

The aim of the above work was to synthesize a single system photochromic liquid crystal material based around the diazocine core unit. The original aim of the work

was to attach the LC mesogen directly to the diazocine core. This was approached by firstly forming the diazocine with amine functional groups and convert these to a halogen. This approach saw the degradation of the azo link which forms the diazocine moiety. The second approach to the formation of diazocine was based on introduction of halogens for direct attachment of the LC mesogen. The reduction and halogenation of the nitro groups was to be performed before the formation of the azo link. This also proved problematic, as the formation of the azo group was unsuccessful. In the final part of this work alkyne spacers were introduced to the diazocine core following work reported by R. Hergers *et al.* The introduction of this alkyne spacer allowed the formation of the azo link due to the higher stability of the TMS protected alkyne group compared to the stability of iodo groups. The issue with this method was the attachment of the LC mesogen via a Sonogashira coupling. The presence of two alkynes in close proximity was not conducive to double functionalisation. The conclusion of the work was that LC mesogens could not be directly attached to the diazocine core but required a spacer group. The type of spacer group needs further investigation to determine the best compromise between synthetic access and targeted properties.

References

(39) J. Wang, J. He, C. Zhi, B. Luo, X. Li, Y. Pan, X. Cao and H. Gu, *RSC Adv.*, Apr. 2014.

(47) R. Siewertsen, H. Neumann, B. Buchheim-Stehn, R. Herges, C. Näther, F. Renth and F. Temps, *J. Am. Chem. Soc.*, 2009, **131**, 15594–15595.

(48) H. Sell, C. Näther and R. Herges, *Beilstein J. Org. Chem.*, 2013, **9**, 1–7.

(49) D. K. Joshi, M. J. Mitchell, D. Bruce, A. J. Lough and H. Yan, *Tetrahedron*, 2012, **68**, 8670–8676.

(85) M. Wang, K. Funabiki and M. Matsui, *Dyes & Pigments*, Apr. 2003, **57**, 77–86.

(86) K. V. Kutonova, M. E. Trusova, P. S. Postnikov, V. D. Filimonov and J. Parello, *Synthesis*, 2013, **45**, 2706–2710.

(87) M. Mihara, T. Nakai, T. Iwai, T. Ito and T. Mizuno, *Synlett*, 2007, **2007**, 2124–2126.

(88) E. Merino, *Chem. Soc. Rev.*, 2011, **40**, 3835–3819.

(89) T. L. Scott and B. C. G. Söderberg, *Tetrahedron*, 2003, **59**, 6323–6332.

(90) M. K. Anwer and A. F. Spatola, *Tetrahedron Lett*, 1985, **26**, 1381–1384.

(91) P. Stepnicka, M. Semler, J. Demel, A. Zukal and J. Cejka, *J Mol Catal A Chem*, 2011, **341**, 97–102.

(92) N. A. Cortese and R. F. Heck, *J. Org. Chem.*, 1994, **59**, 635–638.

(93) D. C. Gowda and B. Mahesh, *Synth. Commun.*, Dec. 2007, **30**, 3639–3644.

(94) C. Zhang and N. Jiao, *Angew. Chem. Int. Ed.*, 2010, **49**, 6174–6177.

(95) K. Orito, T. Hatakeyama, M. Takeo, S. Uchiito, M. Tokuda and H. Suginome, *Tetrahedron*, 1998, **54**, 8403–8410.

(96) T. Tellkamp, J. Shen, Y. Okamoto and R. Herges, *Eur. J. Org. Chem.*, 2014, **2014**, 5456–5461.

(97) A. V. Ellis and M. A. Wilson, *J. Org. Chem.*, 2002, **67**, 8469–8474.

(98) M. Kumar, U. Sharma, S. Sharma, V. Kumar, B. Singh and N. Kumar, *RSC Adv.*, 2013, **3**, 4894–5.

Chapter 5 Summary

5.1 Conclusion

The aim of this work was to design, synthesise, and investigate novel photochromic LC molecules. The first set of novel materials that were synthesised, were based on HABI functionalised with cyanobiphenyl as the LC mesogen attached using a spacer group. This was achieved with different methods of attachment: direct hydrocarbon LC photochrome attachment. The properties of the first method of attachment made in earlier work led to the alteration of the synthesis and the addition of a siloxane linker between the HABI core and the LC mesogen this can be seen in Figure 5.1.

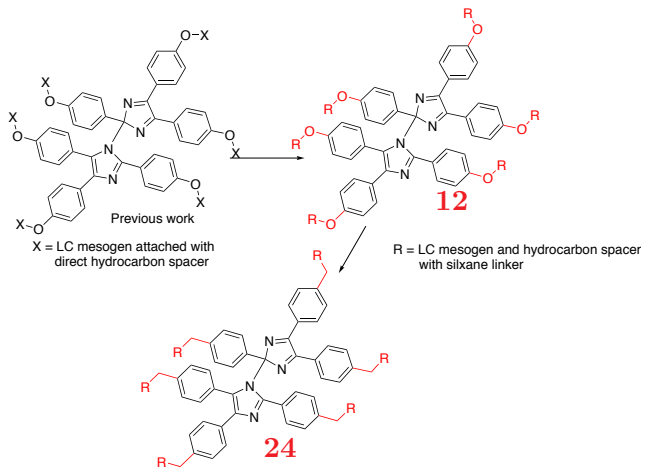

Figure 5.1. The evolution of the functionaliesd HABI.

The alteration of the structure and the incorporation of the siloxane linker reduced the melting point of the material and led to the introduction of a LC phase. The final material **12** was liquid crystaline at room temperature, with a transition to the isotropic at 50°C. Compound **12** exhibited a Smectic A phase which was confirmed using OPM and DSC with a enthalpy value of 1.68 J g^{-1} and finally confirmed using XRD showing the layer spacing at 31.2Å and a lateral intermolecular distance of 4.6 Å, these values match typical values of organic molecules for a SmA phase. The

second material was further altered form **12** to **24** shown in Figure 5.1. The further changes in the structure of the final HABI-LC material **24** did not alter the liquid crystal properties greatly; the transition to isotropic was slightly increased from 48°C for **12** to 55°C. The XRD diffractogram showed a difference in the packing of the material within the SmA phase. In **12** the XRD 2θ plot showed three intensities at 31.2 Å, 6.0 Å and 4.6 Å for the layer spacing, siloxane group, and the intermolecular distance. The XRD 2θ plot for **24** however showed a fourth intensity at 20.5 Å. This was attributed to interdigitation and end-to-end stacking of the the LC mesogens. The packing structure of both the materials is outlined in Figure 5.2

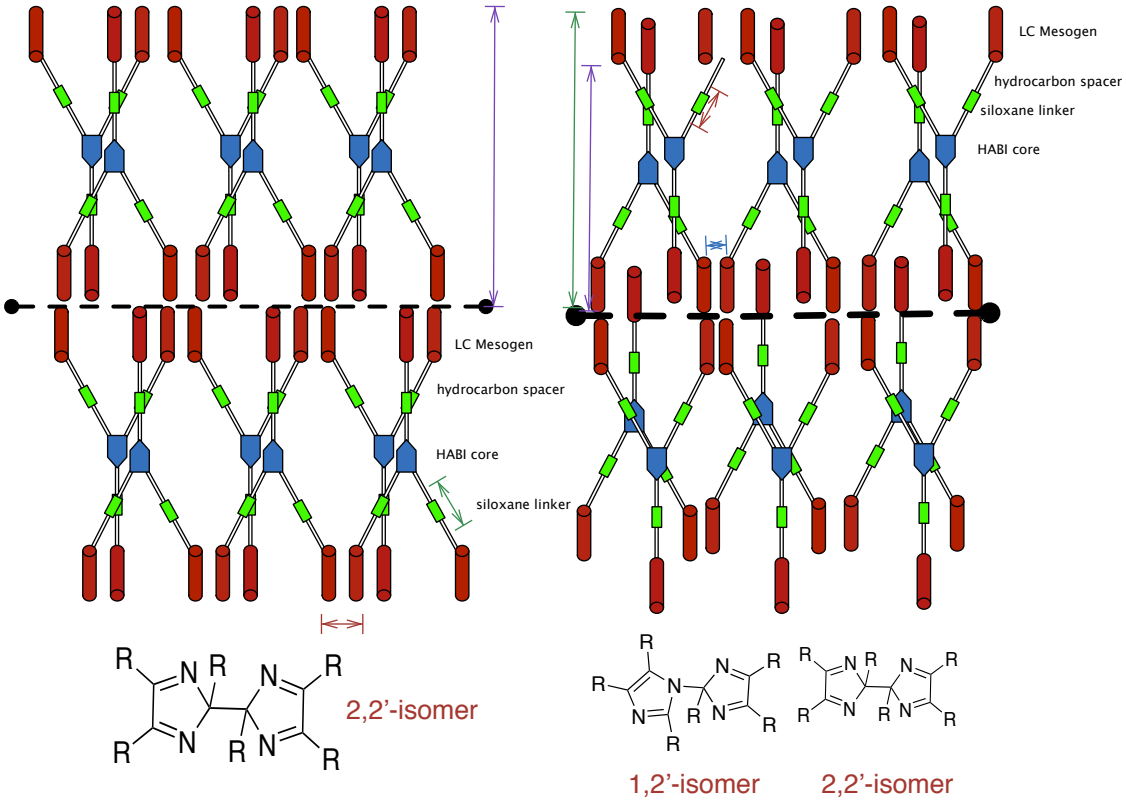

Figure 5.2. Representation of the packing of the functionalised HABIs **12** and **24**.

The alteration of the final HABI-LC material **24** through the removal of the oxy linking group the hydrocarbon spacer to the LC mesogen to the HABI core has no great effect on the liquid crystal phase behaviour or transition temperatures, however it did alter the absorption spectra. The removal of this linker shown in Figure 5.1 caused a further red shift in the maximum absorption value of the radical species,

and although not measured a reduction in the association of the radical material back to the dimer. This decrease in the association speed was only noted visually. The conclusion drawn form the two materials synthesised is that the alteration of the absorption maximum and the association speed of the HABI-LC material is affected by the functionalisation of the HABI core. The result of the work is that a new photochromic LC single system material was synthesised, where upon irradiation a bulk colour change in the material is achieved with no disruption of the liquid crystal phase.

The final section of this work was the synthesis of diazocine functionalised with LC mesogens directly to the photochromic core. The aim of the work was the introduction of a liquid crystal phase through the irradiation isomerisation of the diazocine moiety from the stable *cis* isomer to the less stable but more rod like *trans* isomer. The synthetic routes towards this group were optimised. The second part of the work carried out and looked at the newly emerging diazocine. The combination of this photochromic molecule with LC mesogens has not yet been investigated. This compound was chosen for the isomerisation upon irradiation which unlike in azobenzene which is *trans-cis*, for the diazocine it is *cis-trans*. This property opens up the possibilities of LC phase behaviour introduction or stabilisation upon irradiation. The formulated route for the synthesis of a diazocine with points of direct attachment is a new route different from the previously reported methods for the functionalisation of the compound.[48,99] The proposed route however did not yield the final material and was abanodoned. The direct attachment of the LC mesogen to the diazocine core was altered and an alkyne spacer was introduced following the work by Herges and his colleagues. The introduction of the alkyne protecting the reactive groups on the central core allowed the formation of a functionalised diazocine with points of attachment for the LC mesogen.

Chapter 6 References

(1) P. J. Collings and M. Hird, *Introduction to liquid crystals: chemistry and physics*, 1997.

(2) I. Dierking, *Textures of Liquid Crystals*, Wiley-VCH Verlag GmbH & Co. KGaA, Weinheim, Germany, 2003.

(3) P. Palffy-Muhoray, *Phys Today*, **60**, 54–60.

(4) S. E. Braslavsky, *Pure Appl Chem*, 2007, **79**, 293–465.

(5) F. Fages, J.-P. Desvergne, I. Frisch and H. Bouas-Laurent, *J. Chem. Soc., Chem. Commun.*, 1988, 1413–1415.

(6) E. ter Meer, *Justus Liebigs Ann Chem.*, 1876, **181**, 1–22.

(7) W. Geng, S. Cui and S. Pu, Adv. Mat. Rev. Trans Tech Publications, 2012, pp. 109–112.

(8) Y. Hirshberg, *J. Am. Chem. Soc.*, 1956, **78**, 2304–2312.

(9) H. Nishi, T. Namari and S. Kobatake, *J. Mater. Chem.*, 2011, **21**, 17249–17258.

(10) K. Maeda, in *Processes in Photoreactive Polymers*, Springer US, Boston, MA, 1995, pp. 90–110.

(11) S. Delbaere, G. Vermeersch, M. Frigoli and G. H. Mehl, *Org Lett*, 2010, **12**, 4090–4093.

(12) A. Perrier, F. Maurel and D. Jacquemin, *Acc. Chem. Res.*, 2012, **45**, 1173–1182.

(13) G. Liu, S. Pu and R. Wang, *Org Lett*, 2013, **15**, 980–983.

(14) S. Delbaere, G. Vermeersch, M. Frigoli and G. H. Mehl, *Org. Lett.*, 2006, **8**, 4931–4934.

(15) B. S. Tanaseichuk, *Chem Heterocycl Compd*, 1972, **8**, 1173–1180.

(16) H. Baumgärtel and H. Zimmermann, *Z. Naturforsch. B Chem. Sci.*, 1963, **18**, 406–412.

(17) G. R. Coraor, L. A. Cescon, R. Dessauer, E. F. Silversmith and E. J. Urban, *J. Org. Chem.*, 1971, **36**, 2262–2267.

(18) H. Tanino, T. Kondo, K. Okada and T. Goto, *Bull. Chem. Soc. Jap*, 1972, **45**, 1474–1480.

(19) L. A. Cescon and R. Dessauer, US Pat. 358 503 8A, 1971.

(20) D. M. White and J. Sonnenberg, *J. Am. Chem. Soc.*, 1966, **88**, 3825–3829.

(21) Y. Zhou, W. E. Baker, P. M. Kazmaier and E. Buncel, *Can. J. Chem*, 2011, **76**, 884–895.

(22) S. Delbaere, M. Orio, J. Berthet, M. Sliwa, S. Hatano and J. Abe, *Chem. Commun.*, 2013, **49**, 5841–5843.

(23) Y. Harada, S. Hatano, A. Kimoto and J. Abe, *J. Phys. Chem. Lett.*, 2010, **1**, 1112–1115.

(24) H. Sato, K. Kasatani and S. Murakami, *Chem. Phys. Lett*, 1988, **151**, 97–101.

(25) S. Hatano, T. Horino, A. Tokita, T. Oshima and J. Abe, *J. Am. Chem. Soc.*, 2013, **135**, 3164–3172.

(26) T. Yamaguchi, S. Hatano and J. Abe, *J Phys Chem A*, 2014, **118**, 134–143.

(27) K. Fujita, S. Hatano, D. Kato and J. Abe, *Org Lett*, 2008, **10**, 3105–3108.

(28) K. Mutoh and J. Abe, *Phys. Chem. Ch. Ph.*, 2014, **16**, 17537–17540.

(29) H. Yamashita, T. Ikezawa, Y. Kobayashi and J. Abe, *J Am Chem Soc*, 2015, **137**, 4952–4955.

(30) E. Mitscherlich, *Ann. Pharm.*, 1834, **12**, 311–314.

(31) E. Merino and M. Ribagorda, *Beilstein J. Org. Chem*, July 2012, **8**, 1071–1090.

(32) H. M. D. Bandara and S. C. Burdette, *Chem. Soc. Rev.*, 2012, **41**, 1809–1825.

(33) A. Goulet-Hanssens and C. J. Barrett, *J. Photochem. Photobiol. C*, 2014, **294**, 62–67.

(34) Á. Georgiádes, S. B. Ötvös and F. Fülöp, *ACS Sustainable Chem. Eng.*, 2015, **3**, 3388–3397.

(35) S. Okumura, C.-H. Lin, Y. Takeda and S. Minakata, *J. Org. Chem.*, 2013, **78**, 12090–12105.

(36) S. Wada, M. Urano and H. Suzuki, *J. Org. Chem.*, 2002, **67**, 8254–8257.

(37) M. Malinowski, *J. Prakt. Chem.*, 1988, **330**, 811–813.

(38) L. Racané, H. Čičak, Z. Mihalić, G. Karminski-Zamola and V. Tralić-Kulenović, *Tetrahedron*, 2011, **67**, 2760–2767.

(39) J. Wang, J. He, C. Zhi, B. Luo, X. Li, Y. Pan, X. Cao and H. Gu, *RSC Adv.*, Apr. 2014.

(40) X. A Zhang, H. Zhao, Y. Gao, J. Tong, L. Shan, Y. Chen, S. Zhang, A. Qin, J. Z. Sun and B. Z. Tang, *Polymer*, 2011, **52**, 5290–5301.

(41) Y. Hayata, S. Nagano, Y. Takeoka and T. Seki, *ACS Macro Letters*, 2012, **1**, 1357–1361.

(42) M. K. A. Rahim, T. Fukaminato, T. Kamei and N. Tamaoki, *Langmuir*, 2011, **27**, 10347–10350.

(43) K. G. Yager and C. J. Barrett, *J. Photochem. Photobiol. C*, 2006, **182**, 250–261.

(44) U. Funke and H.-F. Grützmacher, *Tetrahedron*, 1987, **43**, 3787–3795.

(45) Y. Norikane, K. Kitamoto and N. Tamaoki, *J. Org. Chem.*, 2003, **68**, 8291–8304.

(46) W. W. Paudler and A. G. Zeiler, *J. Org. Chem.*, 1969, **34**, 3237–3239.

(47) R. Siewertsen, H. Neumann, B. Buchheim-Stehn, R. Herges, C. Näther, F. Renth and F. Temps, *J. Am. Chem. Soc.*, 2009, **131**, 15594–15595.

(48) H. Sell, C. Näther and R. Herges, *Beilstein J. Org. Chem.*, 2013, **9**, 1–7.

(49) D. K. Joshi, M. J. Mitchell, D. Bruce, A. J. Lough and H. Yan, *Tetrahedron*, 2012, **68**, 8670–8676.

(50) C. H. Legge and G. R. Mitchell, *J Phys. D Appl. Phys.*, 1992, **25**, 492–499.

(51) A. Sobolewska, S. Bartkiewicz, J. Mysliwiec and K. D. Singer, *J. Mater. Chem. C*, 2014.

(52) M. Frigoli and G. H. Mehl, *Chem. Commun. (Camb.)*, 2004, 2040–2041.

(53) M. Frigoli and G. H. Mehl, *Chem. Commun. (Camb.)*, 2004, 818–819.

(54) T. Kosa, L. Sukhomlinova, L. Su, B. Taheri, T. J. White and T. J. Bunning, *Nature*, 2012, **485**, 347–349.

(55) S. Xie, B. Zheng, Q. Kuang, X. Wang, Z. Xie and L. Zheng, *Cryst. Eng. Comm*, 2012, **14**, 7715–6.

(56) M. Frigoli and G. H. Mehl, *Eur. J. Org. Chem.*, 2004, **2004**, 636–642.

(57) S. Delbaere, J. C. Micheau, M. Frigoli, G. H. Mehl and G. Vermeersch, *J. Phys. Org. Chem.*, 2007, **20**, 929–935.

(58) M. Frigoli and G. H. Mehl, *Angew. Chem. Int. Ed.*, 2005, **44**, 5048–5052.

(59) K. Arai, Y. Kobayashi and J. Abe, *Chem. Commun. (Camb.)*, 2015, **51**, 3057–3060.

(60) J. Hussey, *Photochromic Liquid Crystals.* MChem Dissertation, University of Hull, UK, 2012.

(61) B. Atorf, A. Hoischen, M. B. Ros, N. Gimeno, C. Tschierske, G. Dantlgraber and H. Kitzerow, *Applied Physics Letters*, 2012, **100**, 223301.

(62) S. D. Lepore and Y. He, *J. Org. Chem.*, 2003, **68**, 8261–8263.

(63) C. J. Moody and L. M. Harwood, *Experimental organic chemistry: principles and practice*, 1989.

(64) K. Bahrami, M. M. Khodaei and A. Nejati, *Monatsh Chem*, 2011, **142**, 159–162.

(65) K. C. Majumdar, D. Ghosh and S. Ponra, *Synthesis*, 2013, **45**, 2983–2988.

(66) H. Veisi, A. Khazaei, L. Heshmati and S. Hemmati, *Bull. Mater. Sci.*, 2012, **33**, 1231–1234.

(67) A. Sedrpoushan, Z. Joshani and L. Fatollahi, *Lett. Org. Chem.*, 2014, **11**, 287–292.

(68) A. Y. Usyatinsky and Y. L. Khmelnitsky, *Tetrahedron Lett*, June 2000, **41**, 5031–5034.

(69) C. O. Kappe, *Angew. Chem. Int. Ed.*, 2004, **43**, 6250–6284.

(70) C. M. Sousa, J. Berthet, S. Delbaere and P. J. Coelho, *J. Org. Chem.*, 2012, **77**, 3959–3968.

(71) C. M. Sousa, J. Berthet, S. Delbaere, A. Polónia and P. J. Coelho, *J. Org. Chem.*, 2015, **80**, 12177–12181.

(72) R. Adams and C. S. Marvel, *Benzoin*, John Wiley & Sons, Inc., Hoboken, NJ, USA, 1941.

(73) R. Chen, Z. An, F. Li, X. Chen and P. Chen, *Liq. Cryst.*, 2016, **43**, 564–572.

(74) N. Marion, R. S. Ramón and S. P. Nolan, *J Am Chem Soc*, 2009, **131**, 448–449.

(75) N. Xu, D.-W. Gu, Y.-S. Dong, F.-P. Yi, L. Cai, X.-Y. Wu and X.-X. Guo, *Tetrahedron Lett*, 2015, **56**, 1517–1519.

(76) A. Gao, F. Yang, J. Li and Y. Wu, *Tetrahedron*, 2012, **68**, 4950–4954.

(77) M. D. Greenhalgh and S. P. Thomas, *Chem. Commun.*, 2013, **49**, 11230–11233.

(78) J. M. Bakker, S. J. Langford, M. J. Latter, K. A. Lee and C. P. Woodward, *Aust. J. Chem.*, 2005, **58**, 757–755.

(79) A. R. Mulholland, C. P. Woodward and S. J. Langford, *Chem. Commun.*, 2011, **47**, 1494–1496.

(80) L. Ruan, M. Shi, N. Li, X. Ding, F. Yang and J. Tang, *Org. Lett.*, 2014, **16**, 733–735.

(81) C. Giansante, P. Ceroni, V. Balzani, M. Maestri, S.-K. Lee and F. Vögtle, *New J. Chem.*, 2007, **31**, 1250–1259.

(82) E. Ramou, Z. Ahmed, C. Welch, P. K. Karahaliou and G. H. Mehl, *Soft Matter*, 2015, **12**, 888–899.

(83) Z. Ahmed, C. Welch and G. H. Mehl, *RSC Adv.*, 2015, **5**, 93513–93521.

(84) H. Yamashita and J. Abe, *Chem. Commun.*, 2014, **50**, 8468–8465.

(85) M. Wang, K. Funabiki and M. Matsui, *Dyes & Pigments*, Apr. 2003, **57**, 77–86.

(86) K. V. Kutonova, M. E. Trusova, P. S. Postnikov, V. D. Filimonov and J. Parello, *Synthesis*, 2013, **45**, 2706–2710.

(87) M. Mihara, T. Nakai, T. Iwai, T. Ito and T. Mizuno, *Synlett*, 2007, **2007**, 2124–2126.

(88) E. Merino, *Chem. Soc. Rev.*, 2011, **40**, 3835–3819.

(89) T. L. Scott and B. C. G. Söderberg, *Tetrahedron*, 2003, **59**, 6323–6332.

(90) M. K. Anwer and A. F. Spatola, *Tetrahedron Lett*, 1985, **26**, 1381–1384.

(91) P. Stepnicka, M. Semler, J. Demel, A. Zukal and J. Cejka, *J Mol Catal A Chem*, 2011, **341**, 97–102.

(92) N. A. Cortese and R. F. Heck, *J. Org. Chem.*, 1994, **59**, 635–638.

(93) D. C. Gowda and B. Mahesh, *Synth. Commun.*, Dec. 2007, **30**, 3639–3644.

(94) C. Zhang and N. Jiao, *Angew. Chem. Int. Ed.*, 2010, **49**, 6174–6177.

(95) K. Orito, T. Hatakeyama, M. Takeo, S. Uchiito, M. Tokuda and H. Suginome, *Tetrahedron*, 1998, **54**, 8403–8410.

(96) T. Tellkamp, J. Shen, Y. Okamoto and R. Herges, *Eur. J. Org. Chem.*, 2014, **2014**, 5456–5461.

(97) A. V. Ellis and M. A. Wilson, *J. Org. Chem.*, 2002, **67**, 8469–8474.

(98) M. Kumar, U. Sharma, S. Sharma, V. Kumar, B. Singh and N. Kumar, *RSC Adv.*, 2013, **3**, 4894–5.

(99) B. He and O. S. Wenger, *J. Am. Chem. Soc*, 2011, **133**, 17027–17036.